Aided Inertial Navigation With Geometric Features: Observability Analysis

Yulin Yang - yuyang@udel.edu
Guoquan Huang - ghuang@udel.edu

Department of Mechanical Engineering
University of Delaware, Delaware, USA

RPNG

Robot Perception and Navigation Group (RPNG)
Tech Report - RPNG-2017-OBS
Last Updated - May. 13, 2018

Contents

1 Introduction and Related Work **1**

2 Aided INS with Point Features **2**
2.1 IMU Propagation Model . . . 2
2.2 Generic Measurement Model . . . 3

3 Observability Analysis of Aided INS with Point Features **3**
3.1 Global Measurements . . . 4
3.1.1 Global x Measurement . . . 4
3.1.2 Global y Measurement . . . 4
3.1.3 Global z Measurement . . . 5
3.1.4 Global Orientation Measurement . . . 5
3.1.5 Summary . . . 5
3.2 Degenerate Motion . . . 5
3.2.1 Pure Translation . . . 6
3.2.2 Pure Rotation . . . 6
3.2.3 Moving Toward a Feature . . . 7
3.2.4 Constant Acceleration . . . 7

4 Observability Analysis of Aided INS with Line Features **7**
4.1 Line Representation . . . 7
4.2 Observability Analysis: Single Line . . . 8
4.3 Observability Analysis: Multiple Lines . . . 9

5 Observability Analysis of Aided INS with Plane Features **10**
5.1 Observability Analysis: Single Plane . . . 10
5.2 Observability Analysis: Multiple Planes . . . 11

6 Simulation Results **12**

7 Conclusions and Future Work **14**

Appendix A State Transition Matrix **14**

Appendix B Line Jacobians **15**

Appendix C Direct Line Measurement **15**

Appendix D Unobservable Directions for Multiple Lines **16**

Appendix E Unobservable Directions for Multiple Planes **17**

Appendix F Sensor Measurements for Point Features **17**
F.1 1D Range Finder . . . 18
F.2 Mono-camera . . . 18
F.3 2D Imaging Sonar . . . 18
F.4 2D LiDAR . . . 19
F.5 3D LiDAR . . . 19
F.6 RGBD Camera . . . 20
F.7 Stereo Camera . . . 20

Appendix G Unobservable Directions for Point Features **21**
G.1 Nonlinear Observability Analysis 21
G.2 System Propagation Model 22
G.3 Observability Analysis for Point Feature 22
G.3.1 Basis Functions For Point Measurement 23
G.3.2 Unobservable Direction 24

Appendix H Basis Function and Rank Test for Point Measurement **24**
H.1 Basis Functions for Point Measurement 24
H.2 Rank test for $\Xi^{(r)}$ 26
H.3 Rank test for $\Xi^{(b)}$ 28

References **33**

Abstract

In this paper, we perform observability analysis for inertial navigation systems (INS) aided by generic exteroceptive range and/or bearing) sensors with different type of geometric features including points, lines and planes. In particular, while the observability of vision-aided INS (VINS, which uses cameras as bearing sensor) with point features has been extensively studied in the literature, we analytically show that the same observability property remains if using generic range and/or bearing measurements, and if global measurements are also available, as expected, some unobservable directions dismiss. Moreover, we study in-depth the effects of four degenerate motions on the system observability. Building upon the observability analysis of the aided INS with point features, we perform observability analysis for the same system but with line and plane features, respectively, and show that there exist 5 (and 7) unobservable directions for a single line (and plane) feature. Moreover, we, for the first time, analytically derive the unobservable directions for the cases of multiple lines/planes. We validate our observability analysis through Monte Carlo simulations.

1 Introduction and Related Work

Over the past decades, an inertial navigation system (INS) using an inertial measurement unit (IMU) is among the most popular approaches to estimate the 6 degrees-of-freedom (DOF) position and orientation (pose) in 3D, especially in GPS-denied environments such as underwater, indoor, in the urban canyon, and in space. However, simple integration of IMU measurements that are corrupted by noise and bias, often results in estimates unreliable in a long term, although a high-accuracy IMU exists but remains prohibitively expensive for widespread deployment. A camera that is small, light-weight, and energy-efficient, provides rich information about the perceived environment and serves as an idea aiding source for INS, i.e., vision-aided INS (VINS) [1, 2, 3, 4, 5, 6, 7, 8]. Nevertheless, many other exteroceptive sensors such as LiDAR [9], RGBD camera[10] and 2D imaging sonar [11], can also be used to aid INS by providing range and/or bearing measurements to features. To date, various algorithms are available for aided INS problems, among which the EKF-based approaches remain arguably the most popular, for example, observability constrained (OC)-EKF [12, 1], and multi-state constrained Kalman filter (MSCKF) [13, 3].

As system observability plays an important role in developing consistent state estimation [14], the observability of VINS has been extensively studied. In particular, the authors of [15, 16] examined the system's indistinguishable trajectories. By employing the concept of continuous symmetries, [17, 18] showed explicitly that the IMU biases, 3D velocity, and absolute roll and pitch angles in VINS are observable. In [1, 19], observability analysis for the linearized VINS was performed by analytically finding the right null space of the observability matrix. The corresponding nonlinear observability analysis [20] was also carried out, respectively, for monocular vision-aided INS [2] and RGBD-aided INS [21], where the unobservable directions were found analytically. Previous work shows that there are 4 unobservable directions (3 correspond to global translation and 1 to global yaw) for VINS. However, few has studied the observability for INS aided with generic range and/or bearing measurements using different geometric features. Note that aided INS might be fed into global measurements, such as altitude measurements by barometers and orientation measurements by compasses. It is important to understand the effects of such measurements on the system observability. Moreover, it is of practical significance to examine the degenerate motions that may ruin the system observability properties by causing more unobservable directions (e.g., see [22]).

While most current VINS algorithms focus on using point features [3, 1, 2], line and plane features are to prevail [23, 10, 24, 25], because of their advantages: (i) There are plenty of straight lines and planes in common urban or indoor environments (e.g., doors, walls, stairs); (ii) They can be easily detected and tracked continuously over a relatively long time period; (iii) They are more robust in texture-less environments compared to points. In particular, Kottas et al. [25] represented the line with a quaternion and a scalar, and studied the line observability based on this representation with linearized observability matrix. Guo et al. [10] and Panahandeh et al.[24] analyzed the observability of VINS with plane features, while assuming plane orientation is *a priori* known. In contrast, in this work, we make no assumption for lines or planes and advocate to use the minimum parameterization of orthonormal representation [26] to model line features. By performing observability analysis, we show there are 5 (and 7) unobservable directions for INS with a single line (and plane) feature; and moreover, we derive for the first time the unobservable subspace of the aided INS with multiple lines or planes.

Specifically, the main theoretical contributions of this paper are in the following:

- We generalize the VINS observability analysis to INS aided with any type of exteroceptive sensors such as 3D LiDAR, 2D imaging sonar, and stereo cameras, and analytically show that the same observability properties remain (i.e., four unobservable directions).
- We study in-depth the effects of global measurements on the system observability, showing that they, as expected, will improve the system observability.
- By employing the spherical coordinates for the point feature, we identify 4 degenerate motions that cause the aided INS to have more unobservable directions.
- We perform observability analysis for the aided INS with line and plane features, respectively, and show that there exist 5 (and 7) unobservable directions for a single line (and plane) feature. Moreover, we analytically derive the unobservable directions for multiple lines (planes), without any assumption about features.

2 Aided INS with Point Features

In this section, we briefly describe the system and measurement models of the general aided INS, which will form the basis for the ensuing analysis. In particular, the state vector of the aided INS contains the current IMU state $\mathbf{x}_{IMU}$ and the feature ${}^{G}\mathbf{P_f}$ (note that for simplicity of presentation, we consider the case of a single feature):

$$\mathbf{x}= \begin{bmatrix}\mathbf{x}_{IMU}^\top & {}^{G}\mathbf{P}_{\mathbf{f}}^{T}\end{bmatrix} = \begin{bmatrix}{}^{I}_{G}\bar{q}^\top & \mathbf{b}_g^\top & {}^{G}\mathbf{V}_I^\top & \mathbf{b}_a^\top & {}^{G}\mathbf{P}_I^\top & {}^{G}\mathbf{P}_{\mathbf{f}}^\top\end{bmatrix}^\top \tag{1}$$

where ${}^{I}_{G}\bar{q}$ is a unit quaternion represents the rotation of IMU from the global frame to the IMU frame. ${}^{G}\mathbf{V}_I$ and ${}^{G}\mathbf{P}_I$ represents the velocity and position of the IMU in the global frame, while $\mathbf{b}_g$ and $\mathbf{b}_a$ represent the gyroscope and accelerometer biases, respectively.

2.1 IMU Propagation Model

The time evolution of the system is given by [27]:

$$\begin{aligned}&{}^{I}_{G}\dot{\bar{q}}(t) = \frac{1}{2}\mathbf{\Omega}\left({}^{I}\boldsymbol{\omega}(t)\right){}^{I}_{G}\bar{q}(t), \quad {}^{G}\dot{\mathbf{P}}_I(t) = {}^{G}\mathbf{V}_I(t), \quad {}^{G}\dot{\mathbf{V}}_I(t) = {}^{G}\mathbf{a}(t)\\ &\dot{\mathbf{b}}_g(t) = \mathbf{n}_{wg}(t), \quad \dot{\mathbf{b}}_a(t) = \mathbf{n}_{wa}(t), \quad {}^{G}\dot{\mathbf{P}}_{\mathbf{f}}(t) = \mathbf{0}_{3\times 1}\end{aligned} \tag{2}$$

where ${}^{I}\boldsymbol{\omega}$ and ${}^{I}\mathbf{a}$ are the angular velocity and linear acceleration, respectively. $\mathbf{n}_{wg}$ and $\mathbf{n}_{wa}$ are zero-mean Gaussian noises driving the gyroscope and accelerometer biases, and $\mathbf{\Omega}(\boldsymbol{\omega}) \triangleq \begin{bmatrix}-\lfloor\boldsymbol{\omega}\times\rfloor & \boldsymbol{\omega}\\ -\boldsymbol{\omega}^\top & 0\end{bmatrix}$, $\lfloor\boldsymbol{\omega}\times\rfloor$ represents skew-symmetric matrix. The gyroscope and the accelerometer measurements are:

$$\boldsymbol{\omega}_m(t)= {}^{I}\boldsymbol{\omega}(t) + \mathbf{b}_g(t) + \mathbf{n}_g(t) \tag{3}$$

$$\mathbf{a}_m(t)= \mathbf{R}\left({}^{I}_{G}\bar{q}(t)\right)\left({}^{G}\mathbf{a}(t) - {}^{G}\mathbf{g}\right) + \mathbf{b}_a(t) + \mathbf{n}_a(t) \tag{4}$$

where $\mathbf{R}\left(\bar{q}\right)$ represents the rotation corresponding to the quaternion $\bar{q}$, ${}^{G}\mathbf{g} = \begin{bmatrix}0 & 0 & -g\end{bmatrix}^\top$ is the gravity, $\mathbf{n}_g(t)$ and $\mathbf{n}_a(t)$ are zeros-mean Gaussian white noises corrupting angular velocity and linear acceleration measurement. Linearizing the system model (2) at the current state estimates yields the continuous-time error-state equation [27]:

$$\dot{\tilde{\mathbf{x}}}(t) = \begin{bmatrix}\mathbf{F}_c(t) & \mathbf{0}_{15\times 3}\\ \mathbf{0}_{3\times 15} & \mathbf{0}_3\end{bmatrix}\tilde{\mathbf{x}}(t) + \begin{bmatrix}\mathbf{G}(t)\\ \mathbf{0}_{3\times 12}\end{bmatrix}\mathbf{n}(t) = \mathbf{F}(t)\tilde{\mathbf{x}}(t) + \mathbf{G}(t)\mathbf{n}(t) \tag{5}$$

where $\mathbf{F}_c(t)$ is the continuous-time error-state transition matrix, and $\mathbf{G}_c(t)$ is the continuous-time noise Jacobian matrix. The system noise $\mathbf{n}(t) = \begin{bmatrix}\mathbf{n}_g^\top & \mathbf{n}_{wg}^\top & \mathbf{n}_a^\top & \mathbf{n}_{wa}^\top\end{bmatrix}^\top$ are modeled as a zero-mean white Gaussian process with autocorrelation $\mathbb{E}\left[\mathbf{n}(t)\mathbf{n}^\top(\tau)\right] = \mathbf{Q}_c\delta(t-\tau)$. To propagate covariance, we need to compute the

discrete-time state transition matrix $\mathbf{\Phi}_{(k+1,k)}$ from time t_k to t_{k+1}, which is obtained by solving the differential equation $\dot{\mathbf{\Phi}}_{(k+1,k)} = \mathbf{F}(t_k)\mathbf{\Phi}_{(k+1,k)}$ with $\mathbf{\Phi}_{(1,1)} = \mathbf{I}_{18}$ [1]. With that, the discrete-time noise covariance matrix and the propagated covariance can be computed as:

$$\mathbf{Q}_k = \int_{t_k}^{t_{k+1}} \mathbf{\Phi}_{(k,\tau)}\mathbf{G}_c(\tau)\mathbf{Q}_c\mathbf{G}_c^\top(\tau)\mathbf{\Phi}_{(k,\tau)}^\top \mathbf{d}\tau \tag{6}$$

$$\mathbf{P}_{k+1|k} = \mathbf{\Phi}_{(k+1,k)}\mathbf{P}_{k|k}\mathbf{\Phi}_{(k+1,k)}^\top + \mathbf{Q}_k \tag{7}$$

2.2 Generic Measurement Model

A 3D point feature detected from range and/or bearing measurements, can be represented by:

$$\mathbf{P_f} = \begin{bmatrix} x_\mathbf{f} & y_\mathbf{f} & z_\mathbf{f} \end{bmatrix}^\top = r_\mathbf{f}\mathbf{b_f} \tag{8}$$

where $r_\mathbf{f}$ and $\mathbf{b_f}$ are the range and bearing of the point. For simplicity, we assume the sensor frame coincides with the IMU frame. The point in the local sensor frame is given by:

$${}^I\mathbf{P_f} = \begin{bmatrix} {}^Ix_\mathbf{f} & {}^Iy_\mathbf{f} & {}^Iz_\mathbf{f} \end{bmatrix}^\top = {}^I_G\mathbf{R}\left({}^G\mathbf{P_f} - {}^G\mathbf{P}_I\right) \tag{9}$$

While a variety of sensors are available and provide different measurements, all these measurements in the aided INS are in the form of range and/or bearing, which can be modeled as follows (see Appendix F):

$$\mathbf{z} = \begin{bmatrix} z^{(r)} \\ \mathbf{z}^{(b)} \end{bmatrix} \begin{bmatrix} \sqrt{{}^I\mathbf{P_f}^\top {}^I\mathbf{P_f}} + n^{(r)} \\ \mathbf{h_b}\left({}^I\mathbf{P_f}, \mathbf{n}^{(b)}\right) \end{bmatrix} \tag{10}$$

With linearization at the current feature estimate ${}^I\hat{\mathbf{P}}_\mathbf{f}$, we have:

$$\tilde{\mathbf{z}} = \begin{bmatrix} \tilde{z}^{(r)} \\ \tilde{\mathbf{z}}^{(b)} \end{bmatrix} \simeq \begin{bmatrix} \mathbf{H}_r {}^I\tilde{\mathbf{P}}_\mathbf{f} + n^{(r)} \\ \mathbf{H}_b {}^I\tilde{\mathbf{P}}_\mathbf{f} + \mathbf{H}_n\mathbf{n}^{(b)} \end{bmatrix} \tag{11}$$

where $\mathbf{H}_r$ and $\mathbf{H}_b$ denote the range and bearing measurement Jacobians, and $\mathbf{H}_n$ is the noise Jacobian (see Appendix F), n^r and $\mathbf{n}^b$ are the zero-mean Gaussian noises contaminating the range and bearing measurements, respectively.

3 Observability Analysis of Aided INS with Point Features

In this section, we perform observability analysis for the linearized system of aided INS with point features based on generic measurements in a similar way as in [12, 1]. In particular, the observability matrix $\mathbf{M}(\mathbf{x})$ is given by:

$$\mathbf{M}(\mathbf{x}) = \begin{bmatrix} \mathbf{H}_{I_1}\mathbf{\Phi}_{(1,1)} \\ \mathbf{H}_{I_2}\mathbf{\Phi}_{(2,1)} \\ \vdots \\ \mathbf{H}_{I_k}\mathbf{\Phi}_{(k,1)} \end{bmatrix} \tag{12}$$

The unobservable directions of this aided INS span the right null space of $\mathbf{M}(\mathbf{x})$. Specifically, for each block row of $\mathbf{M}(\mathbf{x})$, we have:

$$\begin{aligned} \mathbf{H}_{I_k} &= \begin{bmatrix} \mathbf{H}_{r,k} \\ \mathbf{H}_{b,k} \end{bmatrix} \begin{bmatrix} \lfloor {}^{I_k}_G\hat{\mathbf{R}}\left({}^G\hat{\mathbf{P}}_\mathbf{f} - {}^G\hat{\mathbf{P}}_{I_k}\right)\times\rfloor & \mathbf{0}_3 & \mathbf{0}_3 & \mathbf{0}_3 & -{}^{I_k}_G\hat{\mathbf{R}} & {}^{I_k}_G\hat{\mathbf{R}} \end{bmatrix} \\ &= \mathbf{H}_{proj,k}{}^{I_k}_G\hat{\mathbf{R}} \begin{bmatrix} \lfloor\left({}^G\hat{\mathbf{P}}_\mathbf{f} - {}^G\hat{\mathbf{P}}_{I_k}\right)\times\rfloor {}^{I_k}_G\hat{\mathbf{R}}^\top & \mathbf{0}_3 & \mathbf{0}_3 & \mathbf{0}_3 & -\mathbf{I}_3 & \mathbf{I}_3 \end{bmatrix} \end{aligned} \tag{13}$$

where we have defined $\mathbf{H}_{proj,k} = \begin{bmatrix} \mathbf{H}_{r,k}^\top & \mathbf{H}_{b,k}^\top \end{bmatrix}^\top$. Thus,

$$\mathbf{H}_{I_k}\mathbf{\Phi}_{(k,1)} = \mathbf{H}_{proj,k}{}^{I_k}_G\hat{\mathbf{R}} \begin{bmatrix} \mathbf{\Gamma}_1 & \mathbf{\Gamma}_2 & \mathbf{\Gamma}_3 & \mathbf{\Gamma}_4 & -\mathbf{I}_3 & \mathbf{I}_3 \end{bmatrix} \tag{14}$$

where:

$$\boldsymbol{\Gamma}_1 = \lfloor {}^G\hat{\mathbf{P}}_{\mathbf{f}} - {}^G\hat{\mathbf{P}}_{I_1} - {}^G\hat{\mathbf{V}}_{I_1}\delta t_k + \frac{1}{2}{}^G\mathbf{g}(\delta t_k)^2 \times \rfloor {}^G_{I_1}\hat{\mathbf{R}}$$
$$\boldsymbol{\Gamma}_2 = \lfloor \left({}^G\hat{\mathbf{P}}_{\mathbf{f}} - {}^G\hat{\mathbf{P}}_{I_k}\right) \times \rfloor {}^{I_k}_{G}\hat{\mathbf{R}}^\top \boldsymbol{\Phi}_{12} - \boldsymbol{\Phi}_{52}, \boldsymbol{\Gamma}_3 = -\mathbf{I}_3\delta t_k, \boldsymbol{\Gamma}_4 = -\boldsymbol{\Phi}_{54}$$

By inspection, it is not difficult to see that the null space for the matrix $\mathbf{M}(\mathbf{x})$ is given by:

$$\mathbf{N}^T = \begin{bmatrix}\mathbf{N}_p^T \\ \mathbf{N}_r^T\end{bmatrix} = \begin{bmatrix} \mathbf{0}_3 & \mathbf{0}_3 & \mathbf{0}_3 & \mathbf{0}_3 & \mathbf{I}_3 & \mathbf{I}_3 \\ \left({}^{I_1}_{G}\hat{\mathbf{R}}\,{}^G\mathbf{g}\right)^\top & \mathbf{0}_{1\times 3} & -\left(\lfloor {}^G\hat{\mathbf{V}}_{I_1}\times\rfloor {}^G\mathbf{g}\right)^\top & \mathbf{0}_{1\times 3} & -\left(\lfloor {}^G\hat{\mathbf{P}}_{I_1}\times\rfloor {}^G\mathbf{g}\right)^\top & -\left(\lfloor {}^G\hat{\mathbf{P}}_{\mathbf{f}}\times\rfloor {}^G\mathbf{g}\right)^\top \end{bmatrix}^\top$$

where $\mathbf{N}_p$ corresponds to the sensor's global translation and $\mathbf{N}_r$ relates to the global rotation around the gravity direction. For generic range and bearing sensors, the Jacobians can all be represented by $\mathbf{H}_{proj,k}$. From the above analysis, we see that the system has at least four unobservable directions.

Additionally, in analogy to [12, 2, 21], we have further performed the nonlinear observability analysis based on lie derivatives [20] for the continuous-time nonlinear INS aided by generic measurements, which is summarized as follows:

Lemma 3.1. *The continuous-time nonlinear INS aided by generic range and/or bearing measurements with point features, has 4 unobservable directions.*

Proof. See Appendix G. □

3.1 Global Measurements

In practice the aided INS may also have access to (partial) global measurements provided by, for example, GPS, motion capture systems, barometers and compasses. Intuitively, such measurements would alter the system observability properties, even if only partial (not full 6DOF) information is available. In what follows, we systematically inspect the impacts of such measurements on observability.

3.1.1 Global x Measurement

We consider the case where besides the range and bearing sensors, global position measurements are also available from, for example, GPS and barometer. Specifically, if sensor's translation along x direction is known, the additional measurement is given by $z^{(x)} = \mathbf{e}_1^\top {}^G\mathbf{P}_I$. The measurement Jacobians and the block row of observability matrix at time step k can be computed as:

$$\mathbf{H}_{I_k} = \begin{bmatrix}\mathbf{H}_{r,k} \\ \mathbf{H}_{b,k} \\ \mathbf{H}_{x,k}\end{bmatrix} = \begin{bmatrix}\mathbf{H}_{proj,k}\,{}^{I_k}_{G}\hat{\mathbf{R}} \begin{bmatrix}\lfloor \left({}^G\hat{\mathbf{P}}_{\mathbf{f}} - {}^G\hat{\mathbf{P}}_{I_k}\right)\times\rfloor {}^{I_k}_{G}\hat{\mathbf{R}}^\top & \mathbf{0}_3 & \mathbf{0}_3 & \mathbf{0}_3 & -\mathbf{I}_3 & \mathbf{I}_3 \\ \mathbf{0}_{1\times 3} & \mathbf{0}_{1\times 3} & \mathbf{0}_{1\times 3} & \mathbf{0}_{1\times 3} & \mathbf{e}_1^\top & \mathbf{0}_{1\times 3}\end{bmatrix} \\ \mathbf{0}_{1\times 3} & \mathbf{0}_{1\times 3} & \mathbf{0}_{1\times 3} & \mathbf{0}_{1\times 3} & \mathbf{e}_1^\top & \mathbf{0}_{1\times 3}\end{bmatrix}$$
$$\Rightarrow \mathbf{H}_{I_k}\boldsymbol{\Phi}_{(k,1)} = \begin{bmatrix}\mathbf{H}_{proj,k}\,{}^{I_k}_{G}\hat{\mathbf{R}} \begin{bmatrix}\boldsymbol{\Gamma}_1 & \boldsymbol{\Gamma}_2 & \boldsymbol{\Gamma}_3 & \boldsymbol{\Gamma}_4 & -\mathbf{I}_3 & \mathbf{I}_3\end{bmatrix} \\ \begin{bmatrix}\mathbf{0}_{1\times 3} & \mathbf{0}_{1\times 3} & \mathbf{0}_{1\times 3} & \mathbf{0}_{1\times 3} & \mathbf{e}_1^\top & \mathbf{0}_{1\times 3}\end{bmatrix}\end{bmatrix} \tag{15}$$

where $\mathbf{H}_{x,k}$ is the measurement Jabocians for global x measurement. We can show that the system's unobservable directions now become:

$$\mathbf{N}_x = \begin{bmatrix}\mathbf{0}_{2\times 3} & \mathbf{0}_{2\times 3} & \mathbf{0}_{2\times 3} & \mathbf{0}_{2\times 3} & \begin{bmatrix}\mathbf{0}_{2\times 1} & \mathbf{I}_2\end{bmatrix} & \begin{bmatrix}\mathbf{0}_{2\times 1} & \mathbf{I}_2\end{bmatrix}\end{bmatrix}^\top \tag{16}$$

Compared to $\mathbf{N}$, both sensor's global translation in x direction and the rotation around the gravity direction become observable.

3.1.2 Global y Measurement

Similarly, if the sensor's translation in y direction is known, we have an additional measurement $z^{(y)} = \mathbf{e}_2^\top {}^G\mathbf{P}_I$. The system unobservable direction becomes $\mathbf{N}_y$. Translation in y direction and rotation around gravity direction both become observable:

$$\mathbf{N}_y = \begin{bmatrix}\mathbf{0}_{2\times 3} & \mathbf{0}_{2\times 3} & \mathbf{0}_{2\times 3} & \mathbf{0}_{2\times 3} & \begin{bmatrix}1 & 0 & 0 \\ 0 & 0 & 1\end{bmatrix} & \begin{bmatrix}1 & 0 & 0 \\ 0 & 0 & 1\end{bmatrix}\end{bmatrix}^\top \tag{17}$$

3.1.3 Global z Measurement

Following the similar steps, if the sensor's translation in z direction is directly measured, e.g., by a barometer, we have an additional measurement $z^{(z)} = \mathbf{e}_3^\top {}^G\mathbf{P}_I$. In this case, the block row of the observability matrix at time step k becomes:

$$\mathbf{H}_{I_k}\mathbf{\Phi}_{(k,1)} = \begin{bmatrix} \mathbf{H}_{proj,k}\, {}^{I_k}_{G}\hat{\mathbf{R}} \begin{bmatrix} \mathbf{\Gamma}_1 & \mathbf{\Gamma}_2 & \mathbf{\Gamma}_3 & \mathbf{\Gamma}_4 & -\mathbf{I}_3 & \mathbf{I}_3 \end{bmatrix} \\ \begin{bmatrix} \mathbf{0}_{1\times 3} & \mathbf{0}_{1\times 3} & \mathbf{0}_{1\times 3} & \mathbf{0}_{1\times 3} & \mathbf{e}_3^\top & \mathbf{0}_{1\times 3} \end{bmatrix} \end{bmatrix} \tag{18}$$

Since $\mathbf{e}_3$ is parallel to ${}^G\mathbf{g}$, then $\mathbf{e}_3^\top \lfloor {}^G\mathbf{P}_{I_1}\times \rfloor {}^G\mathbf{g} = 0$. Therefore, the system's unobservable directions become $\mathbf{N}_z$:

$$\mathbf{N}_z^\top = \begin{bmatrix} \mathbf{0}_{2\times 3} & \mathbf{0}_{2\times 3} & \mathbf{0}_{2\times 3} & \mathbf{0}_{2\times 3} & \begin{bmatrix} \mathbf{I}_2 & \mathbf{0}_{1\times 2} \end{bmatrix} & \begin{bmatrix} \mathbf{I}_2 & \mathbf{0}_{1\times 2} \end{bmatrix} \\ \left({}^{I_1}_{G}\hat{\mathbf{R}}\, {}^G\mathbf{g} \right)^\top & \mathbf{0}_{1\times 3} & \left(-\lfloor {}^G\hat{\mathbf{V}}_{I_1}\times \rfloor {}^G\mathbf{g} \right)^\top & \mathbf{0}_{1\times 3} & \left(-\lfloor {}^G\hat{\mathbf{P}}_{I_1}\times \rfloor {}^G\mathbf{g} \right)^\top & \left(-\lfloor {}^G\hat{\mathbf{P}}_{\mathbf{f}}\times \rfloor {}^G\mathbf{g} \right)^\top \end{bmatrix}$$

Clearly, only translation in z becomes observable, while, different from the cases with global x and y measurements, the rotation around gravity direction is still unobservable.

3.1.4 Global Orientation Measurement

If the aided INS is equipped with a magnetic compass, then we also have global orientation measurements given by $z^{(\mathbf{N})} = {}^I\mathbf{N}_n = {}^I_G\mathbf{R}\, {}^G\mathbf{N}_n$. In this case, the Jacobians and the block row of the observability matrix at time step k can be computed as:

$$\begin{aligned} \mathbf{H}_{I_k} &= \begin{bmatrix} \mathbf{H}_{r,k} \\ \mathbf{H}_{b,k} \\ \mathbf{H}_{\mathbf{N},k} \end{bmatrix} = \begin{bmatrix} \mathbf{H}_{proj,k}\, {}^{I_k}_{G}\hat{\mathbf{R}} \begin{bmatrix} \lfloor \left({}^G\hat{\mathbf{P}}_{\mathbf{f}} - {}^G\hat{\mathbf{P}}_{I_k} \right) \times \rfloor {}^{I_k}_{G}\hat{\mathbf{R}}^\top & \mathbf{0}_3 & \mathbf{0}_3 & \mathbf{0}_3 & -\mathbf{I}_3 & \mathbf{I}_3 \end{bmatrix} \\ {}^{I_k}_{G}\hat{\mathbf{R}} \begin{bmatrix} \lfloor {}^G\mathbf{N}_n \times \rfloor {}^{I_k}_{G}\hat{\mathbf{R}}^\top & \mathbf{0}_3 & \mathbf{0}_3 & \mathbf{0}_3 & \mathbf{0}_3 & \mathbf{0}_3 \end{bmatrix} \end{bmatrix} \\ \Rightarrow\ \mathbf{H}_{I_k}\mathbf{\Phi}_{(k,1)} &= \begin{bmatrix} \mathbf{H}_{proj,k}\, {}^{I_k}_{G}\hat{\mathbf{R}} \begin{bmatrix} \mathbf{\Gamma}_1 & \mathbf{\Gamma}_2 & \mathbf{\Gamma}_3 & \mathbf{\Gamma}_4 & -\mathbf{I}_3 & \mathbf{I}_3 \end{bmatrix} \\ {}^{I_k}_{G}\hat{\mathbf{R}} \begin{bmatrix} \lfloor {}^G\mathbf{N}_n \times \rfloor {}^{G}_{I_1}\hat{\mathbf{R}} & \mathbf{\Gamma}_5 & \mathbf{0}_3 & \mathbf{0}_3 & \mathbf{0}_3 & \mathbf{0}_3 \end{bmatrix} \end{bmatrix} \end{aligned} \tag{19}$$

where $\mathbf{H}_{\mathbf{N},k}$ is the Jacobians for orientation measurement, and $\mathbf{\Gamma}_5 = \lfloor {}^G\mathbf{N}_n \times \rfloor {}^{I_k}_{G}\hat{\mathbf{R}}^\top \mathbf{\Phi}_{12}$. If ${}^G\mathbf{N}_n$ is not parallel to ${}^G\mathbf{g}$, $\lfloor {}^G\mathbf{N} \times \rfloor {}^G\mathbf{g} \neq 0$. the rotation around the gravity direction becomes observable, and the unobservable directions become:

$$\mathbf{N}_n = \begin{bmatrix} \mathbf{0}_3 & \mathbf{0}_3 & \mathbf{0}_3 & \mathbf{0}_3 & \mathbf{I}_3 & \mathbf{I}_3 \end{bmatrix}^\top \tag{20}$$

3.1.5 Summary

In summary, as expected, global measurements will make the system more observable. If a global full position measurements by GPS or a prior map are available, the system will become fully observable, while global orientation measurements can make the rotation around gravitational direction observable, as long as this orientation is not parallel to the direction of gravity.

3.2 Degenerate Motion

In what follows, we further investigate degenerate motion for INS aided with generic range and bearing sensors, which is important for healthy estimators. In particular, as compared to [22] where pure translation or constant acceleration have been reported to be generated in VINS, we identify 2 more degenerate cases: pure rotation and translation towards a feature. To ease the analysis, we use range and bearing parameterization (i.e., spherical coordinates) of the point feature, instead of the conventional 3D Euclidean coordinates.

$$\mathbf{P}_{\mathbf{f}} = \begin{bmatrix} x_{\mathbf{f}} \\ y_{\mathbf{f}} \\ z_{\mathbf{f}} \end{bmatrix} = r_{\mathbf{f}}\mathbf{b}_{\mathbf{f}} = r_{\mathbf{f}} \begin{bmatrix} \cos\theta\cos\phi \\ \sin\theta\cos\phi \\ \sin\phi \end{bmatrix} \tag{21}$$

where $r_{\mathbf{f}}$ in the range, θ and ϕ represents the horizontal and elevation angle of point feature. With that, the state becomes:

$$\mathbf{x} = \begin{bmatrix} {}^I_G\bar{q}^\top & \mathbf{b}_{\mathbf{g}}^\top & {}^G\mathbf{V}_I^\top & \mathbf{b}_{\mathbf{a}}^\top & {}^G\mathbf{P}_I^\top & \begin{bmatrix} {}^G r_{\mathbf{f}} & {}^G\theta & {}^G\phi \end{bmatrix} \end{bmatrix}^\top \tag{22}$$

In this case, we can write the block row of the obsevability matrix as:

$$\begin{aligned}
&\mathbf{H}_{I_k} = \mathbf{H}_{proj,k}\,{}^{I_k}_{G}\hat{\mathbf{R}}\begin{bmatrix}\lfloor\left({}^{G}\hat{\mathbf{P}}_{\mathbf{f}} - {}^{G}\hat{\mathbf{P}}_{I_k}\right)\times\rfloor\,{}^{I_k}_{G}\hat{\mathbf{R}}^{\top} & \mathbf{0}_3 & \mathbf{0}_3 & \mathbf{0}_3 & -\mathbf{I}_3 & \begin{bmatrix}\frac{\partial {}^{G}\tilde{\mathbf{P}}_{\mathbf{f}}}{\partial {}^{G}\tilde{r}_{\mathbf{f}}} & \frac{\partial {}^{G}\tilde{\mathbf{P}}_{\mathbf{f}}}{\partial {}^{G}\tilde{\theta}_{\mathbf{f}}} & \frac{\partial {}^{G}\tilde{\mathbf{P}}_{\mathbf{f}}}{\partial {}^{G}\tilde{\phi}_{\mathbf{f}}}\end{bmatrix}\end{bmatrix}\\
&\Rightarrow\ \mathbf{H}_{I_k}\mathbf{\Phi}_{(k,1)} = \mathbf{H}_{b,k}\,{}^{I_k}_{G}\hat{\mathbf{R}}\begin{bmatrix}\mathbf{\Gamma_1} & \mathbf{\Gamma_2} & \mathbf{\Gamma_3} & \mathbf{\Gamma_4} & -\mathbf{I}_3 & \hat{\mathbf{b}}_{\mathbf{f}} & {}^{G}\hat{r}_{\mathbf{f}}\cos\hat{\phi}\hat{\mathbf{b}}_1^{\perp} & {}^{G}\hat{r}_{\mathbf{f}}\hat{\mathbf{b}}_2^{\perp}\end{bmatrix}
\end{aligned} \tag{23}$$

where

$$\begin{aligned}
\frac{\partial {}^{G}\tilde{\mathbf{P}}_{\mathbf{f}}}{\partial {}^{G}\tilde{r}_{\mathbf{f}}} &= \begin{bmatrix}\cos\hat{\theta}\cos\hat{\phi} & \sin\hat{\theta}\cos\hat{\phi} & \sin\hat{\phi}\end{bmatrix}^{\top} \triangleq \hat{\mathbf{b}}_{\mathbf{f}}\\
\frac{\partial {}^{G}\tilde{\mathbf{P}}_{\mathbf{f}}}{\partial {}^{G}\tilde{\theta}_{\mathbf{f}}} &= \begin{bmatrix}-\sin\hat{\theta} & \cos\hat{\theta} & 0\end{bmatrix}^{\top} {}^{G}\hat{r}_{\mathbf{f}}\cos\hat{\phi} \triangleq {}^{G}\hat{r}_{\mathbf{f}}\cos\hat{\phi}\hat{\mathbf{b}}_1^{\perp}\\
\frac{\partial {}^{G}\tilde{\mathbf{P}}_{\mathbf{f}}}{\partial {}^{G}\tilde{\phi}_{\mathbf{f}}} &= \begin{bmatrix}-\cos\hat{\theta}\sin\hat{\phi} & -\sin\hat{\theta}\sin\hat{\phi} & \cos\hat{\phi}\end{bmatrix}^{\top} {}^{G}\hat{r}_{\mathbf{f}} \triangleq {}^{G}\hat{r}_{\mathbf{f}}\hat{\mathbf{b}}_2^{\perp}
\end{aligned}$$

By inspection, the unobservable directions are given by:

$$\mathbf{N}_{rb} = \begin{bmatrix}\mathbf{N}_{rb,p}^{\top} & \mathbf{N}_{rb,r}^{\top}\end{bmatrix}^{\top} = \begin{bmatrix}\mathbf{0}_3 & \mathbf{0}_3 & \mathbf{0}_3 & \mathbf{0}_3 & \mathbf{I}_3 & \hat{\mathbf{b}}_{\mathbf{f}} & \frac{1}{{}^{G}\hat{r}_{\mathbf{f}}\cos\hat{\phi}}\hat{\mathbf{b}}_1^{\perp} & \frac{1}{{}^{G}\hat{r}_{\mathbf{f}}}\hat{\mathbf{b}}_2^{\perp}\\ \left({}^{I_1}_{G}\hat{\mathbf{R}}\,{}^{G}\mathbf{g}\right)^{\top} & \mathbf{0}_{1\times 3} & -\left(\lfloor {}^{G}\hat{\mathbf{V}}_{I_1}\times\rfloor\,{}^{G}\mathbf{g}\right)^{\top} & \mathbf{0}_{1\times 3} & -\left(\lfloor {}^{G}\hat{\mathbf{P}}_{I_1}\times\rfloor\,{}^{G}\mathbf{g}\right)^{\top} & 0 & g & 0\end{bmatrix}^{\top}$$

where $g = \|{}^{G}\mathbf{g}\|$, $\mathbf{N}_{rb,p}$ and $\mathbf{N}_{rb,r}$ denote the unobservable directions related to the global translation and global rotation around the gravity direction, which as expected agrees with the preceding analysis.

3.2.1 Pure Translation

If the sensor undergoes pure translation, the system gain additional unobservable directions:

$$\mathbf{N}_R = \begin{bmatrix}{}^{I_1}_{G}\hat{\mathbf{R}}^{\top} & \mathbf{0}_3 & -\left(\lfloor {}^{G}\hat{\mathbf{V}}_{I_1}\times\rfloor\right)^{\top} & -\left({}^{I_1}_{G}\hat{\mathbf{R}}\lfloor {}^{G}\mathbf{g}\times\rfloor\right)^{\top} & -\left(\lfloor {}^{G}\hat{\mathbf{P}}_{I_1}\times\rfloor\right)^{\top} & -\mathbf{\Theta}^{\top}\end{bmatrix}^{\top} \tag{24}$$

where $\mathbf{\Theta} = \begin{bmatrix}0 & 0 & 0\\ {}^{G}\hat{r}_{\mathbf{f}}\cos\hat{\theta}\tan\hat{\phi} & \sin\hat{\theta}\tan\hat{\phi} & -1\\ -{}^{G}\hat{r}_{\mathbf{f}}\sin\hat{\theta} & \cos\hat{\theta} & 0\end{bmatrix}$. Similar to [22], this unobservable direction can be easily verified as follows:

$$\mathbf{H}_{I_k}\mathbf{\Phi}(k,1)\mathbf{N}_R = \mathbf{H}_{proj,k}\,{}^{I_k}_{G}\hat{\mathbf{R}}\left(\mathbf{\Gamma_4}\,{}^{I_1}_{G}\hat{\mathbf{R}} - \frac{1}{2}\delta t_k^2\mathbf{I}_3\right)\lfloor {}^{G}\mathbf{g}\times\rfloor = \mathbf{0} \tag{25}$$

From $\mathbf{\Theta}$ we see that this unobservable direction only relates to the bearing of the feature, since the first row of $\mathbf{\Theta}$ are all zeros. This indicates that the global rotation of the sensor all becomes unobservable, rather than only global yaw unobservable for general motion. It is important to note that no assumption is made about sensors used in this analysis.

3.2.2 Pure Rotation

If sensor has only rotational motion, then ${}^{G}\mathbf{P}_{I_k} = \mathbf{0}_{3\times 1}$ and we have ${}^{I_k}\mathbf{P}_{\mathbf{f}} = {}^{I_k}_{G}\mathbf{R}\,{}^{G}\mathbf{P}_{\mathbf{f}}$. For mono-camera, the system will gain one more unobservable direction corresponding to the feature's range:

$$\mathbf{N}_1 = \begin{bmatrix}\mathbf{0}_{1\times 3} & \mathbf{0}_{1\times 3} & \mathbf{0}_{1\times 3} & \mathbf{0}_{1\times 3} & \mathbf{0}_{1\times 3} & 1 & 0 & 0\end{bmatrix}^{\top} \tag{26}$$

Since a mono-camera provides only bearing measurements, $\mathbf{H}_{proj,k} = \mathbf{H}_{b,k}$. In this case, we have:

$$\mathbf{H}_{I_k}\mathbf{\Phi}_{(k,1)}\mathbf{N}_1 = \mathbf{H}_{b,k}\,{}^{I}\hat{\mathbf{b}}_{\mathbf{f}} = \mathbf{H}_{b,k}\,{}^{I}_{G}\hat{\mathbf{R}}\,{}^{G}\hat{\mathbf{b}}_{\mathbf{f}} = \mathbf{0}$$

Therefore, we have one more unobservable direction related to the scale of the feature.

3.2.3 Moving Toward a Feature

If the mono-camera is moving towards a feature, then the system will also gain one more unobservable direction related to this feature scale:

$$\mathbf{N}_1 = \begin{bmatrix} \mathbf{0}_{1\times 3} & \mathbf{0}_{1\times 3} & \mathbf{0}_{1\times 3} & \mathbf{0}_{1\times 3} & \mathbf{0}_{1\times 3} & 1 & 0 & 0 \end{bmatrix}^\top \tag{27}$$

This degenerate motion indicates that the sensor is moving along the direction of the feature's bearing direction, that is: ${}^G\mathbf{P}_{I_k} = \alpha {}^G\mathbf{b_f}$, with α denotes the scale of the sensor's motion. Then, we can arrive at:

$${}^{I_k}\mathbf{P_f} = {}^{I_k} r_{\mathbf{f}} {}^{I_k}\mathbf{b_f} = {}^{I_k}_{G}\mathbf{R}\left({}^G\mathbf{P_f} - {}^G\mathbf{P}_{I_k}\right) = {}^{I_k}_{G}\mathbf{R}\left({}^G r_{\mathbf{f}} - \alpha\right){}^G\mathbf{b_f} \tag{28}$$

Similar to the pure rotation, we can show the additional unobservable direction $\mathbf{N}_1$ based on the following:

$$\mathbf{H}_{b,k}\mathbf{\Phi}_{(k,1)}\mathbf{N}_1 = \frac{{}^I\hat{r}_{\mathbf{f}}}{{}^G\hat{r}_{\mathbf{f}} - \alpha}\mathbf{H}_{b,k}{}^I_G\hat{\mathbf{R}}{}^G\hat{\mathbf{b}}_{\mathbf{f}} = \mathbf{0}_{2\times 1}$$

3.2.4 Constant Acceleration

If the mono-camera moves with constant local acceleration, i.e., ${}^I\mathbf{a}$ is constant, then the system will have one more unobservable direction given by:

$$\mathbf{N}_a = \begin{bmatrix} \mathbf{0}_{1\times 3} & \mathbf{0}_{1\times 3} & {}^G\hat{\mathbf{V}}_{I_1} & -{}^I\hat{\mathbf{a}} & {}^G\hat{\mathbf{P}}_{I_1} & {}^G\hat{r}_{\mathbf{f}} & 0 & 0 \end{bmatrix} \tag{29}$$

To see this, we have:

$$\mathbf{H}_{I_k}\mathbf{\Phi}_{(k,1)}\mathbf{N}_a = \mathbf{H}_{b,k}{}^{I_k}_{G}\hat{\mathbf{R}}\left(-{}^G\hat{\mathbf{V}}_{I_1}\delta t_k - \mathbf{\Gamma_4}{}^I\hat{\mathbf{a}} - {}^G\hat{\mathbf{P}}_{I_1} + {}^G r_{\mathbf{f}}{}^G\hat{\mathbf{b}}_{\mathbf{f}}\right) \tag{30}$$

Based on [22], we know:

$$\mathbf{\Gamma_4}{}^I\mathbf{a} = {}^G\hat{\mathbf{P}}_{I_k} - {}^G\hat{\mathbf{P}}_{I_1} - {}^G\hat{\mathbf{V}}_{I_1}\delta t_k \tag{31}$$

Therefore, we arrive at:

$$\mathbf{H}_{I_k}\mathbf{\Phi}_{(k,1)}\mathbf{N}_a = \mathbf{H}_{b,k}{}^{I_k}_{G}\hat{\mathbf{R}}\left({}^G\hat{\mathbf{P}}_{\mathbf{f}} - {}^G\hat{\mathbf{P}}_{I_k}\right) = \mathbf{H}_{b,k}{}^{I_k}\hat{\mathbf{P}}_{\mathbf{f}} = \mathbf{0}_{2\times 1} \tag{32}$$

Clearly, this null space is only related to the scale; thus, if we use sensors such as stereo and RGBD cameras that can recover the scale, this unobservable direction will disappear.

4 Observability Analysis of Aided INS with Line Features

As navigating in structured environments, line features can be used in the aided INS to provide more compact information. Thus, in this section, we perform observability analysis for the aided INS with line features to provide insights for building consistent estimators.

4.1 Line Representation

Inspired by [26], we propose to use the Plücker representation for the line feature in the state vector while *orthonormal representation* (which is minimal) for the error state. The Plücker representation can be initialized by the two end points $\mathbf{P}_{L_1}$ and $\mathbf{P}_{L_2}$ of a line segment L, as:

$$\mathbf{L} = \begin{bmatrix} \lfloor \mathbf{P}_{L_1} \times \rfloor \mathbf{P}_{L_2} \\ \mathbf{P}_{L_2} - \mathbf{P}_{L_1} \end{bmatrix} = \begin{bmatrix} \mathbf{n}_L \\ \mathbf{v}_L \end{bmatrix} \tag{33}$$

where $\mathbf{n}_L$ and $\mathbf{v}_L$ are the normal vector and direction vector for the line $\mathbf{L}$. We need a minimal parameterization for line update. Based on (33), we have:

$$\mathbf{L} = \begin{bmatrix} \mathbf{n}_L | \mathbf{v}_L \end{bmatrix} = \begin{bmatrix} \frac{\mathbf{n}_L}{\|\mathbf{n}_L\|} & \frac{\mathbf{v}_L}{\|\mathbf{v}_L\|} & \frac{\mathbf{n}_L \times \mathbf{v}_L}{\|\mathbf{n}_L \times \mathbf{v}_L\|} \end{bmatrix} \begin{bmatrix} \|\mathbf{n}_L\| & 0 \\ 0 & \|\mathbf{v}_L\| \\ 0 & 0 \end{bmatrix} \tag{34}$$

where we can define:

$$\mathbf{R}_L(\boldsymbol{\theta}_L) = \exp(-\lfloor \boldsymbol{\theta}_L \times \rfloor) = \begin{bmatrix} \frac{\mathbf{n}_L}{\|\mathbf{n}_L\|} & \frac{\mathbf{v}_L}{\|\mathbf{v}_L\|} & \frac{\mathbf{n}_L \times \mathbf{v}_L}{\|\mathbf{n}_L \times \mathbf{v}_L\|} \end{bmatrix} \tag{35}$$

$$\mathbf{W}_L(\phi_L) = \frac{1}{\sqrt{w_1^2 + w_2^2}} \begin{bmatrix} w_1 & -w_2 \\ w_2 & w_1 \end{bmatrix} = \eta \begin{bmatrix} \|\mathbf{n}_L\| & -\|\mathbf{v}_L\| \\ \|\mathbf{v}_L\| & \|\mathbf{n}_L\| \end{bmatrix} \tag{36}$$

where $w_1 = \left\|{}^G\mathbf{n}_L\right\|$, $w_2 = \left\|{}^G\mathbf{v}_L\right\|$ and $\eta = \frac{1}{\sqrt{w_1^2+w_2^2}}$. Since $\mathbf{R}_L \in \mathbf{SO}(3)$ and $\mathbf{W}_L \in \mathbf{SO}(2)$, we can define the error state for these parameters as $\delta\boldsymbol{\theta}_L$ and $\delta\phi_L$ (from $\mathbf{R}_L$ and $\mathbf{W}_L$), respectively. With that, the state can be written as:

$$\mathbf{x} = \begin{bmatrix} {}^I_G\bar{q}^\top & \mathbf{b}_\mathbf{g}^\top & {}^G\mathbf{V}_I^\top & \mathbf{b}_\mathbf{a}^\top & {}^G\mathbf{P}_I^\top & {}^G\mathbf{L}^\top \end{bmatrix}^\top$$

where ${}^G\mathbf{L} = \begin{bmatrix} {}^G\mathbf{n}_L^\top & {}^G\mathbf{v}_L^\top \end{bmatrix}^\top$ and ${}^G\tilde{\mathbf{L}} = \begin{bmatrix} \delta\boldsymbol{\theta}_L^\top & \delta\phi_L^\top \end{bmatrix}^\top$. Their related Jacobians can be seen in Appendix B.

4.2 Observability Analysis: Single Line

Without loss of generality, we consider stereo images are available for detecting and tracking line features. Measurements for the line are given by the distance of the two end points $\mathbf{x}_s$ and $\mathbf{x}_e$ to the line [28]:

$$\mathbf{z} = \begin{bmatrix} \frac{\mathbf{x}_s^\top \mathbf{l}'}{\sqrt{l_1^2+l_2^2}} & \frac{\mathbf{x}_e^\top \mathbf{l}'}{\sqrt{l_1^2+l_2^2}} \end{bmatrix}^\top \tag{37}$$

where we have used:

$${}^I\mathbf{L} = {}^I_G\mathbf{H}\,{}^G\mathbf{L} = \begin{bmatrix} {}^I_G\mathbf{R} & -{}^I_G\mathbf{R}\lfloor {}^G\mathbf{P}_I \times \rfloor \\ \mathbf{0}_3 & {}^I_G\mathbf{R} \end{bmatrix} {}^G\mathbf{L}$$

$$\mathbf{l}' = \begin{bmatrix} \mathbf{K} & \mathbf{0}_3 \end{bmatrix} {}^I\mathbf{L} = \begin{bmatrix} f_2 & 0 & 0 \\ 0 & f_1 & 0 \\ -f_2 c_1 & -f_1 c_2 & f_1 f_2 \end{bmatrix} {}^I\mathbf{n}_L = \begin{bmatrix} l_1 \\ l_2 \\ l_3 \end{bmatrix}$$

With the line measurements, we compute line measurement Jacobians and the block row of the observability matrix at time step k as follows:

$$\frac{\partial \tilde{\mathbf{z}}}{\partial \tilde{\mathbf{x}}} = \frac{\partial \tilde{\mathbf{z}}}{\partial \tilde{\mathbf{l}}'} \mathbf{K}^I_G\hat{\mathbf{R}} \begin{bmatrix} \left(\lfloor {}^G\hat{\mathbf{n}}_L \times \rfloor - \lfloor \lfloor {}^G\hat{\mathbf{P}}_I \times \rfloor {}^G\hat{\mathbf{v}}_L \times \rfloor \right) {}^I_G\hat{\mathbf{R}}^\top & \mathbf{0}_{3\times 9} & \lfloor {}^G\hat{\mathbf{v}}_L \times \rfloor & \boldsymbol{\Gamma}_{l4} & \boldsymbol{\Gamma}_{l5} \end{bmatrix}$$

$$\mathbf{H}_{I_k}\boldsymbol{\Phi}_{(k,1)} = \frac{\partial \tilde{\mathbf{z}}}{\partial \tilde{\mathbf{l}}'} \mathbf{K}^{I_k}_G\hat{\mathbf{R}} \begin{bmatrix} \boldsymbol{\Gamma}_{l1} & \boldsymbol{\Gamma}_{l2} & \lfloor {}^G\hat{\mathbf{v}}_L \times \rfloor \delta t_k & \boldsymbol{\Gamma}_{l3} & \lfloor {}^G\hat{\mathbf{v}}_L \times \rfloor & \boldsymbol{\Gamma}_{l4} & \boldsymbol{\Gamma}_{l5} \end{bmatrix}$$

where $\boldsymbol{\Gamma}_i, i \in \{i \dots 5\}$ are derived as:

$$\begin{aligned}
\boldsymbol{\Gamma}_{l1} &= (\lfloor {}^G\hat{\mathbf{n}}_L \times \rfloor - \lfloor \lfloor {}^G\hat{\mathbf{P}}_{I_k} \times \rfloor {}^G\hat{\mathbf{v}}_L \times \rfloor + \lfloor {}^G\hat{\mathbf{v}}_L \times \rfloor \lfloor {}^G\hat{\mathbf{P}}_{I_1} \times \rfloor + \lfloor {}^G\hat{\mathbf{v}}_L \times \rfloor \lfloor {}^G\hat{\mathbf{V}}_{I_1} \times \rfloor \delta t_k - \frac{1}{2} \lfloor {}^G\hat{\mathbf{v}}_L \times \rfloor \lfloor {}^G\hat{\mathbf{g}} \times \rfloor \delta t_k^2 \\
&\quad - \lfloor {}^G\hat{\mathbf{v}}_L \times \rfloor \lfloor {}^G\hat{\mathbf{P}}_{I_k} \times \rfloor) {}^G_{I_1}\hat{\mathbf{R}} \\
\boldsymbol{\Gamma}_{l2} &= \left(\lfloor {}^G\hat{\mathbf{n}}_L \times \rfloor - \lfloor \lfloor {}^G\hat{\mathbf{P}}_{I_k} \times \rfloor {}^G\hat{\mathbf{v}}_L \times \rfloor \right) {}^{I_k}_G\hat{\mathbf{R}}^\top \boldsymbol{\Phi}_{12} + \lfloor {}^G\hat{\mathbf{v}}_L \times \rfloor \boldsymbol{\Phi}_{52} \\
\boldsymbol{\Gamma}_{l3} &= \lfloor {}^G\hat{\mathbf{v}}_L \times \rfloor \boldsymbol{\Phi}_{54} \\
\boldsymbol{\Gamma}_{l4} &= \lfloor {}^G\hat{\mathbf{n}}_L \times \rfloor - \lfloor {}^G\hat{\mathbf{P}}_{I_k} \times \rfloor \lfloor {}^G\hat{\mathbf{v}}_L \times \rfloor \\
\boldsymbol{\Gamma}_{l5} &= -\left(\frac{w_2}{w_1} {}^G\hat{\mathbf{n}}_L + \frac{w_1}{w_2} \lfloor {}^G\hat{\mathbf{P}}_{I_k} \times \rfloor {}^G\hat{\mathbf{v}}_L \right)
\end{aligned}$$

We also define $e_1 = \mathbf{x}_s^\top \mathbf{l}'$, $e_2 = \mathbf{x}_e^\top \mathbf{l}'$, $l_n = \sqrt{(l_1^2 + l_2^2)}$, $\mathbf{x}_s = [u_1, v_1, 1]^\top$ and $\mathbf{x}_e = [u_2, v_2, 1]^\top$. With these, we have:

$$\frac{\partial \tilde{\mathbf{z}}}{\partial \tilde{\mathbf{l}}'} = \frac{1}{l_n} \begin{bmatrix} u_1 - \frac{l_1 e_1}{l_n^2} & v_1 - \frac{l_2 e_1}{l_n^2} & 1 \\ u_2 - \frac{l_1 e_2}{l_n^2} & v_2 - \frac{l_2 e_2}{l_n^2} & 1 \end{bmatrix} \tag{38}$$

It can be shown that the linearized aided INS system with a line feature will have at least 5 unobservable directions:

$$\begin{aligned}\mathbf{N}_l &= \begin{bmatrix}\mathbf{N}_{l1} & \mathbf{N}_{l2} & \mathbf{N}_{l3} & \mathbf{N}_{l4} & \mathbf{N}_{l5}\end{bmatrix} \\ &= \begin{bmatrix} {}^{I_1}_{G}\hat{\mathbf{R}}{}^{G}\mathbf{g} & \mathbf{0}_{3\times1} & \mathbf{0}_{3\times1} & \mathbf{0}_{3\times1} & \mathbf{0}_{3\times1} \\ \mathbf{0}_{3\times1} & \mathbf{0}_{3\times1} & \mathbf{0}_{3\times1} & \mathbf{0}_{3\times1} & \mathbf{0}_{3\times1} \\ -\lfloor {}^{G}\hat{\mathbf{V}}_{I_1}\times\rfloor {}^{G}\mathbf{g} & \mathbf{0}_{3\times1} & \mathbf{0}_{3\times1} & \mathbf{0}_{3\times1} & {}^{G}\hat{\mathbf{v}}_{\mathbf{e}} \\ \mathbf{0}_{3\times1} & \mathbf{0}_{3\times1} & \mathbf{0}_{3\times1} & \mathbf{0}_{3\times1} & \mathbf{0}_{3\times1} \\ -\lfloor {}^{G}\hat{\mathbf{P}}_{I_1}\times\rfloor {}^{G}\mathbf{g} & {}^{G}\hat{\mathbf{n}}_{\mathbf{e}} & {}^{G}\hat{\mathbf{v}}_{\mathbf{e}} & \lfloor {}^{G}\hat{\mathbf{n}}_{\mathbf{e}}\times\rfloor {}^{G}\hat{\mathbf{v}}_{\mathbf{e}} & \mathbf{0}_{3\times1} \\ -{}^{G}\mathbf{g} & \frac{w_2}{w_1}{}^{G}\hat{\mathbf{v}}_{\mathbf{e}}^{\top} & \mathbf{0}_{3\times1} & \mathbf{0}_{3\times1} & \mathbf{0}_{3\times1} \\ 0 & 0 & 0 & \eta^2 w_2^2 & 0 \end{bmatrix}\end{aligned} \tag{39}$$

where ${}^{G}\hat{\mathbf{n}}_{\mathbf{e}}$ and ${}^{G}\hat{\mathbf{v}}_{\mathbf{e}}$ is the unit direction for ${}^{G}\hat{\mathbf{n}}_{L}$ and ${}^{G}\hat{\mathbf{v}}_{L}$, respectively. For $\mathbf{N}_{l1}$, we have:

$$\mathbf{H}_{I_k}\mathbf{\Phi}_{k,1}\mathbf{N}_{l1} = \frac{\partial\tilde{\mathbf{z}}}{\partial\tilde{\mathbf{l}}'}\mathbf{K}^{I_k}_{G}\hat{\mathbf{R}}\left(\lfloor {}^{G}\mathbf{g}\times\rfloor\lfloor {}^{G}\hat{\mathbf{P}}_{I_k}\times\rfloor {}^{G}\hat{\mathbf{v}}_{L} + \lfloor {}^{G}\hat{\mathbf{v}}_{L}\rfloor\lfloor {}^{G}\mathbf{g}\times\rfloor {}^{G}\hat{\mathbf{P}}_{I_k} + \lfloor {}^{G}\hat{\mathbf{P}}_{I_k}\times\rfloor\lfloor {}^{G}\hat{\mathbf{v}}_{L}\times\rfloor {}^{G}\hat{\mathbf{g}}\right) = \mathbf{0} \tag{40}$$

And for $\mathbf{N}_{l4}$, we have:

$$\mathbf{H}_{I_k}\mathbf{\Phi}_{k,1}\mathbf{N}_{l4} = -\frac{w_1 w_2^2}{w_1^2+w_2^2}\frac{\partial\tilde{\mathbf{z}}}{\partial\tilde{\mathbf{l}}'}\mathbf{K}\underbrace{{}^{I_k}_{G}\hat{\mathbf{R}}\lfloor\left(\frac{w_1}{w_2}\lfloor {}^{G}\hat{\mathbf{n}}_{e}\times\rfloor {}^{G}\mathbf{v}_{e} + {}^{G}\mathbf{P}_{I_k}\right)\times\rfloor {}^{G}\hat{\mathbf{v}}_{e}}_{{}^{I_k}\mathbf{n}'_{L}} \tag{41}$$

According to geometrical analysis, ${}^{I_k}\mathbf{n}'_{L}$ is parallel to ${}^{I_k}\mathbf{n}_{L}$. Since $\mathbf{l} = \mathbf{K}^{I_k}\mathbf{n}_{L}$ is null space of $\frac{\partial\tilde{\mathbf{z}}}{\partial\tilde{\mathbf{l}}'}$, therefore, $\mathbf{K}^{I_k}\mathbf{n}'_{L}$ is also the null space of $\frac{\partial\tilde{\mathbf{z}}}{\partial\tilde{\mathbf{l}}'}$. Then, we can have $\mathbf{H}_{I_k}\mathbf{\Phi}_{k,1}\mathbf{N}_{l4} = \mathbf{0}$. Note that $\mathbf{N}_{l1}$ relates to the rotation around the gravitational direction, $\mathbf{N}_{l2:4}$ relates to the sensor's global translation, while $\mathbf{N}_{l5}$ relates to the sensor motion along the line direction. The above analysis are based on projection model. Hence, for completeness, a direct line measurement model is also considered in Appendix C .

4.3 Observability Analysis: Multiple Lines

Assuming there are $m > 1$ un-parallel lines in the state vector, we define the orientation ${}^{G}_{L_i}\mathbf{R}$ of a line i and the rotation ${}^{Li}_{Lj}\mathbf{R}$ between line i and line j ($i, j \in \{1, \dots m\}$) as:

$${}^{G}_{Li}\hat{\mathbf{R}} = \begin{bmatrix} {}^{G}\hat{\mathbf{n}}_{\mathbf{e}i} & {}^{G}\hat{\mathbf{v}}_{\mathbf{e}i} & \lfloor {}^{G}\hat{\mathbf{n}}_{\mathbf{e}i}\times\rfloor {}^{G}\hat{\mathbf{v}}_{\mathbf{e}i}\end{bmatrix} \tag{42}$$

$${}^{Li}_{Lj}\hat{\mathbf{R}} = {}^{G}_{Li}\hat{\mathbf{R}}^{\top}{}^{G}_{Lj}\hat{\mathbf{R}} \tag{43}$$

We have for the first time proved that the system has at least 4 unobservable directions:

Lemma 4.1. *For the aided INS with $m > 1$ un-parallel line features in the state vector, the system will have*

at least 4 unobservable directions given by:

$$\mathbf{N}_L = \begin{bmatrix} \mathbf{N}_{L1} & \mathbf{N}_{L2:4} \end{bmatrix} \tag{44}$$

$$= \begin{bmatrix} {}^{I_1}_{G}\hat{\mathbf{R}}\,{}^{G}\mathbf{g} & \mathbf{0}_3 \\ \mathbf{0}_{3\times 1} & \mathbf{0}_3 \\ -\lfloor {}^{G}\hat{\mathbf{V}}_{I_1}\times \rfloor {}^{G}\mathbf{g} & \mathbf{0}_3 \\ \mathbf{0}_{1\times 3} & \mathbf{0}_3 \\ -\lfloor {}^{G}\hat{\mathbf{P}}_{I_1}\times \rfloor {}^{G}\mathbf{g} & {}^{G}_{Li}\hat{\mathbf{R}} \\ -{}^{G}\mathbf{g} & \frac{w_{12}}{w_{11}}\,{}^{G}\hat{\mathbf{v}}_{\mathbf{e}1}\mathbf{e}_1^{\top}\,{}^{L1}_{Li}\hat{\mathbf{R}} \\ 0 & \eta_1^2 w_{12}^2 \mathbf{e}_3^{\top}\,{}^{L1}_{Li}\hat{\mathbf{R}} \\ \vdots & \vdots \\ -{}^{G}\mathbf{g} & \frac{w_{i-1,2}}{w_{i-1,1}}\,{}^{G}\hat{\mathbf{v}}_{\mathbf{e}i-1}\mathbf{e}_1^{\top}\,{}^{Li-1}_{Li}\hat{\mathbf{R}} \\ 0 & \eta_{i-1}^2 w_{i-1,2}^2 \mathbf{e}_3^{\top}\,{}^{Li-1}_{Li}\hat{\mathbf{R}} \\ -{}^{G}\mathbf{g} & \frac{w_{i,2}}{w_{i,1}}\,{}^{G}\hat{\mathbf{v}}_{\mathbf{e}i}\mathbf{e}_1^{\top} \\ 0 & \eta_i^2 w_{i,2}^2 \mathbf{e}_3^{\top} \\ -{}^{G}\mathbf{g} & \frac{w_{i+1,2}}{w_{i+1,1}}\,{}^{G}\hat{\mathbf{v}}_{\mathbf{e}i+1}\mathbf{e}_1^{\top}\,{}^{Li}_{Li+1}\hat{\mathbf{R}}^{\top} \\ 0 & \eta_{i+1}^2 w_{i+1,2}^2 \mathbf{e}_3^{\top}\,{}^{Li}_{Li+1}\hat{\mathbf{R}}^{\top} \\ \vdots & \vdots \\ -{}^{G}\mathbf{g} & \frac{w_{m,2}}{w_{m,1}}\,{}^{G}\hat{\mathbf{v}}_{\mathbf{e}m}\mathbf{e}_1^{\top}\,{}^{Li}_{Lm}\hat{\mathbf{R}}^{\top} \\ 0 & \eta_m^2 w_{m,2}^2 \mathbf{e}_3^{\top}\,{}^{Li}_{Lm}\hat{\mathbf{R}}^{\top} \end{bmatrix}$$

where $i \in \{1 \dots m\}$

Proof. See Appendix D. □

5 Observability Analysis of Aided INS with Plane Features

In analogy to the case of line features, in this section we extend the observability analysis to the aided INS with plane features. In particular, for any point $\mathbf{P_f}$ in a plane $\mathbf{\Pi}$, we have $\mathbf{n}_\Pi^\top \mathbf{P_f} + d = 0$, where $\mathbf{n}_\Pi$ is the norm direction of this plane and d is a scalar containing the range information from the origin to plane $\mathbf{\Pi}$. Hence, plane $\mathbf{\Pi}$ can be represented as:

$$\mathbf{\Pi} = \begin{bmatrix} \mathbf{n}_\Pi^\top & d \end{bmatrix}^\top \tag{45}$$

We still need a minimal error state representation for plane update. Notice that a horizontal angle θ and elevation angle ϕ can be used to describe the normal direction $\mathbf{n}_\Pi$ as:

$$\mathbf{n}_\Pi = \begin{bmatrix} n_1 \\ n_2 \\ n_3 \end{bmatrix} = \begin{bmatrix} \cos\theta\cos\phi \\ \sin\theta\cos\phi \\ \sin\phi \end{bmatrix} \tag{46}$$

Thus, the error state for the plane can be denoted as $\tilde{\mathbf{\Pi}} = \begin{bmatrix} \tilde{\theta} & \tilde{\phi} & \tilde{d} \end{bmatrix}^\top$. Accordingly, the state vector of the system with one plane feature becomes:

$$\mathbf{x} = \begin{bmatrix} {}^{I}_{G}\bar{q}^\top & \mathbf{b}_\mathbf{g}^\top & {}^{G}\mathbf{V}_I^\top & \mathbf{b}_\mathbf{a}^\top & {}^{G}\mathbf{P}_I^\top & {}^{G}\mathbf{\Pi}^\top \end{bmatrix}^\top \tag{47}$$

5.1 Observability Analysis: Single Plane

Plane features can be extracted from point cloud (of RGBD and stereo cameras and 3D LiDAR), the corresponding plane measurements are given by:

$$\mathbf{z} = \begin{bmatrix} {}^{I}\theta \\ {}^{I}\phi \\ {}^{I}d \end{bmatrix} \tag{48}$$

The measurement Jacobian w.r.t. the plane can be computed as follows:

$$\mathbf{H}_{\Pi} = \frac{\partial \tilde{z}}{\partial \mathbf{\Pi}} = \begin{bmatrix} -\frac{\hat{n}_2}{\hat{n}_1^2+\hat{n}_2^2} & \frac{\hat{n}_1}{\hat{n}_1^2+\hat{n}_2^2} & 0 & 0 \\ -\frac{\hat{n}_1\hat{n}_3}{\sqrt{\hat{n}_1^2+\hat{n}_2^2}} & -\frac{\hat{n}_2\hat{n}_3}{\sqrt{\hat{n}_1^2+\hat{n}_2^2}} & \sqrt{\hat{n}_1^2+\hat{n}_2^2} & 0 \\ 0 & 0 & 0 & 1 \end{bmatrix} \tag{49}$$

Hence, we get the measurement Jacobians w.r.t. the state $\mathbf{x}$ as:

$$\begin{aligned} \frac{\partial \tilde{\mathbf{z}}}{\partial \tilde{\mathbf{x}}} &= \mathbf{H}_{\Pi} \begin{bmatrix} \lfloor {}^{I}_{G}\hat{\mathbf{R}}\, {}^{G}\hat{\mathbf{n}}_{\Pi} \times \rfloor & \mathbf{0}_3 & \mathbf{0}_3 & \mathbf{0}_3 & \mathbf{0}_3 & {}^{I}_{G}\hat{\mathbf{R}}\, {}^{G}\hat{\mathbf{n}}_1^{\perp} \cos\hat{\phi} & {}^{I}_{G}\hat{\mathbf{R}}\, {}^{G}\hat{\mathbf{n}}_2^{\perp} & \mathbf{0}_{3\times 1} \\ \mathbf{0}_{1\times 3} & \mathbf{0}_{1\times 3} & \mathbf{0}_{1\times 3} & \mathbf{0}_{1\times 3} & {}^{G}\hat{\mathbf{n}}_{\Pi}^{\top} & {}^{G}\hat{\mathbf{P}}_I^{\top}\, {}^{G}\hat{\mathbf{n}}_1^{\perp} \cos\hat{\phi} & {}^{G}\hat{\mathbf{P}}_I^{\top}\, {}^{G}\hat{\mathbf{n}}_2^{\perp} & 1 \end{bmatrix} \\ \Rightarrow\ \mathbf{H}_{I_k}\mathbf{\Phi}_{(k,1)} &= \mathbf{H}_{\Pi} \begin{bmatrix} \mathbf{\Gamma}_{\Pi 1} & \mathbf{\Gamma}_{\Pi 2} & \begin{bmatrix} \mathbf{0}_3 \\ {}^{G}\hat{\mathbf{n}}_{\Pi}^{\top}\delta t_k \end{bmatrix} & \mathbf{\Gamma}_{\Pi 3} & \begin{bmatrix} \mathbf{0}_3 \\ {}^{G}\hat{\mathbf{n}_{\Pi}}^{\top} \end{bmatrix} & \mathbf{\Gamma}_{\Pi 4} \end{bmatrix} \end{aligned}$$

where:

$$\begin{aligned} \mathbf{\Gamma}_{\Pi 1} &= \begin{bmatrix} {}^{I_k}_{G}\hat{\mathbf{R}} \lfloor {}^{G}\hat{\mathbf{n}}_{\Pi} \times \rfloor \\ {}^{G}\mathbf{n}_{\Pi}^{\top} \lfloor \left({}^{G}\hat{\mathbf{P}}_{I_1} + {}^{G}\hat{\mathbf{V}}_{I_1}\delta t_k - \frac{1}{2}{}^{G}\mathbf{g}\delta t_k^2 - {}^{G}\hat{\mathbf{P}}_{I_k} \right) \times \rfloor \end{bmatrix} {}^{G}_{I_1}\hat{\mathbf{R}} \\ \mathbf{\Gamma}_{\Pi 2} &= \begin{bmatrix} {}^{I_k}_{G}\hat{\mathbf{R}} \lfloor {}^{G}\hat{\mathbf{n}}_{\Pi} \times \rfloor {}^{I_k}_{G}\hat{\mathbf{R}}^{\top} \mathbf{\Phi}_{12} \\ {}^{G}\hat{\mathbf{n}}_{\Pi}^{\top}\mathbf{\Phi}_{52} \end{bmatrix}, \quad \mathbf{\Gamma}_{\Pi 3} = \begin{bmatrix} \mathbf{0}_3 \\ {}^{G}\hat{\mathbf{n}}_{\Pi}^{\top}\mathbf{\Phi}_{54} \end{bmatrix} \\ \mathbf{\Gamma}_{\Pi 4} &= \begin{bmatrix} {}^{I}_{G}\hat{\mathbf{R}}\, {}^{G}\hat{\mathbf{n}}_1^{\perp} \cos\hat{\phi} & {}^{I}_{G}\hat{\mathbf{R}}\, {}^{G}\hat{\mathbf{n}}_2^{\perp} & \mathbf{0}_{3\times 1} \\ {}^{G}\hat{\mathbf{P}}_I^{\top}\, {}^{G}\hat{\mathbf{n}}_1^{\perp} \cos\hat{\phi} & {}^{G}\hat{\mathbf{P}}_I^{\top}\, {}^{G}\hat{\mathbf{n}}_2^{\perp} & 1 \end{bmatrix} \\ {}^{G}\mathbf{n}_1^{\perp} &= \begin{bmatrix} -\sin\hat{\theta} & \cos\hat{\theta} & 0 \end{bmatrix}^{\top} \\ {}^{G}\mathbf{n}_2^{\perp} &= \begin{bmatrix} -\cos\hat{\theta}\sin\hat{\phi} & -\sin\hat{\theta}\sin\hat{\phi} & \cos\hat{\phi} \end{bmatrix}^{\top} \end{aligned}$$

It is not difficult to see that the aided INS with a plane feature will have at least 7 unobservable directions:

$$\begin{aligned} \mathbf{N}_{\pi} &= \begin{bmatrix} \mathbf{N}_{\pi 1} & \mathbf{N}_{\pi 2:4} & \mathbf{N}_{\pi 5:7} \end{bmatrix} \\ &= \begin{bmatrix} {}^{I_1}_{G}\hat{\mathbf{R}}\, {}^{G}\mathbf{g} & \mathbf{0}_{3\times 1} & \mathbf{0}_{3\times 1} & \mathbf{0}_{3\times 1} & \mathbf{0}_{3\times 1} & \mathbf{0}_{3\times 1} & {}^{I_1}_{G}\hat{\mathbf{R}}\, {}^{G}\mathbf{n}_{\Pi} \\ \mathbf{0}_{3\times 1} & \mathbf{0}_{3\times 1} & \mathbf{0}_{3\times 1} & \mathbf{0}_{3\times 1} & \mathbf{0}_{3\times 1} & \mathbf{0}_{3\times 1} & \mathbf{0}_{3\times 1} \\ -\lfloor {}^{G}\hat{\mathbf{V}}_{I_1} \times \rfloor {}^{G}\mathbf{g} & \mathbf{0}_{3\times 1} & \mathbf{0}_{3\times 1} & \mathbf{0}_{3\times 1} & {}^{G}\hat{\mathbf{n}}_1^{\perp} & {}^{G}\hat{\mathbf{n}}_2^{\perp} & \mathbf{0}_{3\times 1} \\ \mathbf{0}_{3\times 1} & \mathbf{0}_{3\times 1} & \mathbf{0}_{3\times 1} & \mathbf{0}_{3\times 1} & \mathbf{0}_{3\times 1} & \mathbf{0}_{3\times 1} & \mathbf{0}_{3\times 1} \\ -\lfloor {}^{G}\hat{\mathbf{P}}_{I_1} \times \rfloor {}^{G}\mathbf{g} & {}^{G}\hat{\mathbf{n}}_1^{\perp} & {}^{G}\hat{\mathbf{n}}_2^{\perp} & {}^{G}\hat{\mathbf{n}}_{\Pi} & \mathbf{0}_{3\times 1} & \mathbf{0}_{3\times 1} & \mathbf{0}_{3\times 1} \\ -g & 0 & 0 & 0 & 0 & 0 & 0 \\ 0 & 0 & 0 & 0 & 0 & 0 & 0 \\ 0 & 0 & 0 & -1 & 0 & 0 & 0 \end{bmatrix} \end{aligned} \tag{50}$$

Note that $\mathbf{N}_{\pi 1}$ relates to the rotation around the gravitational direction, $\mathbf{N}_{\pi 2:4}$ relates to the sensor's global translation, $\mathbf{N}_{\pi 5:6}$ relate to the sensor motion perpendicular to the plane's norm direction while $\mathbf{N}_{\pi 7}$ relates to the rotation around the plane normal direction.

5.2 Observability Analysis: Multiple Planes

Assuming that there are $m > 1$ plane features in the state vector, we define the orientation of the plane i and the rotation between plane i and plane j ($i, j \in \{1, \dots m\}$) as:

$${}^{G}_{\Pi_i}\hat{\mathbf{R}} = \begin{bmatrix} {}^{G}\hat{\mathbf{n}}_{\Pi i1}^{\perp} & {}^{G}\hat{\mathbf{n}}_{\Pi i2}^{\perp} & {}^{G}\hat{\mathbf{n}}_{\Pi i} \end{bmatrix} \tag{51}$$

$${}^{\Pi i}_{\Pi j}\hat{\mathbf{R}} = {}^{G}_{\Pi i}\hat{\mathbf{R}}^{\top}\, {}^{G}_{\Pi j}\hat{\mathbf{R}} \tag{52}$$

Lemma 5.1. *For aided INS system with m plane features in the state vector,*

- *If $m = 2$ and the planes are not parallel, the system will have at least 5 unobservable directions as $\mathbf{N}_{\Pi 1:5}$.*

- *If $m \geq 3$ and these planes' intersections are not parallel, the system will have at least 4 unobservable directions as $\mathbf{N}_{\Pi 1:4}$.*

$$\mathbf{N}_\Pi = \begin{bmatrix} \mathbf{N}_{\Pi 1} & \mathbf{N}_{\Pi 2:4} & \mathbf{N}_{\Pi 5} \end{bmatrix} \tag{53}$$
$$= \begin{bmatrix} {}^{I_1}_{G}\hat{\mathbf{R}}\,{}^{G}\mathbf{g} & \mathbf{0}_3 & \mathbf{0}_{3\times 1} \\ \mathbf{0}_{3\times 1} & \mathbf{0}_3 & \mathbf{0}_{3\times 1} \\ -\lfloor {}^{G}\hat{\mathbf{V}}_{I_1} \times \rfloor {}^{G}\mathbf{g} & \mathbf{0}_3 & \lfloor {}^{G}\hat{\mathbf{n}}_{\Pi i} \times \rfloor {}^{G}\hat{\mathbf{n}}_{\Pi j} \\ \mathbf{0}_{3\times 1} & \mathbf{0}_3 & \mathbf{0}_{3\times 1} \\ -\lfloor {}^{G}\hat{\mathbf{P}}_{I_1} \times \rfloor {}^{G}\mathbf{g} & {}^{G}_{\Pi i}\hat{\mathbf{R}} & \mathbf{0}_{3\times 1} \\ -g & \mathbf{0}_{1\times 3} & 0 \\ 0 & \mathbf{0}_{1\times 3} & 0 \\ 0 & -\mathbf{e}_3^{\top\,\Pi 1}_{\Pi i}\hat{\mathbf{R}} & 0 \\ \vdots & \vdots & \vdots \\ -g & \mathbf{0}_{1\times 3} & 0 \\ 0 & \mathbf{0}_{1\times 3} & 0 \\ 0 & -\mathbf{e}_3^{\top\,\Pi i-1}_{\Pi i}\hat{\mathbf{R}} & 0 \\ -g & \mathbf{0}_{1\times 3} & 0 \\ 0 & \mathbf{0}_{1\times 3} & 0 \\ 0 & -\mathbf{e}_3^{\top} & 0 \\ -g & \mathbf{0}_{1\times 3} & 0 \\ 0 & \mathbf{0}_{1\times 3} & 0 \\ 0 & -\mathbf{e}_3^{\top\,\Pi i}_{\Pi i+1}\hat{\mathbf{R}}^{\top} & 0 \\ \vdots & \vdots & \vdots \\ -g & \mathbf{0}_{1\times 3} & 0 \\ 0 & \mathbf{0}_{1\times 3} & 0 \\ 0 & -\mathbf{e}_3^{\top\,\Pi i}_{\Pi m}\hat{\mathbf{R}}^{\top} & 0 \end{bmatrix}$$

where $i, j \in \{1 \dots m\}$.

Proof. See Appendix E. □

Note that $\mathbf{N}_{\Pi 1}$ relates to the rotation around the gravitational direction, $\mathbf{N}_{\Pi 2:4}$ relates to the sensor's global translation. $\mathbf{N}_{\Pi 5}$ is for the case with 2 planes, and it refers to the sensor motion along the intersection line of the two planes.

6 Simulation Results

To validate our observability analysis, we perform 100 Monte Carlo simulations of visual inertial odometry (VIO) using point [13], line and plane features, respectively. The simulated trajectory and different geometric features are shown in Fig. 1, where we assume a stereo camera with IMU is moving on spacial sine trajectories to get the feature measurements. In the results presented below, we implemented the MSCKF [13] as the VIO estimator to validate our observability analysis, since the MSCKF has been widely used for VINS with point features and its observability analysis [1, 2]. In particular, we have compared two difference versions of MSCKF – the *ideal* MSCKF which uses true states as the linearization points and was shown to have correct observability properties and thus being consistent, and the *standard* MSCKF which uses current state estimates as the linearization points and was found to be overconfident (inconsistent) [1, 2]. We compute the root mean squared error (RMSE) and the normalized estimation error squared (NEES) to quantify estimation accuracy and consistency [29]. The results are shown in Fig. 1. It is clear from these figures that standard MSCKF performs worse than the ideal MSCKF which is consistent (though the comparison of orientation estimates is not as apparent as position estimates). This implies the importance of understanding system observability properties for the design of consistent INS state estimators.

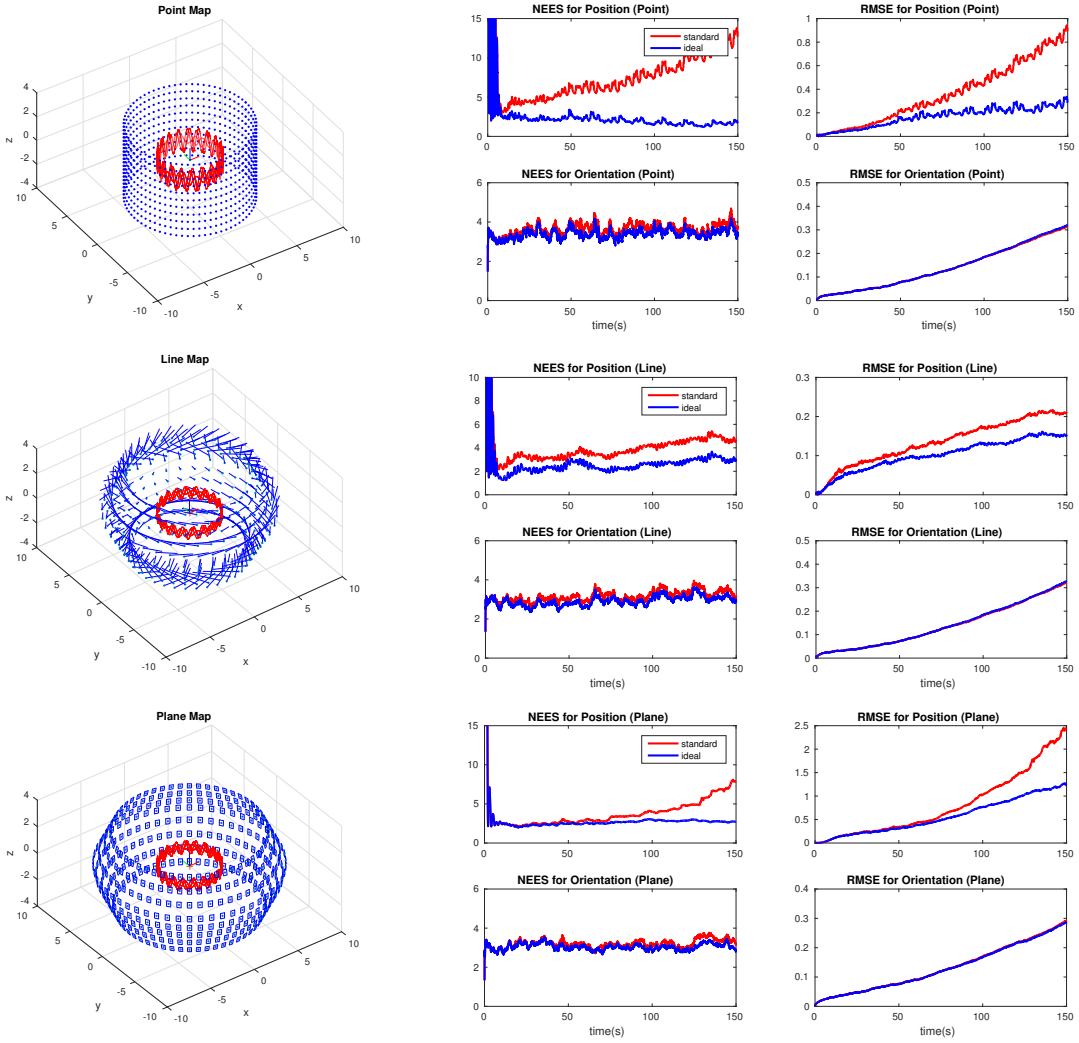

Figure 1: Monte Carlo results of the standard and ideal MSCKFs for different geometric features: (top) points, (middle) lines, and (bottom) planes.

7 Conclusions and Future Work

We have performed observability analysis from INS aided by generic range and/or bearing measurements with different geometric features including points, lines and planes, which encapsulates the vision-aided INS as a special case. In particular, in the case of point features, we have systematically investigated the effects of global measurements on the aided INS observability and as expected, we found that the global measurements improve the system observability. Moreover, we have also identified four types of degenerate motion which should be avoided when performing aided INS. We further generalized the observability analysis to the aided INS with line and plane features, respectively, analytically proved that there exist at least 5 (7) unobservable directions with a single line (plane) feature, and for the first time, derived the unobservable directions for multiple lines or planes. The analysis is validated in the MSCKF-based VIO Monte Carlo simulations. In the future, we will leverage the presented observability analysis to design consistent estimators for different aided INS with geometric features. We will also investigate the (stochastic) observability of aided INS under adversarial attacks [30] or unknown inputs [31] in order to design secure estimators for robot navigation.

Appendix A: State Transition Matrix

Follow the reference [1], the state transition matrix $\mathbf{\Phi}_{(k,1)}$ is defined as:

$$\mathbf{\Phi}_{(k,1)} = \begin{bmatrix} \mathbf{\Phi}_{11} & \mathbf{\Phi}_{12} & \mathbf{0}_3 & \mathbf{0}_3 & \mathbf{0}_3 & \mathbf{0}_3 \\ \mathbf{0}_3 & \mathbf{I}_3 & \mathbf{0}_3 & \mathbf{0}_3 & \mathbf{0}_3 & \mathbf{0}_3 \\ \mathbf{\Phi}_{31} & \mathbf{\Phi}_{32} & \mathbf{I}_3 & \mathbf{\Phi}_{34} & \mathbf{0}_3 & \mathbf{0}_3 \\ \mathbf{0}_3 & \mathbf{0}_3 & \mathbf{0}_3 & \mathbf{I}_3 & \mathbf{0}_3 & \mathbf{0}_3 \\ \mathbf{\Phi}_{51} & \mathbf{\Phi}_{52} & \mathbf{\Phi}_{53} & \mathbf{\Phi}_{54} & \mathbf{I}_3 & \mathbf{0}_3 \\ \mathbf{0}_3 & \mathbf{0}_3 & \mathbf{0}_3 & \mathbf{0}_3 & \mathbf{0}_3 & \mathbf{I}_3 \end{bmatrix} \tag{54}$$

where we have:

$$\mathbf{\Phi}_{11} = {}^{I_k}_{I_1}\mathbf{R} \tag{55}$$

$$\mathbf{\Phi}_{31} = -\lfloor \left({}^{G}\mathbf{V}_{I_k} - {}^{G}\mathbf{V}_{I_1}\right) + {}^{G}\mathbf{g}\delta t_k \times \rfloor {}^{G}_{I_1}\mathbf{R} \tag{56}$$

$$\mathbf{\Phi}_{51} = \lfloor {}^{G}\mathbf{P}_{I_1} + {}^{G}\mathbf{V}_{I_1}\delta t_k - \frac{1}{2}{}^{G}\mathbf{g}\delta t_k^2 - {}^{G}\mathbf{P}_{I_k} \times \rfloor {}^{G}_{I_1}\mathbf{R} \tag{57}$$

$$\mathbf{\Phi}_{12} = -\int_{t_1}^{t_k} {}^{I_\tau}_{I_k}\mathbf{R}^\top \mathbf{d}\tau \tag{58}$$

$$\mathbf{\Phi}_{32} = \int_{t_1}^{t_k} {}^{I_s}_{G}\mathbf{R}^\top \lfloor {}^{I_s}\mathbf{a} \times \rfloor \int_{t_1}^{s} {}^{I_\tau}_{I_s}\mathbf{R}^\top \mathbf{d}\tau \mathbf{d}s \tag{59}$$

$$\mathbf{\Phi}_{52} = \int_{t_1}^{t_k} \int_{t_1}^{\theta} {}^{I_s}_{G}\mathbf{R}^\top \lfloor {}^{I_s}\mathbf{a} \times \rfloor \int_{t_1}^{t_s} {}^{I_\tau}_{I_s}\mathbf{R}^\top \mathbf{d}\tau \mathbf{d}s \mathbf{d}\theta \tag{60}$$

$$\mathbf{\Phi}_{53} = \mathbf{I}_3 \delta t_k \tag{61}$$

$$\mathbf{\Phi}_{34} = -\int_{t_1}^{t_k} {}^{I_\tau}_{G}\mathbf{R}^\top \mathbf{d}\tau \tag{62}$$

$$\mathbf{\Phi}_{54} = -\int_{t_1}^{t_k} \int_{t_1}^{t_s} {}^{I_\tau}_{G}\mathbf{R}^\top \mathbf{d}\tau \mathbf{d}s \tag{63}$$

Appendix B: Line Jacobians

We would like to compute the Jacobians of $\frac{\partial {}^G\mathbf{L}}{\partial \delta \boldsymbol{\theta}_L}$ and $\frac{\partial {}^G\mathbf{L}}{\partial \delta \boldsymbol{\phi}_L}$. We first disturb the system with $\delta\boldsymbol{\theta}_L$, and arrive at:

$$
\begin{aligned}
{}^G\mathbf{L} &= \mathbf{R}_L \begin{bmatrix} \left\| {}^G\mathbf{n}_L \right\| & 0 \\ 0 & \left\| {}^G\mathbf{v}_L \right\| \\ 0 & 0 \end{bmatrix} \simeq (\mathbf{I} - \lfloor \delta\boldsymbol{\theta}_L \rfloor) \hat{\mathbf{R}}_L \begin{bmatrix} \left\| {}^G\hat{\mathbf{n}}_L \right\| & 0 \\ 0 & \left\| {}^G\hat{\mathbf{v}}_L \right\| \\ 0 & 0 \end{bmatrix} && (64) \\
&= {}^G\hat{\mathbf{L}} - \lfloor \delta\boldsymbol{\theta}_L \rfloor \begin{bmatrix} {}^G\hat{\mathbf{n}}_L & {}^G\hat{\mathbf{v}}_L \end{bmatrix} = {}^G\hat{\mathbf{L}} + \begin{bmatrix} \lfloor {}^G\hat{\mathbf{n}}_L \rfloor & \lfloor {}^G\hat{\mathbf{v}}_L \rfloor \end{bmatrix} \delta\boldsymbol{\theta}_L && (65)
\end{aligned}
$$

Note that we take ${}^G\mathbf{L} = [{}^G\mathbf{n}_L \ {}^G\mathbf{v}_L]$ in the above derivation for convenience. We then disturb the system with $\delta\boldsymbol{\phi}_L$, and we can arrive at:

$$
\begin{aligned}
\mathbf{W}_L &= \begin{bmatrix} \cos\phi_L & -\sin\phi_L \\ \sin\phi_L & \cos\phi_L \end{bmatrix} = \begin{bmatrix} \cos\left(\hat{\phi}_L + \tilde{\phi}_L\right) & -\sin\left(\hat{\phi}_L + \tilde{\phi}_L\right) \\ \sin\left(\hat{\phi}_L + \tilde{\phi}_L\right) & \cos\left(\hat{\phi}_L + \tilde{\phi}_L\right) \end{bmatrix} && (66) \\
&\simeq \begin{bmatrix} \cos\hat{\phi}_L - \delta\phi_L \sin\hat{\phi}_L & -\sin\hat{\phi}_L - \delta\phi_L \cos\hat{\phi}_L \\ \sin\hat{\phi}_L + \delta\phi_L \cos\hat{\phi}_L & \cos\hat{\phi}_L - \delta\phi_L \sin\hat{\phi}_L \end{bmatrix} && (67)
\end{aligned}
$$

From the above definition, we have $\cos\phi_L = \frac{\left\| {}^G\mathbf{n}_L \right\|}{\sqrt{\|{}^G\mathbf{n}_L\|^2 + \|{}^G\mathbf{v}_L\|^2}}$, $\sin\phi_L = \frac{\left\| {}^G\mathbf{v}_L \right\|}{\sqrt{\|{}^G\mathbf{n}_L\|^2 + \|{}^G\mathbf{v}_L\|^2}}$. Therefore, we have:

$$
\begin{aligned}
\left\| {}^G\mathbf{n}_L \right\| &= \sqrt{\|{}^G\mathbf{n}_L\|^2 + \|{}^G\mathbf{v}_L\|^2} \cos\phi_L = \sqrt{\|{}^G\hat{\mathbf{n}}_L\|^2 + \|{}^G\hat{\mathbf{v}}_L\|^2} \left(\cos\hat{\phi}_L - \delta\phi_L \sin\hat{\phi}_L\right) = \left\| {}^G\hat{\mathbf{n}}_L \right\| - \left\| {}^G\hat{\mathbf{v}}_L \right\| \delta\phi_L \\
\left\| {}^G\mathbf{v}_L \right\| &= \sqrt{\|{}^G\mathbf{n}_L\|^2 + \|{}^G\mathbf{v}_L\|^2} \sin\phi_L = \sqrt{\|{}^G\hat{\mathbf{n}}_L\|^2 + \|{}^G\hat{\mathbf{v}}_L\|^2} \left(\sin\hat{\phi}_L + \delta\phi_L \cos\hat{\phi}_L\right) = \left\| {}^G\hat{\mathbf{v}}_L \right\| + \left\| {}^G\hat{\mathbf{n}}_L \right\| \delta\phi_L
\end{aligned}
$$

Therefore, we have:

$$
\begin{aligned}
{}^G\mathbf{L} &= \mathbf{R}_L \begin{bmatrix} \left\| {}^G\mathbf{n}_L \right\| & 0 \\ 0 & \left\| {}^G\mathbf{v}_L \right\| \\ 0 & 0 \end{bmatrix} \simeq \begin{bmatrix} {}^G\hat{\mathbf{n}}_L - \frac{\left\| {}^G\hat{\mathbf{v}}_L \right\|}{\left\| {}^G\hat{\mathbf{n}}_L \right\|} {}^G\hat{\mathbf{n}}_L \delta\phi_L & {}^G\hat{\mathbf{v}}_L + \frac{\left\| {}^G\hat{\mathbf{n}}_L \right\|}{\left\| {}^G\hat{\mathbf{v}}_L \right\|} {}^G\hat{\mathbf{v}}_L \delta\phi_L \end{bmatrix} && (68) \\
&= \begin{bmatrix} {}^G\hat{\mathbf{n}}_L - \frac{w_2}{w_1} {}^G\hat{\mathbf{n}}_L \delta\phi_L & {}^G\hat{\mathbf{v}}_L + \frac{w_1}{w_2} {}^G\hat{\mathbf{v}}_L \delta\phi_L \end{bmatrix} && (69)
\end{aligned}
$$

Appendix C: Direct Line Measurement

Given a point cloud, the 3D line feature can be directly extracted with its direction ${}^I\mathbf{v}_m$ and distance to the sensor ${}^Id = \frac{\left\| {}^I\mathbf{n}_L \right\|}{\left\| {}^I\mathbf{v}_L \right\|}$. Therefore, we also consider a direct line measurement as:

$$
\mathbf{z} = \begin{bmatrix} \lfloor {}^I\mathbf{v}_m \times \rfloor {}^I\mathbf{v}_L \\ {}^Id \end{bmatrix} \tag{70}
$$

where ${}^I\mathbf{v}_m$ and ${}^Id$ is the line direction measurement and distance measurement in the IMU frame. Therefore, we have:

$$
\begin{aligned}
\frac{\partial \tilde{\mathbf{z}}}{\partial \tilde{\mathbf{x}}} &= \frac{\partial \tilde{\mathbf{z}}}{\partial {}^I\mathbf{L}} \frac{\partial {}^I\mathbf{L}}{\partial \tilde{\mathbf{x}}} && (71) \\
\frac{\partial \tilde{\mathbf{z}}}{\partial {}^I\mathbf{L}} &= \begin{bmatrix} \mathbf{0}_3 & \lfloor {}^I\mathbf{v}_m \times \rfloor \\ \frac{{}^I\mathbf{n}_L^\top}{\left\| {}^I\mathbf{n}_L \right\| \left\| {}^I\mathbf{v}_L \right\|} & -\frac{\left\| {}^I\mathbf{n}_L \right\|}{\left\| {}^I\mathbf{v}_L \right\|^3} {}^I\mathbf{v}_L^\top \end{bmatrix} && (72) \\
\frac{\partial {}^I\mathbf{L}}{\partial \tilde{\mathbf{x}}} &= \begin{bmatrix} {}^I_G\hat{\mathbf{R}} & \mathbf{0}_3 \\ \mathbf{0}_3 & {}^I_G\hat{\mathbf{R}} \end{bmatrix} \begin{bmatrix} \left(\lfloor {}^G\hat{\mathbf{n}}_L \times \rfloor - \lfloor \lfloor {}^G\hat{\mathbf{P}}_I \times \rfloor {}^G\hat{\mathbf{v}}_L \times \rfloor \right) {}^I_G\hat{\mathbf{R}}^\top & \mathbf{0}_{3\times 9} & \lfloor {}^G\hat{\mathbf{v}}_L \times \rfloor & \boldsymbol{\Gamma}_{l4} & \boldsymbol{\Gamma}_{l5} \\ \lfloor {}^G\hat{\mathbf{v}}_L \times \rfloor {}^I_G\hat{\mathbf{R}}^\top & & \mathbf{0}_{3\times 9} & \mathbf{0}_3 & \lfloor {}^G\hat{\mathbf{v}}_L \times \rfloor & \frac{w_1}{w_2} {}^G\hat{\mathbf{v}}_L \end{bmatrix} && (73)
\end{aligned}
$$

Therefore, we can compute the block row of the observability matrix at time step k as follows:

$$\mathbf{H}_{I_k}\mathbf{\Phi}_{(k,1)} = \frac{\partial\tilde{\mathbf{z}}}{\partial^I\mathbf{L}}\begin{bmatrix}{}^I_G\hat{\mathbf{R}} & \mathbf{0}_3\\ \mathbf{0}_3 & {}^I_G\hat{\mathbf{R}}\end{bmatrix}\begin{bmatrix}\mathbf{\Gamma}_{l1} & \mathbf{\Gamma}_{l2} & \lfloor{}^G\hat{\mathbf{v}}_L\times\rfloor\delta t_k & \mathbf{\Gamma}_{l3} & \lfloor{}^G\hat{\mathbf{v}}_L\times\rfloor & \mathbf{\Gamma}_{l4} & \mathbf{\Gamma}_{l5}\\ \lfloor{}^G\hat{\mathbf{v}}_L\times\rfloor{}^G_{I_1}\hat{\mathbf{R}} & \lfloor{}^G\hat{\mathbf{v}}_L\times\rfloor{}^G_{I_k}\hat{\mathbf{R}}\mathbf{\Phi}_{12} & \mathbf{0}_3 & \mathbf{0}_3 & \mathbf{0}_3 & \lfloor{}^G\hat{\mathbf{v}}_L\times\rfloor & \frac{w_1}{w_2}{}^G\hat{\mathbf{v}}_L\end{bmatrix}$$

It can be shown that the linearized aided INS system with a line feature will have at least 5 unobservable directions:

$$\begin{aligned}\mathbf{N}_l &= \begin{bmatrix}\mathbf{N}_{l1} & \mathbf{N}_{l2} & \mathbf{N}_{l3} & \mathbf{N}_{l4} & \mathbf{N}_{l5}\end{bmatrix} \\ &= \begin{bmatrix}{}^{I_1}_G\hat{\mathbf{R}}{}^G\mathbf{g} & \mathbf{0}_{3\times1} & \mathbf{0}_{3\times1} & \mathbf{0}_{3\times1} & \mathbf{0}_{3\times1}\\ \mathbf{0}_{3\times1} & \mathbf{0}_{3\times1} & \mathbf{0}_{3\times1} & \mathbf{0}_{3\times1} & \mathbf{0}_{3\times1}\\ -\lfloor{}^G\hat{\mathbf{V}}_{I_1}\times\rfloor{}^G\mathbf{g} & \mathbf{0}_{3\times1} & \mathbf{0}_{3\times1} & \mathbf{0}_{3\times1} & {}^G\hat{\mathbf{v}}_\mathbf{e}\\ \mathbf{0}_{3\times1} & \mathbf{0}_{3\times1} & \mathbf{0}_{3\times1} & \mathbf{0}_{3\times1} & \mathbf{0}_{3\times1}\\ -\lfloor{}^G\hat{\mathbf{P}}_{I_1}\times\rfloor{}^G\mathbf{g} & {}^G\hat{\mathbf{n}}_\mathbf{e} & {}^G\hat{\mathbf{v}}_\mathbf{e} & \lfloor{}^G\hat{\mathbf{n}}_\mathbf{e}\times\rfloor{}^G\hat{\mathbf{v}}_\mathbf{e} & \mathbf{0}_{3\times1}\\ -{}^G\mathbf{g} & \frac{w_2}{w_1}{}^G\hat{\mathbf{v}}_\mathbf{e}^\top & \mathbf{0}_{3\times1} & \mathbf{0}_{3\times1} & \mathbf{0}_{3\times1}\\ 0 & 0 & 0 & \eta^2w_2^2 & 0\end{bmatrix}\end{aligned} \tag{74}$$

We first verify $\mathbf{N}_{l1}$ and have:

$$\mathbf{H}_{I_k}\mathbf{\Phi}_{k,1}\mathbf{N}_{l1} = \frac{\partial\tilde{\mathbf{z}}}{\partial^I\mathbf{L}}\begin{bmatrix}{}^I_G\hat{\mathbf{R}} & \mathbf{0}_3\\ \mathbf{0}_3 & {}^I_G\hat{\mathbf{R}}\end{bmatrix}\begin{bmatrix}\lfloor{}^G\mathbf{g}\times\rfloor\lfloor{}^G\hat{\mathbf{P}}_{I_k}\times\rfloor{}^G\hat{\mathbf{v}}_L + \lfloor{}^G\hat{\mathbf{v}}_L\rfloor\lfloor{}^G\mathbf{g}\times\rfloor{}^G\hat{\mathbf{P}}_{I_k} + \lfloor{}^G\hat{\mathbf{P}}_{I_k}\times\rfloor\lfloor{}^G\hat{\mathbf{v}}_L\times\rfloor{}^G\hat{\mathbf{g}}\\ \lfloor{}^G\hat{\mathbf{v}}_L\times\rfloor{}^G\hat{\mathbf{g}} - \lfloor{}^G\hat{\mathbf{v}}_L\times\rfloor{}^G\hat{\mathbf{g}}\end{bmatrix} = \begin{bmatrix}\mathbf{0}\\ \mathbf{0}\end{bmatrix}$$

And for $\mathbf{N}_{l4}$, we have:

$$\begin{aligned}\mathbf{H}_{I_k}\mathbf{\Phi}_{k,1}\mathbf{N}_{l4} &= \frac{w_1w_2^2}{w_1^2+w_2^2}\frac{\partial\tilde{\mathbf{z}}}{\partial^I\mathbf{L}}\begin{bmatrix}\underbrace{-{}^{I_k}_G\hat{\mathbf{R}}\lfloor\left(\frac{w_1}{w_2}\lfloor{}^G\hat{\mathbf{n}}_e\times\rfloor{}^G\mathbf{v}_e + {}^G\mathbf{P}_{I_k}\right)\times\rfloor{}^G\hat{\mathbf{v}}_e}_{{}^{I_k}\mathbf{n}'_L}\\ {}^{I_k}_G\hat{\mathbf{R}}{}^G\hat{\mathbf{v}}_e\end{bmatrix} = \frac{w_1w_2^2}{w_1^2+w_2^2}\frac{\partial\tilde{\mathbf{z}}}{\partial^I\mathbf{L}}\begin{bmatrix}{}^{I_k}d{}^{I_k}\mathbf{n}_e\\ {}^{I_k}\mathbf{v}_e\end{bmatrix}\\ &= \frac{w_1w_2^2}{w_1^2+w_2^2}\begin{bmatrix}\lfloor{}^{I_k}\mathbf{v}_m\rfloor{}^{I_k}\mathbf{v}_e\\ \frac{\left\|{}^{I_k}\mathbf{n}_L\right\|}{\left\|{}^{I_k}\mathbf{v}_L\right\|^2}{}^{I_k}\mathbf{n}_e^\top{}^{I_k}\mathbf{n}_e - \frac{\left\|{}^{I_k}\mathbf{n}_L\right\|}{\left\|{}^{I_k}\mathbf{v}_L\right\|^2}{}^{I_k}\mathbf{v}_e^\top{}^{I_k}\mathbf{v}_e\end{bmatrix} = \begin{bmatrix}\mathbf{0}\\ \mathbf{0}\end{bmatrix}\end{aligned} \tag{75}$$

where ${}^{I_k}\mathbf{n}_e$ is the unit direction vector of ${}^{I_k}\mathbf{n}_L$, ${}^{I_k}d$ is the distance of line to sensor in frame $\{I_k\}$, and ${}^{I_k}\mathbf{n}'_L = -{}^{I_k}d{}^{I_k}\mathbf{n}_e$. Then, we can have $\mathbf{H}_{I_k}\mathbf{\Phi}_{k,1}\mathbf{N}_{l4} = \mathbf{0}$. Note that $\mathbf{N}_{l1}$ relates to the rotation around the gravitational direction, $\mathbf{N}_{l2:4}$ relates to the sensor's global translation, while $\mathbf{N}_{l5}$ relates to the sensor motion along the line direction.

Appendix D: Unobservable Directions for Multiple Lines

Since that we have m line features in the state vector, the Observability Gramian at time step k can be constructed as:

$$\mathbf{H}_{I_k}\mathbf{\Phi}_{(k,1)} = \begin{bmatrix}\mathbf{H}^{L1}_{I_k}\mathbf{\Phi}_{(k,1)}\\ \mathbf{H}^{L2}_{I_k}\mathbf{\Phi}_{(k,1)}\\ \mathbf{H}^{L3}_{I_k}\mathbf{\Phi}_{(k,1)}\\ \vdots\\ \mathbf{H}^{Lm}_{I_k}\mathbf{\Phi}_{(k,1)}\end{bmatrix} = \begin{bmatrix}\mathbf{M}^{L1}_k\\ \mathbf{M}^{L2}_k\\ \mathbf{M}^{L3}_k\\ \vdots\\ \mathbf{M}^{Lm}_k\end{bmatrix} \tag{76}$$

It is straightforward to verify $\mathbf{N}_{L1}$, which relates to the rotation around the gravitational direction. Since we have multiple un-parallel lines, the unobservable direction along the line direction deceases. Therefore, the main task to prove that $\mathbf{N}_{L2:4}$ are the null space of $\mathbf{H}_{I_k}\mathbf{\Phi}_{(k,1)}$. $\mathbf{N}_{L2:4}$ are related to the sensor position and from the analysis for a single line feature, we can easily find vectors $\boldsymbol{\alpha}_j, \boldsymbol{\beta}_j, \boldsymbol{\gamma}_j$ which are the null space for $\mathbf{M}^{Lj}_k$ for feature j, and $\boldsymbol{\alpha}_i, \boldsymbol{\beta}_i, \boldsymbol{\gamma}_i$ which are the null space for $\mathbf{M}^{Li}_k$ for feature i. Therefore, we have:

$$\mathbf{M}^{Li}_k\begin{bmatrix}\alpha_i & \beta_i & \gamma_i\end{bmatrix} = \mathbf{0}_{3\times1} \tag{77}$$

$$\mathbf{M}^{Lj}_k\begin{bmatrix}\alpha_j & \beta_j & \gamma_j\end{bmatrix} = \mathbf{0}_{3\times1} \tag{78}$$

If we can show that $\{\alpha_j, \beta_j, \gamma_j\}$ can be linearly represented by the $\{\alpha_i, \beta_i, \gamma_i\}$ as:

$$\begin{bmatrix}\alpha_j & \beta_j & \gamma_j\end{bmatrix} = \begin{bmatrix}\alpha_i & \beta_i & \gamma_i\end{bmatrix} \mathbf{\Lambda} \tag{79}$$

If $\mathbf{\Lambda}$ is invertible, both $\alpha_i, \beta_i, \gamma_i$ and $\alpha_j, \beta_j, \gamma_j$ share the same bases, and they are the null space for both $\mathbf{M}_k^{Lj}$ and $\mathbf{M}_k^{Li}$, that is:

$$\begin{bmatrix}\mathbf{M}_k^{Li} \\ \mathbf{M}_k^{Lj}\end{bmatrix} \begin{bmatrix}\alpha_i & \beta_i & \gamma_i & \alpha_j & \beta_j & \gamma_j\end{bmatrix} = \mathbf{0}_{6\times 1} \tag{80}$$

Based on the definition of $\mathbf{N}_{L2:4}$, we can have:

$$\mathbf{N}_{L2:4}^{(j)} = \begin{bmatrix}\alpha_j & \beta_j & \gamma_j\end{bmatrix} = \begin{bmatrix}\alpha_i & \beta_i & \gamma_i\end{bmatrix} {}^{Li}_{Lj}\mathbf{R} = \mathbf{N}_{L2:4}^{(i)} {}^{Li}_{Lj}\mathbf{R} \tag{81}$$

Since ${}^{Li}_{Lj}\mathbf{R}$ is a rotation matrix, it is invertible. Hence, according to the analysis, we have that both $\mathbf{N}_{L2:4}^{(i)}$ and $\mathbf{N}_{L2:4}^{(j)}$ are the null space for both $\mathbf{M}_k^{Lj}$ and $\mathbf{M}_k^{Li}$. Since we have no assumption for the choice of i and j, $\mathbf{N}_{L2:4}^{(i)}$ can also serve as the null space for $\mathbf{H}_{I_k}\mathbf{\Phi}_{(k,1)}$.

Appendix E: Unobservable Directions for Multiple Planes

Since we have m plane features in the state vector, we can construct the Observability Gramian at time step k as:

$$\mathbf{H}_{I_k}\mathbf{\Phi}_{(k,1)} = \begin{bmatrix}\mathbf{H}_{I_k}^{\Pi 1}\mathbf{\Phi}_{(k,1)} \\ \mathbf{H}_{I_k}^{\Pi 2}\mathbf{\Phi}_{(k,1)} \\ \mathbf{H}_{I_k}^{\Pi 3}\mathbf{\Phi}_{(k,1)} \\ \vdots \\ \mathbf{H}_{I_k}^{\Pi m}\mathbf{\Phi}_{(k,1)}\end{bmatrix} = \begin{bmatrix}\mathbf{M}_k^{\Pi 1} \\ \mathbf{M}_k^{\Pi 2} \\ \mathbf{M}_k^{\Pi 3} \\ \vdots \\ \mathbf{M}_k^{\Pi m}\end{bmatrix} \tag{82}$$

It is straightforward to verify $\mathbf{N}_{\Pi 1}$ which is related to the rotation around the gravitational direction. If $m = 2$, the state vector has two plane features, and their intersection line $\lfloor {}^G\mathbf{n}_{\Pi 1}\times \rfloor {}^G\mathbf{n}_{\Pi 2}$ perpendicular to both planes normal directions. Therefore, the sensor motion along this intersection line will be unobservable. Similar to the proof of line, the main task is to prove $\mathbf{N}_{\Pi 2:4}$ are the null space of $\mathbf{H}_{I_k}\mathbf{\Phi}_{(k,1)}$. We can easily find vectors $\boldsymbol{\alpha}_j, \boldsymbol{\beta}_j, \boldsymbol{\gamma}_j$ which are the null space for $\mathbf{M}_k^{\Pi j}$ for feature j, and $\boldsymbol{\alpha}_i, \boldsymbol{\beta}_i, \boldsymbol{\gamma}_i$ which are the null space for $\mathbf{M}_k^{\Pi i}$ for feature i. Therefore, we have:

$$\mathbf{M}_k^{\Pi i}\begin{bmatrix}\alpha_i & \beta_i & \gamma_i\end{bmatrix} = \mathbf{0}_{3\times 1} \tag{83}$$

$$\mathbf{M}_k^{\Pi j}\begin{bmatrix}\alpha_j & \beta_j & \gamma_j\end{bmatrix} = \mathbf{0}_{3\times 1} \tag{84}$$

If we can show that $\{\alpha_j, \beta_j, \gamma_j\}$ can be linearly represented by the $\{\alpha_i, \beta_i, \gamma_i\}$ as:

$$\begin{bmatrix}\alpha_j & \beta_j & \gamma_j\end{bmatrix} = \begin{bmatrix}\alpha_i & \beta_i & \gamma_i\end{bmatrix} \mathbf{\Lambda} \tag{85}$$

And if $\mathbf{\Lambda}$ is invertible, both $\alpha_i, \beta_i, \gamma_i$ and $\alpha_j, \beta_j, \gamma_j$ share the same bases, and they are the null space for both $\mathbf{M}_k^{\Pi j}$ and $\mathbf{M}_k^{\Pi i}$, that is:

$$\begin{bmatrix}\mathbf{M}_k^{\Pi i} \\ \mathbf{M}_k^{\Pi j}\end{bmatrix} \begin{bmatrix}\alpha_i & \beta_i & \gamma_i & \alpha_j & \beta_j & \gamma_j\end{bmatrix} = \mathbf{0}_{6\times 1} \tag{86}$$

Based on the definition of $\mathbf{N}_{\Pi 2:4}$, we can have:

$$\mathbf{N}_{\Pi 2:4}^{(j)} = \begin{bmatrix}\alpha_j & \beta_j & \gamma_j\end{bmatrix} = \begin{bmatrix}\alpha_i & \beta_i & \gamma_i\end{bmatrix} {}^{\Pi i}_{\Pi j}\mathbf{R} = \mathbf{N}_{\Pi 2:4}^{(i)} {}^{\Pi i}_{\Pi j}\mathbf{R} \tag{87}$$

Since ${}^{\Pi i}_{\Pi j}\mathbf{R}$ is a rotation matrix, it is invertible. Hence, according to the analysis, we have that both $\mathbf{N}_{\Pi 2:4}^{(i)}$ and $\mathbf{N}_{\Pi 2:4}^{(j)}$ are the null space for both $\mathbf{M}_k^{\Pi j}$ and $\mathbf{M}_k^{Li}$. Since we have no assumption for the choice of i and j, $\mathbf{N}_{\Pi 2:4}^{(i)}$ can also serve as the null space for $\mathbf{H}_{I_k}\mathbf{\Phi}_{(k,1)}$.

Appendix F: Sensor Measurements for Point Features

In this section, we will analyze the measurement model for lase sensors, camera sensors and 2D imaging sonars.

F.1: 1D Range Finder

1D range Finder can only get the range measurement of the point feature, and the measurement model can be described as:

$$z^{(r)} = \sqrt{{}^x\mathbf{P}_\mathbf{f}^\top {}^x\mathbf{P}_\mathbf{f}} + \mathbf{n}^{(r)} = \sqrt{({}^x x_\mathbf{f})^2 + ({}^x y_\mathbf{f})^2 + ({}^x z_\mathbf{f})^2} + \mathbf{n}^{(r)} \tag{88}$$

where ${}^x r_\mathbf{f} = \sqrt{{}^x\mathbf{p}_f^\top {}^x\mathbf{p}_f}$ represents the range for the point feature in the frame $\{X\}$. And we can linearizing the measurement model at ${}^x\hat{\mathbf{P}}_\mathbf{f}$ as:

$$\tilde{z}^{(r)} \simeq \mathbf{H}_r {}^x\tilde{\mathbf{P}}_\mathbf{f} + \mathbf{n}^{(r)} = \frac{{}^x\hat{\mathbf{P}}_\mathbf{f}^\top}{{}^x\hat{r}_\mathbf{f}} {}^x\tilde{\mathbf{P}}_\mathbf{f} + \mathbf{n}^{(r)} \tag{89}$$

F.2: Mono-camera

Mono-camera can only get the bearing measurements of the point feature, and the measurement model can be represented as:

$$\mathbf{z}^{(b)} = \begin{bmatrix} \frac{\mathbf{e}_1^\top {}^x\mathbf{P}_\mathbf{f}}{\mathbf{e}_3^\top {}^x\mathbf{P}_\mathbf{f}} \\ \frac{\mathbf{e}_2^\top {}^x\mathbf{P}_\mathbf{f}}{\mathbf{e}_3^\top {}^x\mathbf{P}_\mathbf{f}} \end{bmatrix} + \mathbf{n}^{(b)} = \begin{bmatrix} \frac{{}^x x_\mathbf{f}}{{}^x z_\mathbf{f}} \\ \frac{{}^x y_\mathbf{f}}{{}^x z_\mathbf{f}} \end{bmatrix} + \mathbf{n}^{(b)} \tag{90}$$

where $\mathbf{e}_i \in \mathbb{R}^{3\times 1}$ for $i = 1, 2, 3$ and $\mathbf{e}_1 = [1 \quad 0 \quad 0]^\top$, $\mathbf{e}_2 = [0 \quad 1 \quad 0]^\top$ and $\mathbf{e}_3 = [0 \quad 0 \quad 1]^\top$. Inspired by [32], we use a more universal measurement model for point feature with Mono-camera as:

$$\mathbf{z}^{(b)} = \mathbf{h}_b\left({}^x\mathbf{P}_\mathbf{f}, \mathbf{n}^{(b)}\right) = \begin{bmatrix} {}^x\mathbf{b}_{\perp 1}^\top \\ {}^x\mathbf{b}_{\perp 2}^\top \end{bmatrix} {}^x\mathbf{P}_\mathbf{f} + {}^x z_\mathbf{f} \begin{bmatrix} {}^x\mathbf{b}_{\perp 1}^\top \\ {}^x\mathbf{b}_{\perp 2}^\top \end{bmatrix} \begin{bmatrix} \mathbf{I}_2 \\ \mathbf{0}_{1\times 2} \end{bmatrix} \mathbf{n}^{(b)} \tag{91}$$

where $\mathbf{b}_{\perp i}, i \in \{1, 2\}$ are two perpendicular vectors to the bearing ${}^x\mathbf{b}_\mathbf{f}$, and they can be constructed from [32]. The advantage of this model is that it is suitable for both fish eye and normal projective camera model. And the linearized model with ${}^x\hat{\mathbf{P}}_\mathbf{f}$ is:

$$\tilde{\mathbf{z}}^{(b)} \simeq \mathbf{H}_b {}^x\tilde{\mathbf{P}}_\mathbf{f} + \mathbf{H}_n \mathbf{n}^{(b)} = \begin{bmatrix} {}^x\mathbf{b}_{\perp 1}^\top \\ {}^x\mathbf{b}_{\perp 2}^\top \end{bmatrix} {}^x\tilde{\mathbf{P}}_\mathbf{f} + {}^x\hat{z}_\mathbf{f} \begin{bmatrix} {}^x\hat{\mathbf{b}}_{\perp 1}^\top \\ {}^x\hat{\mathbf{b}}_{\perp 2}^\top \end{bmatrix} \begin{bmatrix} \mathbf{I}_2 \\ \mathbf{0}_{1\times 2} \end{bmatrix} \mathbf{n}^{(b)} \tag{92}$$

F.3: 2D Imaging Sonar

2D imaging sonar's measurement contains the range and horizontal bearing measurement of a point [11], and the model can be represented as:

$$\mathbf{z} = \begin{bmatrix} z^{(r)} \\ z^{(b)} \end{bmatrix} + \begin{bmatrix} \mathbf{n}^{(r)} \\ \mathbf{n}^{(b)} \end{bmatrix} = \begin{bmatrix} \sqrt{{}^x\mathbf{P}_\mathbf{f}^\top {}^x\mathbf{P}_\mathbf{f}} \\ {}^x\theta_\mathbf{f} \end{bmatrix} + \begin{bmatrix} \mathbf{n}^{(r)} \\ \mathbf{n}^{(b)} \end{bmatrix} = \begin{bmatrix} \sqrt{({}^x x_\mathbf{f})^2 + ({}^x y_\mathbf{f})^2 + ({}^x z_\mathbf{f})^2} \\ {}^x\theta_\mathbf{f} \end{bmatrix} + \begin{bmatrix} \mathbf{n}^{(r)} \\ \mathbf{n}^{(b)} \end{bmatrix} \tag{93}$$

and similar to the case of the Mono-camera, we rewrite the bearing measurement as:

$$z^{(b)} = \mathbf{h}_b\left({}^x\mathbf{P}_\mathbf{f}, \mathbf{n}^{(b)}\right) = {}^x r_\mathbf{f} \begin{bmatrix} \cos\left({}^x\theta_\mathbf{f} + n^{(b)}\right)\cos\phi & \sin\left({}^x\theta_\mathbf{f} + n^{(b)}\right)\cos\phi & \sin\phi \end{bmatrix} {}^x\mathbf{b}_\perp \tag{94}$$

where ${}^x\mathbf{b}_\perp = \begin{bmatrix} -\sin\theta & \cos\theta & 0 \end{bmatrix}^\top$. Therefore, the linearized sonar measurement model with ${}^x\hat{\mathbf{P}}_\mathbf{f}$ as:

$$\tilde{\mathbf{z}} = \begin{bmatrix} \tilde{z}^{(r)} \\ \tilde{z}^{(b)} \end{bmatrix} \begin{bmatrix} \mathbf{H}_r {}^x\tilde{\mathbf{P}}_\mathbf{f} + \mathbf{n}^{(r)} \\ \mathbf{H}_b {}^x\tilde{\mathbf{P}}_\mathbf{f} + \mathbf{H}_n \mathbf{n}^{(b)} \end{bmatrix} \tag{95}$$

$$\mathbf{H}_b = {}^x\mathbf{b}_\perp^\top \tag{96}$$

$$\mathbf{H}_n = {}^x\mathbf{b}_\perp^\top {}^x\hat{\mathbf{P}}_\mathbf{f} \left(-sin\left({}^x\hat{\theta}_\mathbf{f}\right)\cos\left({}^x\hat{\phi}_\mathbf{f}\right) + \cos\left({}^x\hat{\theta}_\mathbf{f}\right)\cos\left({}^x\hat{\phi}_\mathbf{f}\right)\right) \tag{97}$$

where ${}^x\hat{\theta}_\mathbf{f} = \arctan\frac{{}^x\hat{y}_\mathbf{f}}{{}^x\hat{x}_\mathbf{f}}$, ${}^x\hat{\phi}_\mathbf{f} = \arctan\frac{{}^x\hat{z}_\mathbf{f}}{\sqrt{{}^x\hat{x}_\mathbf{f}^2 + {}^x\hat{y}_\mathbf{f}^2}}$.

F.4: 2D LiDAR

2D lidar measurement is quite similar to sonar measurement, except for an extra constraint that ${}^{x}z_f = \mathbf{e}_3^\top {}^{x}\mathbf{p}_f = 0$ (or we can see as $\phi = 0$). In order to distinguish with Eq. (93), we add this constrain to the model, and hence:

$$\mathbf{z} = \begin{bmatrix} z^{(r)} \\ \mathbf{z}^{(b)} \end{bmatrix} = \begin{bmatrix} \sqrt{{}^{x}\mathbf{P}_\mathbf{f}^\top {}^{x}\mathbf{P}_\mathbf{f}} \\ {}^{x}\theta_\mathbf{f} \\ \mathbf{e}_3^\top {}^{x}\mathbf{P}_\mathbf{f} \end{bmatrix} + \begin{bmatrix} n^{(r)} \\ \mathbf{n}^{(b)}_{2\times 1} \end{bmatrix} = \begin{bmatrix} \sqrt{({}^{x}x_\mathbf{f})^2 + ({}^{x}y_\mathbf{f})^2 + ({}^{x}z_\mathbf{f})^2} \\ {}^{x}\theta_\mathbf{f} \\ {}^{x}z_\mathbf{f} \end{bmatrix} + \begin{bmatrix} n^{(r)} \\ \mathbf{n}^{(b)}_{2\times 1} \end{bmatrix} \tag{98}$$

where $\mathbf{n}^{(b)} = \begin{bmatrix} n_1^{(b)} & n_2^{(b)} \end{bmatrix}^\top$. Similarly, we can rewrite the bearing measurement as:

$$\mathbf{z}^{(b)} = \mathbf{h}_b\left({}^{x}\mathbf{P}_\mathbf{f}, \mathbf{n}^{(b)}\right) = \begin{bmatrix} {}^{x}\mathbf{b}_{\perp 1}^\top {}^{x}r_\mathbf{f} \begin{bmatrix} \cos\left({}^{x}\theta_\mathbf{f} + n_1^{(b)}\right)\cos\phi & \sin\left({}^{x}\theta_\mathbf{f} + n_1^{(b)}\right)\cos\phi & \sin\phi \end{bmatrix}^\top \\ {}^{x}\mathbf{b}_{\perp 2}^\top {}^{x}\mathbf{P}_\mathbf{f} + n_2^{(b)} \end{bmatrix} \tag{99}$$

where $\mathbf{b}_{\perp 1} = \begin{bmatrix} -\sin({}^{x}\theta_\mathbf{f}) & \cos({}^{x}\theta_\mathbf{f}) & 0 \end{bmatrix}^\top$, $\mathbf{b}_{\perp 2} = \begin{bmatrix} 0 & 0 & 1 \end{bmatrix}^\top$. Therefore, the linearized system with ${}^{x}\hat{\mathbf{P}}_\mathbf{f}$ can be described as:

$$\tilde{\mathbf{z}} = \begin{bmatrix} \tilde{z}^{(r)} \\ \tilde{\mathbf{z}}^{(b)} \end{bmatrix} = \begin{bmatrix} \mathbf{H}_r {}^{x}\tilde{\mathbf{P}}_\mathbf{f} + n^{(r)} \\ \mathbf{H}_b {}^{x}\tilde{\mathbf{P}}_\mathbf{f} + \mathbf{H}_n \mathbf{n}^{(b)} \end{bmatrix} \tag{100}$$

where:

$$\mathbf{H}_b = \begin{bmatrix} \mathbf{b}_{\perp 1}^\top \\ \mathbf{b}_{\perp 2}^\top \end{bmatrix} \tag{101}$$

$$\mathbf{H}_n = \begin{bmatrix} {}^{x}\mathbf{b}_{\perp 1}^\top {}^{x}\hat{\mathbf{P}}_\mathbf{f} \left(-sin\left({}^{x}\hat{\theta}_\mathbf{f}\right)\cos\left({}^{x}\hat{\phi}_\mathbf{f}\right) + \cos\left({}^{x}\hat{\theta}_\mathbf{f}\right)\cos\left({}^{x}\hat{\phi}_\mathbf{f}\right)\right) \\ {}^{x}\mathbf{b}_{\perp 2}^\top \end{bmatrix} \tag{102}$$

where ${}^{x}\hat{\theta}_\mathbf{f} = \arctan\frac{{}^{x}\hat{y}_\mathbf{f}}{{}^{x}\hat{x}_\mathbf{f}}$, ${}^{x}\hat{\phi}_\mathbf{f} = \arctan\frac{{}^{x}\hat{z}_\mathbf{f}}{\sqrt{{}^{x}\hat{x}_\mathbf{f}^2 + {}^{x}\hat{y}_\mathbf{f}^2}}$.

F.5: 3D LiDAR

3D LiDAR can directly get the range and bearing information of the feature, therefore the measurement model can be denoted as:

$$\mathbf{z} = \begin{bmatrix} z^{(r)} \\ \mathbf{z}^{(b)} \end{bmatrix} = \begin{bmatrix} \sqrt{{}^{x}\mathbf{p}_\mathbf{f}^\top {}^{x}\mathbf{p}_\mathbf{f}} \\ {}^{x}\theta_\mathbf{f} \\ {}^{x}\phi_\mathbf{f} \end{bmatrix} + \begin{bmatrix} n^{(r)} \\ \mathbf{n}^{(b)} \end{bmatrix} = \begin{bmatrix} \sqrt{({}^{x}x_\mathbf{f})^2 + ({}^{x}y_\mathbf{f})^2 + ({}^{x}z_\mathbf{f})^2} \\ {}^{x}\theta_\mathbf{f} \\ {}^{x}\phi_\mathbf{f} \end{bmatrix} + \begin{bmatrix} n^{(r)} \\ \mathbf{n}^{(b)} \end{bmatrix} \tag{103}$$

where $\mathbf{n}^{(b)} = \begin{bmatrix} n_1^{(b)} & n_2^{(b)} \end{bmatrix}^\top$. Similarly, we can rewrite the bearing measurement as:

$$\mathbf{z}^{(b)} = \mathbf{h}_b\left({}^{x}\mathbf{P}_\mathbf{f}, \mathbf{n}^{(b)}\right) = \begin{bmatrix} {}^{x}\mathbf{b}_{\perp 1}^\top {}^{x}r_\mathbf{f} \begin{bmatrix} \cos\left({}^{x}\theta_\mathbf{f} + n_1^{(b)}\right)\cos\phi & \sin\left({}^{x}\theta_\mathbf{f} + n_1^{(b)}\right)\cos\phi & \sin\phi \end{bmatrix}^\top \\ {}^{x}\mathbf{b}_{\perp 2}^\top {}^{x}r_\mathbf{f} \begin{bmatrix} \cos({}^{x}\theta_\mathbf{f})\cos\left({}^{x}\phi_\mathbf{f} + n_2^{(b)}\right) & \sin({}^{x}\theta_\mathbf{f})\cos\left({}^{x}\phi_\mathbf{f} + n_2^{(b)}\right) & \sin\left({}^{x}\phi_\mathbf{f} + n_2^{(b)}\right) \end{bmatrix}^\top \end{bmatrix} \tag{104}$$

where $\mathbf{b}_{\perp i}, i \in \{1, 2\}$ are two perpendicular vectors to the bearing ${}^{x}\mathbf{b}_\mathbf{f}$, and they can be constructed from [32]. Therefore, the linearized system with ${}^{x}\hat{\mathbf{P}}_\mathbf{f}$ can be described as:

$$\tilde{\mathbf{z}} = \begin{bmatrix} \tilde{z}^{(r)} \\ \tilde{\mathbf{z}}^{(b)} \end{bmatrix} = \begin{bmatrix} \mathbf{H}_r {}^{x}\tilde{\mathbf{P}}_\mathbf{f} + n^{(r)} \\ \mathbf{H}_b {}^{x}\tilde{\mathbf{P}}_\mathbf{f} + \mathbf{H}_n \mathbf{n}^{(b)} \end{bmatrix} \tag{105}$$

where:

$$\mathbf{H}_b = \begin{bmatrix} \mathbf{b}_{\perp 1}^\top \\ \mathbf{b}_{\perp 2}^\top \end{bmatrix} \tag{106}$$

$$\mathbf{H}_n = \begin{bmatrix} {}^{x}\mathbf{b}_{\perp 1}^\top {}^{x}\hat{\mathbf{P}}_\mathbf{f} \left(-\sin\left({}^{x}\hat{\theta}_\mathbf{f}\right)\cos\left({}^{x}\hat{\phi}_\mathbf{f}\right) + \cos\left({}^{x}\hat{\theta}_\mathbf{f}\right)\cos\left({}^{x}\hat{\phi}_\mathbf{f}\right)\right) \\ {}^{x}\mathbf{b}_{\perp 2}^\top {}^{x}\hat{\mathbf{P}}_\mathbf{f} \left(-\cos\left({}^{x}\hat{\theta}_\mathbf{f}\right)\sin\left({}^{x}\hat{\phi}_\mathbf{f}\right) - \sin\left({}^{x}\hat{\theta}_\mathbf{f}\right)\sin\left({}^{x}\hat{\phi}_\mathbf{f}\right) + \cos\left({}^{x}\hat{\phi}_\mathbf{f}\right)\right) \end{bmatrix} \tag{107}$$

where ${}^x\hat{\theta}_\mathbf{f} = \arctan \frac{{}^x\hat{y}_\mathbf{f}}{{}^x\hat{x}_\mathbf{f}}$, ${}^x\hat{\phi}_\mathbf{f} = \arctan \frac{{}^x\hat{z}_\mathbf{f}}{\sqrt{{}^x\hat{x}_\mathbf{f}^2 + {}^x\hat{y}_\mathbf{f}^2}}$.

F.6: RGBD Camera

RGBD camera can also get the range and bearing information of the feature, therefore:

$$\mathbf{z} = \begin{bmatrix} z^{(r)} \\ \mathbf{z}^{(b)} \end{bmatrix} = \begin{bmatrix} \sqrt{{}^x\mathbf{P}_\mathbf{f}^\top {}^x\mathbf{P}_\mathbf{f}} \\ \frac{\mathbf{e}_1^\top {}^x\mathbf{P}_\mathbf{f}}{\mathbf{e}_3^\top {}^x\mathbf{P}_\mathbf{f}} \\ \frac{\mathbf{e}_2^\top {}^x\mathbf{P}_\mathbf{f}}{\mathbf{e}_3^\top {}^x\mathbf{P}_\mathbf{f}} \end{bmatrix} + \begin{bmatrix} n^{(r)} \\ \mathbf{n}^{(b)} \end{bmatrix} = \begin{bmatrix} \sqrt{({}^x x_\mathbf{f})^2 + ({}^x y_\mathbf{f})^2 + ({}^x z_\mathbf{f})^2} \\ \frac{{}^x x_\mathbf{f}}{{}^x z_\mathbf{f}} \\ \frac{{}^x y_\mathbf{f}}{{}^x z_\mathbf{f}} \end{bmatrix} + \begin{bmatrix} n^{(r)} \\ \mathbf{n}^{(b)} \end{bmatrix} \tag{108}$$

Therefore, we can rewrite the measurement model as:

$$\mathbf{z} = \begin{bmatrix} z^{(r)} \\ \mathbf{z}^{(b)} \end{bmatrix} = \begin{bmatrix} \sqrt{{}^x\mathbf{P}_\mathbf{f}^\top {}^x\mathbf{P}_\mathbf{f}} + \mathbf{n}^{(r)} \\ \mathbf{h}_b\left({}^x\mathbf{P}_\mathbf{f}, \mathbf{n}^{(b)}\right) \end{bmatrix} = \begin{bmatrix} \sqrt{{}^x\mathbf{P}_\mathbf{f}^\top {}^x\mathbf{P}_\mathbf{f}} + \mathbf{n}^{(r)} \\ \begin{bmatrix} {}^x\mathbf{b}_{\perp 1}^\top \\ {}^x\mathbf{b}_{\perp 2}^\top \end{bmatrix} {}^x\mathbf{P}_\mathbf{f} + {}^x z_\mathbf{f} \begin{bmatrix} {}^x\mathbf{b}_{\perp 1}^\top \\ {}^x\mathbf{b}_{\perp 2}^\top \end{bmatrix} \begin{bmatrix} \mathbf{I}_2 \\ \mathbf{0}_{1\times 2} \end{bmatrix} \mathbf{n}^{(b)} \end{bmatrix} \tag{109}$$

And we can linearize the system with ${}^x\hat{\mathbf{P}}_\mathbf{f}$ as:

$$\tilde{\mathbf{z}} = \begin{bmatrix} \tilde{z}^{(r)} \\ \tilde{\mathbf{z}}^{(b)} \end{bmatrix} \simeq \begin{bmatrix} \mathbf{H}_r {}^x\tilde{\mathbf{P}}_\mathbf{f} + n^{(r)} \\ \mathbf{H}_b {}^x\tilde{\mathbf{P}}_\mathbf{f} + \mathbf{H}_n \mathbf{n}^{(b)} \end{bmatrix} = \begin{bmatrix} \frac{{}^x\hat{\mathbf{P}}_\mathbf{f}^\top}{{}^x\hat{r}_\mathbf{f}} {}^x\tilde{\mathbf{P}}_\mathbf{f} + \mathbf{n}^{(r)} \\ \begin{bmatrix} {}^x\hat{\mathbf{b}}_{\perp 1}^\top \\ {}^x\hat{\mathbf{b}}_{\perp 2}^\top \end{bmatrix} {}^x\tilde{\mathbf{P}}_\mathbf{f} + {}^x\hat{z}_\mathbf{f} \begin{bmatrix} {}^x\hat{\mathbf{b}}_{\perp 1}^\top \\ {}^x\hat{\mathbf{b}}_{\perp 2}^\top \end{bmatrix} \begin{bmatrix} \mathbf{I}_2 \\ \mathbf{0}_{1\times 2} \end{bmatrix} \mathbf{n}^{(b)} \end{bmatrix} \tag{110}$$

F.7: Stereo Camera

Stereo-camera are two mono-cameras with known extrinsic transformations. Without lost of generalities, we assume input images have already been rectified, thus the measurement model can be described as:

$$\mathbf{z} = \begin{bmatrix} \frac{\mathbf{e}_1^\top {}^x\mathbf{P}_\mathbf{f}}{\mathbf{e}_3^\top {}^x\mathbf{P}_\mathbf{f}} \\ \frac{\mathbf{e}_1^\top {}^x\mathbf{P}_\mathbf{f} - b_s}{\mathbf{e}_3^\top {}^x\mathbf{P}_\mathbf{f}} \\ \frac{\mathbf{e}_2^\top {}^x\mathbf{P}_\mathbf{f}}{\mathbf{e}_3^\top {}^x\mathbf{P}_\mathbf{f}} \end{bmatrix} + \begin{bmatrix} n_1^{(b)} \\ n_1^{(b)} \\ n_2^{(b)} \end{bmatrix} = \begin{bmatrix} \frac{{}^x x_\mathbf{f}}{{}^x z_\mathbf{f}} \\ \frac{{}^x x_\mathbf{f} - b_s}{{}^x z_\mathbf{f}} \\ \frac{{}^x y_\mathbf{f}}{{}^x z_\mathbf{f}} \end{bmatrix} + \begin{bmatrix} n_1^{(b)} \\ n_1^{(b)} \\ n_2^{(b)} \end{bmatrix} \tag{111}$$

where b is the baseline for the stereo-camera, which is a known scalar. Similar to the case of Mono-camera, we can rewrite the Stereo camera measurement as:

$$\mathbf{z} = \begin{bmatrix} \mathbf{z}_L^{(b)} \\ \mathbf{z}_R^{(b)} \end{bmatrix} = \begin{bmatrix} \mathbf{h}_{b_L}\left({}^x\mathbf{P}_\mathbf{f}, \mathbf{n}^{(b)}\right) \\ \mathbf{h}_{b_R}\left({}^x\mathbf{P}_\mathbf{f}, \mathbf{n}^{(b)}\right) \end{bmatrix} = \begin{bmatrix} \begin{bmatrix} {}^x\mathbf{b}_{\perp 1L}^\top \\ {}^x\mathbf{b}_{\perp 2L}^\top \end{bmatrix} {}^x\mathbf{P}_\mathbf{f} + {}^x z_\mathbf{f} \begin{bmatrix} {}^x\mathbf{b}_{\perp 1L}^\top \\ {}^x\mathbf{b}_{\perp 2L}^\top \end{bmatrix} \begin{bmatrix} \mathbf{I}_2 \\ \mathbf{0}_{1\times 2} \end{bmatrix} \mathbf{n}^{(b)} \\ \begin{bmatrix} {}^x\mathbf{b}_{\perp 1R}^\top \\ {}^x\mathbf{b}_{\perp 2R}^\top \end{bmatrix} {}^x\mathbf{P}'_\mathbf{f} + {}^x z_\mathbf{f} \begin{bmatrix} {}^x\mathbf{b}_{\perp 1R}^\top \\ {}^x\mathbf{b}_{\perp 2R}^\top \end{bmatrix} \begin{bmatrix} \mathbf{I}_2 \\ \mathbf{0}_{1\times 2} \end{bmatrix} \mathbf{n}^{(b)} \end{bmatrix} \tag{112}$$

where $\mathbf{z}_L^{(b)}$ and $\mathbf{z}_R^{(b)}$ represents the bearing measurement from the left-and right camera, respectively, ${}^x\mathbf{P}'_\mathbf{f} = \begin{bmatrix} {}^x x_\mathbf{f} - b_s & {}^x y_\mathbf{f} & {}^x z_\mathbf{f} \end{bmatrix}^\top$. With ${}^x\hat{\mathbf{P}}_\mathbf{f}$, we can linearize the system as:

$$\tilde{\mathbf{z}} = \begin{bmatrix} \tilde{\mathbf{z}}_L^{(b)} \\ \tilde{\mathbf{z}}_R^{(b)} \end{bmatrix} = \begin{bmatrix} \mathbf{H}_{b_L} {}^x\tilde{\mathbf{P}}_\mathbf{f} + \mathbf{H}_n \mathbf{n}^{(\mathbf{b})} \\ \mathbf{H}_{b_R} {}^x\tilde{\mathbf{P}}_\mathbf{f} + \mathbf{H}_n \mathbf{n}^{(\mathbf{b})} \end{bmatrix} = \begin{bmatrix} \begin{bmatrix} {}^x\hat{\mathbf{b}}_{\perp 1_L}^\top \\ {}^x\hat{\mathbf{b}}_{\perp 2_L}^\top \end{bmatrix} {}^x\tilde{\mathbf{P}}_\mathbf{f} + {}^x\hat{z}_\mathbf{f} \begin{bmatrix} {}^x\hat{\mathbf{b}}_{\perp 1_L}^\top \\ {}^x\hat{\mathbf{b}}_{\perp 2_L}^\top \end{bmatrix} \begin{bmatrix} \mathbf{I}_2 \\ \mathbf{0}_{1\times 2} \end{bmatrix} \mathbf{n}^{(b)} \\ \begin{bmatrix} {}^x\hat{\mathbf{b}}_{\perp 1_R}^\top \\ {}^x\hat{\mathbf{b}}_{\perp 2_R}^\top \end{bmatrix} {}^x\tilde{\mathbf{P}}_\mathbf{f} + {}^x\hat{z}_\mathbf{f} \begin{bmatrix} {}^x\hat{\mathbf{b}}_{\perp 1_R}^\top \\ {}^x\hat{\mathbf{b}}_{\perp 2_R}^\top \end{bmatrix} \begin{bmatrix} \mathbf{I}_2 \\ \mathbf{0}_{1\times 2} \end{bmatrix} \mathbf{n}^{(b)} \end{bmatrix} \tag{113}$$

To sum up, the measurement model and its linearized model for aided INS can be generalized as (10) and (11).

All the sensor measurements to point feature can be seen as the combination of range measurements and bearing measurements (as shown in Table 1). (Be noted from the table that camera sensors can get the full bearing measurements, which in some sense is equivalent that we get the information of θ and ϕ. The sonar can only get partial bearing information (θ), so we label it as partial bearing measurement in the table.) Therefore, in order to fully analyze the observability property of aided INS, we will analyze the range only measurement model and bearing only measurement model in the next section respectively.

Table 1: Measurement Model for Different Sensors

Sensor	Range	Full Bearing	Partial Bearing
1D range finder	✓		
mono-camera		✓	
sonar	✓		✓
2D lidar	✓	✓	
3D lidar	✓	✓	
RGBD-camera	✓	✓	
stereo-camera	✓	✓	

Appendix G: Unobservable Directions for Point Features

G.1: Nonlinear Observability Analysis

we first provide an overview of the nonlinear observability rank condition test [20] and summarize the method in [12][21][33][2] for finding the unobservable modes of nonlinear system. Consider a nonlinear system:

$$\begin{cases} \dot{\mathbf{x}} = \mathbf{f}_0(\mathbf{x}) + \sum_{i=1}^{\ell} \mathbf{f}_i(\mathbf{x}) u_i \\ \mathbf{z} = \mathbf{h}(\mathbf{x}) \end{cases} \tag{114}$$

where $\mathbf{x} \in \mathbb{R}^m$ is the state vector, $\mathbf{u} = [u_1 \quad \cdots \quad u_\ell] \in \mathbb{R}^\ell$ is the system input, $\mathbf{z} \in \mathbb{R}^k$ is the system output, and $\mathbf{f}_i$ for $i \in \{0, \ldots, \ell\}$ is the process function.

The zeroth order Lie derivative of a measurement function $\mathbf{h}$ is the function itself, i.e., $\mathcal{L}^0\mathbf{h} = \mathbf{h}(\mathbf{x})$. For any n-th order Lie derivative, $\mathcal{L}^n\mathbf{h}$, the $n+1$-th order Lie derivative $\mathcal{L}_{\mathbf{f}_i}^{n+1}\mathbf{h}$ with respect to a process function $\mathbf{f}_i$ can be computed as:

$$\mathcal{L}_{\mathbf{f}_i}^{n+1}\mathbf{h} = \nabla \mathcal{L}^n\mathbf{h} \cdot \mathbf{f}_i \tag{115}$$

where ∇ denotes the gradient operator with respect to $\mathbf{x}$ and " $\cdot$ " represents the vector inner product. Similarly, mixed higher order Lie derivatives can be defined as:

$$\mathcal{L}_{\mathbf{f}_i\mathbf{f}_{j\ldots}\mathbf{f}_k}^{n}\mathbf{h} = \mathcal{L}_{\mathbf{f}_i}(\mathcal{L}_{\mathbf{f}_{j\ldots}\mathbf{f}_k}^{n-1}\mathbf{h}) = \nabla \mathcal{L}_{\mathbf{f}_{j\ldots}\mathbf{f}_k}^{n-1}\mathbf{h} \cdot \mathbf{f}_i \tag{116}$$

where $i, j, k \in \{0, \ldots, \ell\}$.

The observability of a nonlinear system is determined by calculating the dimension of the space spanned by the gradients of Lie derivative of its output functions[20]. Hence, the observability matrix $\mathbf{O}$ of system (114) is defined as:

$$\mathbf{O} \triangleq \begin{bmatrix} \nabla \mathcal{L}^0\mathbf{h} \\ \nabla \mathcal{L}_{\mathbf{f}_i}^1\mathbf{h} \\ \vdots \\ \nabla \mathcal{L}_{\mathbf{f}_i\mathbf{f}_{j\ldots}\mathbf{f}_k}^n\mathbf{h} \\ \vdots \end{bmatrix} \tag{117}$$

To prove that a system is observable, it suffices to show that $\mathbf{O}$ is of full column rank. However, to prove that a system is unobservable, we have to find the null space of matrix $\mathbf{O}$, which may have infinitely many rows. This can be very challenging especially for high-dimensional systems, such as aided INS. To address this issue, we adopt the method proposed by [21] for analyzing observability of nonlinear systems in the form of Eq. (114).

Theorem G.1. *Assume that there exists a nonlinear transformation $\boldsymbol{\beta}(\mathbf{x}) = [\boldsymbol{\beta}_1(\mathbf{x})^\top \ldots \boldsymbol{\beta}_n(\mathbf{x})^\top]^\top$ (i.e., a set of basis functions) of the variable $\mathbf{x}$, such that:*

1. *The system measurement equation can be written as a function of $\boldsymbol{\beta}$, i.e., $\mathbf{z} = \mathbf{h}(\mathbf{x}) = \overline{\mathbf{h}}(\boldsymbol{\beta})$*
2. *$\frac{\partial \boldsymbol{\beta}}{\partial \mathbf{x}}\mathbf{f}_j$, for $j = \{0, \ldots, \ell\}$, is a function of $\boldsymbol{\beta}$*

Then the observability matrix of system (114) can be factorized as: $\mathbf{O} = \Xi\Omega$ *where* Ξ *is the observability matrix of the system:*

$$\begin{cases} \dot{\boldsymbol{\beta}} = \mathbf{g}_0(\boldsymbol{\beta}) + \sum_{i=1}^{\ell} \mathbf{g}_i(\boldsymbol{\beta}) u_i \\ \mathbf{z} = \overline{\mathbf{h}}(\boldsymbol{\beta}) \end{cases} \tag{118}$$

and Ω *can be represented as:*

$$\Omega = \frac{\partial \boldsymbol{\beta}}{\partial \mathbf{x}} \tag{119}$$

Proof. See [21]. □

Note that system (118) results by pre-multiplying the process function to system (114) with $\frac{\partial \boldsymbol{\beta}}{\partial \mathbf{x}}$:

$$\begin{cases} \frac{\partial \boldsymbol{\beta}}{\partial \mathbf{x}} \frac{\partial \mathbf{x}}{\partial t} = \frac{\partial \boldsymbol{\beta}}{\partial \mathbf{x}} \mathbf{f}_0(\mathbf{x}) + \frac{\partial \boldsymbol{\beta}}{\partial \mathbf{x}} \sum_{i=1}^{\ell} \mathbf{f}_i(\mathbf{x}) u_i \\ \mathbf{z} = \mathbf{h}(\mathbf{x}) \end{cases} \Rightarrow \begin{cases} \dot{\boldsymbol{\beta}} = \mathbf{g}_0(\boldsymbol{\beta}) + \sum_{i=1}^{\ell} \mathbf{g}_i(\boldsymbol{\beta}) u_i \\ \mathbf{z} = \overline{\mathbf{h}}(\boldsymbol{\beta}) \end{cases}$$

where $\mathbf{g}_i(\boldsymbol{\beta}) \triangleq \frac{\partial \boldsymbol{\beta}}{\partial \mathbf{x}}$ and $\overline{\mathbf{h}}(\boldsymbol{\beta}) \triangleq \mathbf{h}(\mathbf{x})$.

Corollary G.2. *If* Ξ *is of full column rank, i.e., system (118) is observable, then the unobservable directions of system (118) will be spanned by the null vectors of* Ω*.*

Proof. From $\mathbf{O} = \Xi\Omega$, we have $null(\mathbf{O}) = null(\Omega) \cup (null(\Xi) \cap range(\Omega))$. Therefore, if Ξ is of full column rank, i.e., system (118) is observable, then $null(\mathbf{O}) = null(\Omega)$. □

Base on Theorem G.1 and Corollary G.2, to find the unobservable directions of a system, we first need to define the basis functions, $\boldsymbol{\beta}$, which fulfill the first and second conditions of Theorem G.1. Then, we should prove that the infinite-dimensional matrix Ξ has full column rank, which satisfies the conditions of Corollary G.2.

G.2: System Propagation Model

For the aided INS, the IMU measurements are used for state propagation while the measurements from exteroceptive sensor are used for state update. The INS state $\mathbf{x}_I$ can be defined as:

$$\mathbf{x}_I = [{}^I_G\mathbf{s}^\top \quad \mathbf{b}_g^\top \quad {}^G\mathbf{v}_I^\top \quad \mathbf{b}_a^\top \quad {}^G\mathbf{p}_I^\top]^\top \tag{120}$$

where ${}^I_G\mathbf{s}$ is the Cayley-Gibbs-Rodriguez parameterization [34] representing the orientation of the global frame $\{G\}$ in the IMU frame of reference $\{I\}$. The time-continuous system evolution model:

$$\begin{aligned} {}^I_G\dot{\mathbf{s}}(t) &= \mathbf{D}({}^I\boldsymbol{\omega}(t) - \mathbf{b}_g(t)) \\ \dot{\mathbf{b}}_g(t) &= \mathbf{n}_g \\ {}^G\dot{\mathbf{V}}_I(t) &= {}^G\mathbf{a}(t) = {}^G\mathbf{g} + \mathbf{R}({}^I_G\mathbf{s}(t))^\top({}^I\mathbf{a}(t) - \mathbf{b}_a(t)) \\ \dot{\mathbf{b}}_a(t) &= \mathbf{n}_a \\ {}^G\dot{\mathbf{P}}_I(t) &= {}^G\mathbf{V}_I(t) \end{aligned} \tag{121}$$

where $\mathbf{D} \triangleq \frac{\partial \mathbf{s}}{\partial \boldsymbol{\theta}} = \frac{1}{2}(\mathbf{I} + \lfloor \mathbf{s}\times \rfloor + \mathbf{s}\mathbf{s}^\top)$, $\boldsymbol{\theta} = \alpha\hat{\mathbf{k}}$ represents a rotation by an angle α around the axis $\hat{\mathbf{k}}$, ${}^I\boldsymbol{\omega}(t) = [\omega_1 \quad \omega_2 \quad \omega_3]^\top$ and ${}^I\mathbf{a}(t) = [a_1 \quad a_2 \quad a_3]^\top$ are the rotational velocity and linear acceleration respectively, measured by the IMU and represented in $\{I\}$. ${}^G\mathbf{g}$ is the gravitational acceleration, $\mathbf{R}(\mathbf{s})$ is the rotation matrix corresponding to $\mathbf{s}$, and $\mathbf{n}_g$ and $\mathbf{n}_a$ are the gyroscope and accelerometer biases driving white Gaussian noises.

G.3: Observability Analysis for Point Feature

Based on the above analysis, the key is to prove Ξ is of full rank and then to find the unobservable direction from the Ω. Ω is determined by the basis functions $\boldsymbol{\beta}$. That means if we can find the same basis functions set $\boldsymbol{\beta}$ for aided INS, we can prove that these systems have the same unobservable directions. Therefore, the only job left unfinished is to check the rank of different Ξs for these systems.

G.3.1: Basis Functions For Point Measurement

With the generalized point measurement model and state propagation model, we can define the state vector as:

$$\mathbf{x} = [{}^{I}_{G}\mathbf{s}^\top \quad \mathbf{b}_g^\top \quad {}^{G}\mathbf{V}_I^\top \quad \mathbf{b}_a^\top \quad {}^{G}\mathbf{P}_I^\top \quad {}^{G}\mathbf{P}_\mathbf{f}^\top]^\top \tag{122}$$

For simplicity, we retain only a few of the subscripts and superscripts in the state elements and denote the system state vector as:

$$\mathbf{x} = [\mathbf{s}^\top \quad \mathbf{b}_g^\top \quad \mathbf{V}^\top \quad \mathbf{b}_a^\top \quad \mathbf{P}^\top \quad \mathbf{P}_\mathbf{f}^\top]^\top \tag{123}$$

Then the system state equation can be rewritten as:

$$\begin{bmatrix} \dot{\mathbf{s}} \\ \dot{\mathbf{b}}_g \\ \dot{\mathbf{V}} \\ \dot{\mathbf{b}}_a \\ \dot{\mathbf{P}} \\ \dot{\mathbf{P}}_\mathbf{f} \end{bmatrix} = \underbrace{\begin{bmatrix} -\mathbf{D}\mathbf{b}_g \\ \mathbf{0} \\ \mathbf{g} - \mathbf{R}^\top \mathbf{b}_a \\ \mathbf{0} \\ \mathbf{v} \\ \mathbf{0} \end{bmatrix}}_{\mathbf{f}_0} + \underbrace{\begin{bmatrix} \mathbf{D} \\ \mathbf{0} \\ \mathbf{0} \\ \mathbf{0} \\ \mathbf{0} \\ \mathbf{0} \end{bmatrix}}_{\mathbf{F}_1} \boldsymbol{\omega} + \underbrace{\begin{bmatrix} \mathbf{0} \\ \mathbf{0} \\ \mathbf{R}^\top \\ \mathbf{0} \\ \mathbf{0} \\ \mathbf{0} \end{bmatrix}}_{\mathbf{F}_2} \mathbf{a} \tag{124}$$

where $\mathbf{R} \triangleq \mathbf{R}(\mathbf{s})$. Note that $\mathbf{f}_0$ is a 18×1 vector, while $\mathbf{F}_1$ and $\mathbf{F_2}$ are both 24×3 matrices which is a compact form for representing process functions as:

$$\mathbf{F}_1\boldsymbol{\omega} = \mathbf{f}_{11}\omega_1 + \mathbf{f}_{12}\omega_2 + \mathbf{f}_{13}\omega_3 \tag{125}$$

$$\mathbf{F}_2\mathbf{a} = \mathbf{f}_{21}a_1 + \mathbf{f}_{22}a_2 + \mathbf{f}_{23}a_3 \tag{126}$$

Since all the terms in the preceding projections are defined based on the existing basis functions, we have found a complete basis set (see H.1):

$$\boldsymbol{\beta} = \begin{bmatrix} \boldsymbol{\beta}_1 \\ \boldsymbol{\beta}_2 \\ \boldsymbol{\beta}_3 \\ \boldsymbol{\beta}_4 \\ \boldsymbol{\beta}_5 \end{bmatrix} = \begin{bmatrix} \mathbf{R}(\mathbf{p}_\mathbf{f} - \mathbf{p}) \\ \mathbf{b}_g \\ \mathbf{R}\mathbf{v} \\ \mathbf{b}_a \\ \mathbf{R}\mathbf{g} \end{bmatrix} \tag{127}$$

Therefore, the new system with $\boldsymbol{\beta}$ basis:

$$\begin{bmatrix} \dot{\boldsymbol{\beta}}_1 \\ \dot{\boldsymbol{\beta}}_2 \\ \dot{\boldsymbol{\beta}}_3 \\ \dot{\boldsymbol{\beta}}_4 \\ \dot{\boldsymbol{\beta}}_5 \end{bmatrix} = \underbrace{\begin{bmatrix} -\lfloor \boldsymbol{\beta}_1 \times \rfloor \boldsymbol{\beta}_2 - \boldsymbol{\beta}_3 \\ \mathbf{0} \\ -\lfloor \boldsymbol{\beta}_3 \times \rfloor \boldsymbol{\beta}_2 + \boldsymbol{\beta}_5 - \boldsymbol{\beta}_4 \\ \mathbf{0} \\ -\lfloor \boldsymbol{\beta}_5 \times \rfloor \boldsymbol{\beta}_2 \end{bmatrix}}_{\mathbf{g}_0} + \underbrace{\begin{bmatrix} \lfloor \boldsymbol{\beta}_1 \times \rfloor \\ \mathbf{0} \\ \lfloor \boldsymbol{\beta}_3 \times \rfloor \\ \mathbf{0} \\ \lfloor \boldsymbol{\beta}_5 \times \rfloor \end{bmatrix}}_{\mathbf{G}_1} \boldsymbol{\omega} + \underbrace{\begin{bmatrix} \mathbf{0} \\ \mathbf{0} \\ \mathbf{I}_3 \\ \mathbf{0} \\ \mathbf{0} \end{bmatrix}}_{\mathbf{G}_2} \mathbf{a} \tag{128}$$

where $\mathbf{g}_0$ is a 18×1 vector, while $\mathbf{G}_1$ and $\mathbf{G}_2$ are both 24×3 matrices which is compact form for representing process functions as:

$$\mathbf{G}_1\boldsymbol{\omega} = \mathbf{g}_{11}\omega_1 + \mathbf{g}_{12}\omega_2 + \mathbf{g}_{13}\omega_3 \tag{129}$$

$$\mathbf{G}_2\mathbf{a} = \mathbf{g}_{21}a_1 + \mathbf{g}_{22}a_2 + \mathbf{g}_{23}a_3 \tag{130}$$

Base on the Theorem G.1, the observability matrix $\mathbf{O}$ of the aided INS is the product of observability matrix Ξ with the derivatives of the basis functions Ω. In what follows, we will first prove that matrix Ξ is of full column rank. Then, the null space of matrix Ω corresponds to the unobservable directions of the aided INS.

From the generalized measurement model Eq. (10), the Ξ contains two parts:

$$\Xi = \begin{bmatrix} \Xi^{(r)} \\ \Xi^{(b)} \end{bmatrix} \tag{131}$$

where $\Xi^{(r)}$ and $\Xi^{(b)}$ represents observability matrix from the range measurement and bearing measurement respectively. Therefore, in order to prove that matrix Ξ is of full column rank, we will inspect the column rank of $\Xi^{(r)}$ and $\Xi^{(b)}$ respectively. In Appendix H.2 and H.3 we showed that for range measurement and fulling bearing measurement $\Xi^{(r)}$ and $\Xi^{(b)}$ will have full column rank

G.3.2: Unobservable Direction

According to the basis set of $\boldsymbol{\beta}$, we have:

$$\Omega = \frac{\partial \boldsymbol{\beta}}{\partial \mathbf{x}} = \begin{bmatrix} \lfloor \mathbf{R}(\mathbf{p_f} - \mathbf{p}) \times \rfloor \frac{\partial \boldsymbol{\theta}}{\partial \mathbf{s}} & \mathbf{0} & \mathbf{0} & \mathbf{0} & -\mathbf{R} & \mathbf{R} \\ \mathbf{0} & \mathbf{I}_3 & \mathbf{0} & \mathbf{0} & \mathbf{0} & \mathbf{0} \\ \lfloor \mathbf{R}\mathbf{v} \times \rfloor \frac{\partial \boldsymbol{\theta}}{\partial \mathbf{s}} & \mathbf{0} & \mathbf{R} & \mathbf{0} & \mathbf{0} & \mathbf{0} \\ \mathbf{0} & \mathbf{0} & \mathbf{0} & \mathbf{I}_3 & \mathbf{0} & \mathbf{0} \\ \lfloor \mathbf{R}\mathbf{g} \times \rfloor \frac{\partial \boldsymbol{\theta}}{\partial \mathbf{s}} & \mathbf{0} & \mathbf{0} & \mathbf{0} & \mathbf{0} & \mathbf{0} \end{bmatrix} \tag{132}$$

Assuming A is the null space of Ω, and A should have the following form:

$$\mathbf{A} = \begin{bmatrix} \mathbf{A}_1^\top & \mathbf{A}_2^\top & \mathbf{A}_3^\top & \mathbf{A}_4^\top & \mathbf{A}_5^\top & \mathbf{A}_6^\top \end{bmatrix}^\top \neq \mathbf{0} \tag{133}$$

such that:

$$\Omega \mathbf{A} = \mathbf{0} \tag{134}$$

Hence, the system's unobservable directions can be described as:

$$\mathbf{A} = \begin{bmatrix} \frac{\partial \mathbf{s}}{\partial \theta} \mathbf{R}\mathbf{g} & \mathbf{0} \\ \mathbf{0} & \mathbf{0} \\ -\lfloor \mathbf{v} \times \rfloor \mathbf{g} & \mathbf{0} \\ \mathbf{0} & \mathbf{0} \\ -\lfloor \mathbf{p} \times \rfloor \mathbf{g} & \mathbf{I}_3 \\ -\lfloor \mathbf{p_f} \times \rfloor \mathbf{g} & \mathbf{I}_3 \end{bmatrix} \tag{135}$$

Therefore, the unobservable directions are the global position of exteroceptive sensor and the the point landmark, and the rotation about the gravity vector.

Appendix H: Basis Function and Rank Test for Point Measurement

H.1: Basis Functions for Point Measurement

According to the two conditions of Theorem G.1, we define the system's first basis function according to Eq. (9):

$$\boldsymbol{\beta_1} \triangleq \mathbf{R}(\mathbf{p_f} - \mathbf{p}) \tag{136}$$

According to the second condition of Theorem G.1, we will compute:

$$\frac{\partial \boldsymbol{\beta}_1}{\partial \mathbf{x}} = \begin{bmatrix} \frac{\partial \boldsymbol{\beta}_1}{\partial \mathbf{s}} & \frac{\partial \boldsymbol{\beta}_1}{\partial \mathbf{b}_g} & \frac{\partial \boldsymbol{\beta}_1}{\partial \mathbf{v}} & \frac{\partial \boldsymbol{\beta}_1}{\partial \mathbf{b}_a} & \frac{\partial \boldsymbol{\beta}_1}{\partial \mathbf{p}} & \frac{\partial \boldsymbol{\beta}_1}{\partial \mathbf{p_f}} \end{bmatrix} \tag{137}$$

$$= \begin{bmatrix} \lfloor \mathbf{R}(\mathbf{p_f} - \mathbf{p}) \times \rfloor \frac{\partial \boldsymbol{\theta}}{\partial \mathbf{s}} & \mathbf{0} & \mathbf{0} & \mathbf{0} & -\mathbf{R} & \mathbf{R} \end{bmatrix} \tag{138}$$

$$\frac{\partial \boldsymbol{\beta}_1}{\partial \mathbf{x}} \mathbf{f}_0 = -\lfloor \mathbf{R}(\mathbf{p_f} - \mathbf{p}) \times \rfloor \mathbf{b}_g - \mathbf{R}\mathbf{v} \triangleq -\lfloor \boldsymbol{\beta}_1 \times \rfloor \boldsymbol{\beta}_2 - \boldsymbol{\beta}_3 \tag{139}$$

$$\frac{\partial \boldsymbol{\beta}_1}{\partial \mathbf{x}} \mathbf{f}_{1i} = \lfloor \mathbf{R}(\mathbf{p_f} - \mathbf{p}) \times \rfloor \mathbf{e}_i \triangleq \lfloor \boldsymbol{\beta}_1 \times \rfloor \mathbf{e}_i \tag{140}$$

$$\frac{\partial \boldsymbol{\beta}_1}{\partial \mathbf{x}} \mathbf{f}_{2i} = \mathbf{0} \tag{141}$$

where $\frac{\partial \boldsymbol{\theta}}{\partial \mathbf{s}} \mathbf{D} = \frac{\partial \boldsymbol{\theta}}{\partial \mathbf{s}} \frac{\partial \mathbf{s}}{\partial \boldsymbol{\theta}} = \mathbf{I}_3$, $i \in \{1, 2, 3\}$ and we have defined two new basis elements: $\boldsymbol{\beta}_2 \triangleq \mathbf{b}_a$, $\boldsymbol{\beta}_3 \triangleq \mathbf{R}\mathbf{v}$.

Similarly, for the span of $\boldsymbol{\beta}_2$, we have:

$$\frac{\partial \boldsymbol{\beta}_2}{\partial \mathbf{x}} = \left[\frac{\partial \boldsymbol{\beta}_2}{\partial \mathbf{s}} \quad \frac{\partial \boldsymbol{\beta}_2}{\partial \mathbf{b}_g} \quad \frac{\partial \boldsymbol{\beta}_2}{\partial \mathbf{v}} \quad \frac{\partial \boldsymbol{\beta}_2}{\partial \mathbf{b}_a} \quad \frac{\partial \boldsymbol{\beta}_2}{\partial \mathbf{p}} \quad \frac{\partial \boldsymbol{\beta}_2}{\partial \mathbf{p_f}}\right] \tag{142}$$

$$= [\mathbf{0} \quad \mathbf{I}_3 \quad \mathbf{0} \quad \mathbf{0} \quad \mathbf{0} \quad \mathbf{0}] \tag{143}$$

$$\frac{\partial \boldsymbol{\beta}_2}{\partial \mathbf{x}} \mathbf{f}_0 = \mathbf{0} \tag{144}$$

$$\frac{\partial \boldsymbol{\beta}_2}{\partial \mathbf{x}} \mathbf{f}_{1i} = \mathbf{0} \tag{145}$$

$$\frac{\partial \boldsymbol{\beta}_2}{\partial \mathbf{x}} \mathbf{f}_{2i} = \mathbf{0} \tag{146}$$

where $i \in \{1, 2, 3\}$.

Then, for the span of $\boldsymbol{\beta}_3$, we have:

$$\frac{\partial \boldsymbol{\beta}_3}{\partial \mathbf{x}} = \left[\frac{\partial \boldsymbol{\beta}_3}{\partial \mathbf{s}} \quad \frac{\partial \boldsymbol{\beta}_3}{\partial \mathbf{b}_g} \quad \frac{\partial \boldsymbol{\beta}_3}{\partial \mathbf{v}} \quad \frac{\partial \boldsymbol{\beta}_3}{\partial \mathbf{b}_a} \quad \frac{\partial \boldsymbol{\beta}_3}{\partial \mathbf{p}} \quad \frac{\partial \boldsymbol{\beta}_3}{\partial \mathbf{p_f}}\right] \tag{147}$$

$$= \left[\lfloor \mathbf{R}\mathbf{v} \times \rfloor \frac{\partial \boldsymbol{\theta}}{\partial \mathbf{s}} \quad \mathbf{0} \quad \mathbf{R} \quad \mathbf{0} \quad \mathbf{0} \quad \mathbf{0}\right] \tag{148}$$

$$\frac{\partial \boldsymbol{\beta}_3}{\partial \mathbf{x}} \mathbf{f}_0 = -\lfloor \mathbf{R}\mathbf{v} \times \rfloor \mathbf{b}_g + \mathbf{R}\mathbf{g} - \mathbf{b}_a \triangleq -\lfloor \boldsymbol{\beta}_3 \times \rfloor \boldsymbol{\beta}_2 + \boldsymbol{\beta}_5 - \boldsymbol{\beta}_4 \tag{149}$$

$$\frac{\partial \boldsymbol{\beta}_3}{\partial \mathbf{x}} \mathbf{f}_{1i} = \lfloor \mathbf{R}\mathbf{v} \times \rfloor \mathbf{e}_i \triangleq \lfloor \boldsymbol{\beta} \times \rfloor \mathbf{e}_i \tag{150}$$

$$\frac{\partial \boldsymbol{\beta}_3}{\partial \mathbf{x}} \mathbf{f}_{2i} = \mathbf{I}_3 \mathbf{e}_i \tag{151}$$

where $i \in \{1, 2, 3\}$, and we have defined $\boldsymbol{\beta}_4 \triangleq \mathbf{b}_a$ and $\boldsymbol{\beta}_5 \triangleq \mathbf{R}\mathbf{g}$.

Then, for the span of $\boldsymbol{\beta}_4$ and $\boldsymbol{\beta}_5$ we have:

$$\frac{\partial \boldsymbol{\beta}_4}{\partial \mathbf{x}} = \left[\frac{\partial \boldsymbol{\beta}_4}{\partial \mathbf{s}} \quad \frac{\partial \boldsymbol{\beta}_4}{\partial \mathbf{b}_g} \quad \frac{\partial \boldsymbol{\beta}_4}{\partial \mathbf{v}} \quad \frac{\partial \boldsymbol{\beta}_4}{\partial \mathbf{b}_a} \quad \frac{\partial \boldsymbol{\beta}_4}{\partial \mathbf{p}} \quad \frac{\partial \boldsymbol{\beta}_4}{\partial \mathbf{p_f}}\right] \tag{152}$$

$$= [\mathbf{0} \quad \mathbf{0} \quad \mathbf{0} \quad \mathbf{I}_3 \quad \mathbf{0} \quad \mathbf{0}] \tag{153}$$

$$\frac{\partial \boldsymbol{\beta}_4}{\partial \mathbf{x}} \mathbf{f}_0 = \mathbf{0} \tag{154}$$

$$\frac{\partial \boldsymbol{\beta}_4}{\partial \mathbf{x}} \mathbf{f}_{1i} = \mathbf{0} \tag{155}$$

$$\frac{\partial \boldsymbol{\beta}_4}{\partial \mathbf{x}} \mathbf{f}_{2i} = \mathbf{0} \tag{156}$$

where $i \in \{1, 2, 3\}$.

$$\frac{\partial \boldsymbol{\beta}_5}{\partial \mathbf{x}} = \left[\frac{\partial \boldsymbol{\beta}_5}{\partial \mathbf{s}} \quad \frac{\partial \boldsymbol{\beta}_5}{\partial \mathbf{b}_g} \quad \frac{\partial \boldsymbol{\beta}_5}{\partial \mathbf{v}} \quad \frac{\partial \boldsymbol{\beta}_5}{\partial \mathbf{b}_a} \quad \frac{\partial \boldsymbol{\beta}_5}{\partial \mathbf{p}} \quad \frac{\partial \boldsymbol{\beta}_5}{\partial \mathbf{p_f}}\right] \tag{157}$$

$$= \left[\lfloor \mathbf{R}\mathbf{g} \times \rfloor \frac{\partial \boldsymbol{\theta}}{\partial \mathbf{s}} \quad \mathbf{0} \quad \mathbf{0} \quad \mathbf{0} \quad \mathbf{0} \quad \mathbf{0}\right] \tag{158}$$

$$\frac{\partial \boldsymbol{\beta}_5}{\partial \mathbf{x}} \mathbf{f}_0 = -\lfloor \mathbf{R}\mathbf{g} \times \rfloor \mathbf{b}_g \triangleq -\lfloor \boldsymbol{\beta}_5 \times \rfloor \boldsymbol{\beta}_2 \tag{159}$$

$$\frac{\partial \boldsymbol{\beta}_5}{\partial \mathbf{x}} \mathbf{f}_{1i} = \lfloor \mathbf{R}\mathbf{g} \times \rfloor \mathbf{e}_i \triangleq \lfloor \boldsymbol{\beta}_5 \times \rfloor \mathbf{e}_i \tag{160}$$

$$\frac{\partial \boldsymbol{\beta}_5}{\partial \mathbf{x}} \mathbf{f}_{2i} = \mathbf{0} \tag{161}$$

where $i \in \{1, 2, 3\}$.

H.2: Rank test for $\Xi^{(r)}$

Since the for the range measurement:$r = \sqrt{{}^{x}\mathbf{P}_{\mathbf{f}}^{\top}\,{}^{x}\mathbf{P}_{\mathbf{f}}}$ and $r \geq 0$, we take $r^2 = {}^{x}\mathbf{P}_{\mathbf{f}}^{\top}\,{}^{x}\mathbf{P}_{\mathbf{f}}$ as the equivalent measurement to simplify the mathematical analysis. Hence, the range measurement model can be expressed in terms of basis functions as:

$$\overline{\mathbf{h}}^{(r)} = \boldsymbol{\beta}_1^{\top}\boldsymbol{\beta}_1 \tag{162}$$

Then we will perform the nonlinear observability rank condition test according to [20].

- The zeroth-order Lie derivatives of the measurement function is:

$$\mathcal{L}^0\overline{\mathbf{h}}^{(r)} = \boldsymbol{\beta}_1^{\top}\boldsymbol{\beta}_1 \tag{163}$$

Then, the gradient of the zeroth order Lie derivative is:

$$\nabla\mathcal{L}^0\overline{\mathbf{h}}^{(r)} = \frac{\partial\overline{\mathbf{h}}^{(r)}}{\partial\boldsymbol{\beta}} = \begin{bmatrix} 2\boldsymbol{\beta}_1^{\top} & \mathbf{0} & \mathbf{0} & \mathbf{0} & \mathbf{0} \end{bmatrix} \tag{164}$$

- The first-order Lie derivative of $\overline{\mathbf{h}}^{(r)}$ with respect to $\mathbf{g}_0$, $\mathbf{g}_{1i}$ and $\mathbf{g}_{2i}$ are computed respectively, as:

$$\mathcal{L}^1_{\mathbf{g}_0}\overline{\mathbf{h}}^{(r)} = \nabla\mathcal{L}^0\overline{\mathbf{h}}^{(r)} \cdot \mathbf{g}_0 = -2\boldsymbol{\beta}_1^{\top}\boldsymbol{\beta}_3 \tag{165}$$

$$\mathcal{L}^1_{\mathbf{g}_{1i}}\overline{\mathbf{h}}^{(r)} = \nabla\mathcal{L}^0\overline{\mathbf{h}}^{(r)} \cdot \mathbf{g}_{1i} = \mathbf{0} \tag{166}$$

$$\mathcal{L}^1_{\mathbf{g}_{2i}}\overline{\mathbf{h}}^{(r)} = \nabla\mathcal{L}^0\overline{\mathbf{h}}^{(r)} \cdot \mathbf{g}_{2i} = \mathbf{0} \tag{167}$$

while the corresponding gradients are given by:

$$\nabla\mathcal{L}^1_{\mathbf{g}_0}\overline{\mathbf{h}}^{(r)} = \frac{\partial\mathcal{L}^1_{\mathbf{g}_0}\overline{\mathbf{h}}^{(r)}}{\partial\boldsymbol{\beta}} = \begin{bmatrix} -2\boldsymbol{\beta}_3^{\top} & \mathbf{0} & -2\boldsymbol{\beta}_1^{\top} & \mathbf{0} & \mathbf{0} \end{bmatrix} \tag{168}$$

$$\nabla\mathcal{L}^1_{\mathbf{g}_{1i}}\overline{\mathbf{h}}^{(r)} = \frac{\partial\mathcal{L}^1_{\mathbf{g}_{1i}}\overline{\mathbf{h}}^{(r)}}{\partial\boldsymbol{\beta}} = [\mathbf{0} \quad \mathbf{0} \quad \mathbf{0} \quad \mathbf{0} \quad \mathbf{0}] \tag{169}$$

$$\nabla\mathcal{L}^1_{\mathbf{g}_{2i}}\overline{\mathbf{h}}^{(r)} = \frac{\partial\mathcal{L}^1_{\mathbf{g}_{2i}}\overline{\mathbf{h}}^{(r)}}{\partial\boldsymbol{\beta}} = [\mathbf{0} \quad \mathbf{0} \quad \mathbf{0} \quad \mathbf{0} \quad \mathbf{0}] \tag{170}$$

- The second-order Lie derivatives are as following:

$$\mathcal{L}^2_{\mathbf{g}_0\mathbf{g}_0}\overline{\mathbf{h}}^{(r)} = \nabla\mathcal{L}^1_{\mathbf{g}_0}\overline{\mathbf{h}}^{(r)} \cdot \mathbf{g}_0 = 2\boldsymbol{\beta}_3^{\top}\boldsymbol{\beta}_3 - 2\boldsymbol{\beta}_1^{\top}\boldsymbol{\beta}_5 + 2\boldsymbol{\beta}_1^{\top}\boldsymbol{\beta}_4 \tag{171}$$

$$\mathcal{L}^2_{\mathbf{g}_0\mathbf{g}_{1i}}\overline{\mathbf{h}}^{(r)} = \nabla\mathcal{L}^2_{\mathbf{g}_0}\overline{\mathbf{h}}^{(r)} \cdot \mathbf{g}_{1i} = \mathbf{0} \tag{172}$$

$$\mathcal{L}^2_{\mathbf{g}_0\mathbf{g}_{2i}}\overline{\mathbf{h}}^{(r)} = \nabla\mathcal{L}^1_{\mathbf{g}_0}\overline{\mathbf{h}}^{(r)} \cdot \mathbf{g}_{2i} = -2\boldsymbol{\beta}_1^{\top}\mathbf{e}_i \tag{173}$$

while the corresponding gradients are:

$$\nabla\mathcal{L}^2_{\mathbf{g}_0\mathbf{g}_0}\overline{\mathbf{h}}^{(r)} = \frac{\partial\mathcal{L}^2_{\mathbf{g}_0\mathbf{g}_0}\overline{\mathbf{h}}^{(r)}}{\partial\boldsymbol{\beta}} = \begin{bmatrix} -2(\boldsymbol{\beta}_5^{\top} - \boldsymbol{\beta}_4^{\top}) & \mathbf{0} & 4\boldsymbol{\beta}_3^{\top} & 2\boldsymbol{\beta}_1^{\top} & -2\boldsymbol{\beta}_1^{\top} \end{bmatrix} \tag{174}$$

$$\nabla\mathcal{L}^2_{\mathbf{g}_0\mathbf{g}_{1i}}\overline{\mathbf{h}}^{(r)} = \frac{\partial\mathcal{L}^2_{\mathbf{g}_0\mathbf{g}_{1i}}\overline{\mathbf{h}}^{(r)}}{\partial\boldsymbol{\beta}} = [\mathbf{0} \quad \mathbf{0} \quad \mathbf{0} \quad \mathbf{0} \quad \mathbf{0}] \tag{175}$$

$$\nabla\mathcal{L}^2_{\mathbf{g}_0\mathbf{g}_{2i}}\overline{\mathbf{h}}^{(r)} = \frac{\partial\mathcal{L}^2_{\mathbf{g}_0\mathbf{g}_{2i}}\overline{\mathbf{h}}^{(r)}}{\partial\boldsymbol{\beta}} = \begin{bmatrix} -2\mathbf{e}_1^{\top} & \mathbf{0} & \mathbf{0} & \mathbf{0} & \mathbf{0} \end{bmatrix} \tag{176}$$

- The third-order Lie derivatives are as following:

$$\mathcal{L}^3_{\mathbf{g}_0\mathbf{g}_0\mathbf{g}_0}\overline{\mathbf{h}}^{(r)} = \nabla\mathcal{L}^2_{\mathbf{g}_0\mathbf{g}_0}\overline{\mathbf{h}}^{(r)}\cdot\mathbf{g}_0 = 6\boldsymbol{\beta}_3^\top\boldsymbol{\beta}_5 - 6\boldsymbol{\beta}_3^\top\boldsymbol{\beta}_4 - 2\boldsymbol{\beta}_4^\top\lfloor\boldsymbol{\beta}_1\times\rfloor\boldsymbol{\beta}_2 \tag{177}$$

$$\mathcal{L}^3_{\mathbf{g}_0\mathbf{g}_0\mathbf{g}_{1i}}\overline{\mathbf{h}}^{(r)} = \nabla\mathcal{L}^2_{\mathbf{g}_0\mathbf{g}_0}\overline{\mathbf{h}}^{(r)}\cdot\mathbf{g}_{1i} = 2\boldsymbol{\beta}_4^\top\lfloor\boldsymbol{\beta}_1\times\rfloor\mathbf{e}_i \tag{178}$$

$$\mathcal{L}^3_{\mathbf{g}_0\mathbf{g}_0\mathbf{g}_{2i}}\overline{\mathbf{h}}^{(r)} = \nabla\mathcal{L}^2_{\mathbf{g}_0\mathbf{g}_0}\overline{\mathbf{h}}^{(r)}\cdot\mathbf{g}_{2i} = 4\boldsymbol{\beta}_3^\top\mathbf{e}_i \tag{179}$$

$$\mathcal{L}^3_{\mathbf{g}_0\mathbf{g}_{2i}\mathbf{g}_0}\overline{\mathbf{h}}^{(r)} = \nabla\mathcal{L}^2_{\mathbf{g}_0\mathbf{g}_{2i}}\overline{\mathbf{h}}^{(r)}\cdot\mathbf{g}_0 = 2\mathbf{e}_i^\top\lfloor\boldsymbol{\beta}_1\times\rfloor\boldsymbol{\beta}_2 + 2\mathbf{e}_i^\top\boldsymbol{\beta}_3 \tag{180}$$

$$\mathcal{L}^3_{\mathbf{g}_0\mathbf{g}_{2i}\mathbf{g}_{1j}}\overline{\mathbf{h}}^{(r)} = \nabla\mathcal{L}^2_{\mathbf{g}_0\mathbf{g}_{2i}}\overline{\mathbf{h}}^{(r)}\cdot\mathbf{g}_{1j} = -2\mathbf{e}_i^\top\lfloor\boldsymbol{\beta}_1\times\rfloor\mathbf{e}_j \tag{181}$$

while the corresponding gradients are:

$$\nabla\mathcal{L}^3_{\mathbf{g}_0\mathbf{g}_0\mathbf{g}_0}\overline{\mathbf{h}}^{(r)} = \frac{\partial\mathcal{L}^3_{\mathbf{g}_0\mathbf{g}_0\mathbf{g}_0}\overline{\mathbf{h}}^{(r)}}{\partial\boldsymbol{\beta}} \tag{182}$$

$$= \begin{bmatrix}2\boldsymbol{\beta}_4^\top\lfloor\boldsymbol{\beta}_2\times\rfloor & -2\boldsymbol{\beta}_4\lfloor\boldsymbol{\beta}_1\times\rfloor & 6(\boldsymbol{\beta}_5^\top-\boldsymbol{\beta}_4^\top) & -6\boldsymbol{\beta}_3^\top+2\boldsymbol{\beta}_2^\top\lfloor\boldsymbol{\beta}_1\times\rfloor & 6\boldsymbol{\beta}_3^\top\end{bmatrix}$$

$$\nabla\mathcal{L}^3_{\mathbf{g}_0\mathbf{g}_0\mathbf{g}_{1i}}\overline{\mathbf{h}}^{(r)} = \frac{\partial\mathcal{L}^3_{\mathbf{g}_0\mathbf{g}_0\mathbf{g}_{1i}}\overline{\mathbf{h}}^{(r)}}{\partial\boldsymbol{\beta}} = \begin{bmatrix}-2\boldsymbol{\beta}_4^\top\lfloor\mathbf{e}_i\times\rfloor & \mathbf{0} & \mathbf{0} & -2\mathbf{e}_i^\top\lfloor\boldsymbol{\beta}_1\times\rfloor & \mathbf{0}\end{bmatrix} \tag{183}$$

$$\nabla\mathcal{L}^3_{\mathbf{g}_0\mathbf{g}_0\mathbf{g}_{2i}}\overline{\mathbf{h}}^{(r)} = \frac{\partial\mathcal{L}^3_{\mathbf{g}_0\mathbf{g}_0\mathbf{g}_{2i}}\overline{\mathbf{h}}^{(r)}}{\partial\boldsymbol{\beta}} = \begin{bmatrix}\mathbf{0} & \mathbf{0} & 4\mathbf{e}_i^\top & \mathbf{0} & \mathbf{0}\end{bmatrix} \tag{184}$$

$$\nabla\mathcal{L}^3_{\mathbf{g}_0\mathbf{g}_{2i}\mathbf{g}_0}\overline{\mathbf{h}}^{(r)} = \frac{\partial\mathcal{L}^3_{\mathbf{g}_0\mathbf{g}_{2i}\mathbf{g}_0}\overline{\mathbf{h}}^{(r)}}{\partial\boldsymbol{\beta}} = \begin{bmatrix}-2\mathbf{e}_i^\top\lfloor\boldsymbol{\beta}_2\times\rfloor & 2\mathbf{e}_i^\top\lfloor\boldsymbol{\beta}_1\times\rfloor & 2\mathbf{e}_i^\top & \mathbf{0} & \mathbf{0}\end{bmatrix} \tag{185}$$

$$\nabla\mathcal{L}^3_{\mathbf{g}_0\mathbf{g}_{2i}\mathbf{g}_{1j}}\overline{\mathbf{h}}^{(r)} = \frac{\partial\mathcal{L}^3_{\mathbf{g}_0\mathbf{g}_{2i}\mathbf{g}_{1j}}\overline{\mathbf{h}}^{(r)}}{\partial\boldsymbol{\beta}} = \begin{bmatrix}2\mathbf{e}_i^\top\lfloor\mathbf{e}_j\times\rfloor & \mathbf{0} & \mathbf{0} & \mathbf{0} & \mathbf{0}\end{bmatrix} \tag{186}$$

- The fourth-order Lie derivatives are as following:

$$\mathcal{L}^4_{\mathbf{g}_0\mathbf{g}_0\mathbf{g}_0\mathbf{g}_0}\overline{\mathbf{h}}^{(r)} = \nabla\mathcal{L}^3_{\mathbf{g}_0\mathbf{g}_0\mathbf{g}_0}\overline{\mathbf{h}}^{(r)}\cdot\mathbf{g}_0$$

$$= -2\boldsymbol{\beta}_4^\top\lfloor\boldsymbol{\beta}_2\times\rfloor\lfloor\boldsymbol{\beta}_1\times\rfloor\boldsymbol{\beta}_2 - 8\boldsymbol{\beta}_4^\top\lfloor\boldsymbol{\beta}_2\times\rfloor\boldsymbol{\beta}_3 + 6(\boldsymbol{\beta}_4^\top-\boldsymbol{\beta}_5^\top)(\boldsymbol{\beta}_4-\boldsymbol{\beta}_5) \tag{187}$$

$$\mathcal{L}^4_{\mathbf{g}_0\mathbf{g}_0\mathbf{g}_{2i}\mathbf{g}_0}\overline{\mathbf{h}}^{(r)} = \nabla\mathcal{L}^4_{\mathbf{g}_0\mathbf{g}_0\mathbf{g}_{2i}}\overline{\mathbf{h}}^{(r)}\cdot\mathbf{g}_0 = -4\mathbf{e}_i^\top\lfloor\boldsymbol{\beta}_3\times\rfloor\boldsymbol{\beta}_2 + 4\mathbf{e}_i^\top\boldsymbol{\beta}_5 - 4\mathbf{e}_i^\top\boldsymbol{\beta}_4 \tag{188}$$

while the corresponding gradients are:

$$\nabla\mathcal{L}^4_{\mathbf{g}_0\mathbf{g}_0\mathbf{g}_0\mathbf{g}_0}\overline{\mathbf{h}}^{(r)} = \begin{bmatrix}\frac{\partial\mathcal{L}^4_{\mathbf{g}_0\mathbf{g}_0\mathbf{g}_0\mathbf{g}_0}\overline{\mathbf{h}}^{(r)}}{\partial\boldsymbol{\beta}_1} & \frac{\partial\mathcal{L}^4_{\mathbf{g}_0\mathbf{g}_0\mathbf{g}_0\mathbf{g}_0}\overline{\mathbf{h}}^{(r)}}{\partial\boldsymbol{\beta}_2} & \frac{\partial\mathcal{L}^4_{\mathbf{g}_0\mathbf{g}_0\mathbf{g}_0\mathbf{g}_0}\overline{\mathbf{h}}^{(r)}}{\partial\boldsymbol{\beta}_3} & \frac{\partial\mathcal{L}^4_{\mathbf{g}_0\mathbf{g}_0\mathbf{g}_0\mathbf{g}_0}\overline{\mathbf{h}}^{(r)}}{\partial\boldsymbol{\beta}_4} & \frac{\partial\mathcal{L}^4_{\mathbf{g}_0\mathbf{g}_0\mathbf{g}_0\mathbf{g}_0}\overline{\mathbf{h}}^{(r)}}{\partial\boldsymbol{\beta}_5}\end{bmatrix} \tag{189}$$

$$\nabla\mathcal{L}^4_{\mathbf{g}_0\mathbf{g}_0\mathbf{g}_{2i}\mathbf{g}_0}\overline{\mathbf{h}}^{(r)} = \frac{\partial\mathcal{L}^4_{\mathbf{g}_0\mathbf{g}_0\mathbf{g}_{2i}\mathbf{g}_0}\overline{\mathbf{h}}^{(r)}}{\partial\boldsymbol{\beta}} = \begin{bmatrix}\mathbf{0} & -4\mathbf{e}_i^\top\lfloor\boldsymbol{\beta}_3\times\rfloor & 4\mathbf{e}_i^\top\lfloor\boldsymbol{\beta}_2\times\rfloor & -4\mathbf{e}_i^\top & 4\mathbf{e}_i^\top\end{bmatrix} \tag{190}$$

where the terms in Eq. (189) are:

$$\frac{\partial\mathcal{L}^4_{\mathbf{g}_0\mathbf{g}_0\mathbf{g}_0\mathbf{g}_0}\overline{\mathbf{h}}^{(r)}}{\partial\boldsymbol{\beta}_1} = 2\boldsymbol{\beta}_4^\top\lfloor\boldsymbol{\beta}_2\times\rfloor^2 \tag{191}$$

$$\frac{\partial\mathcal{L}^4_{\mathbf{g}_0\mathbf{g}_0\mathbf{g}_0\mathbf{g}_0}\overline{\mathbf{h}}^{(r)}}{\partial\boldsymbol{\beta}_2} = -2\boldsymbol{\beta}_4^\top\lfloor\boldsymbol{\beta}_2\times\rfloor\lfloor\boldsymbol{\beta}_1\times\rfloor + 2\boldsymbol{\beta}_2^\top\lfloor\boldsymbol{\beta}_1\times\rfloor\lfloor\boldsymbol{\beta}_4\times\rfloor + 8\boldsymbol{\beta}_4^\top\lfloor\boldsymbol{\beta}_3\times\rfloor \tag{192}$$

$$\frac{\partial\mathcal{L}^4_{\mathbf{g}_0\mathbf{g}_0\mathbf{g}_0\mathbf{g}_0}\overline{\mathbf{h}}^{(r)}}{\partial\boldsymbol{\beta}_3} = -8\boldsymbol{\beta}_4^\top\lfloor\boldsymbol{\beta}_2\times\rfloor \tag{193}$$

$$\frac{\partial\mathcal{L}^4_{\mathbf{g}_0\mathbf{g}_0\mathbf{g}_0\mathbf{g}_0}\overline{\mathbf{h}}^{(r)}}{\partial\boldsymbol{\beta}_4} = -2\boldsymbol{\beta}_2^\top\lfloor\boldsymbol{\beta}_1\times\rfloor\lfloor\boldsymbol{\beta}_2\times\rfloor + 8\boldsymbol{\beta}_3^\top\lfloor\boldsymbol{\beta}_2\times\rfloor + 12(\boldsymbol{\beta}_4^\top-\boldsymbol{\beta}_5^\top) \tag{194}$$

$$\frac{\partial\mathcal{L}^4_{\mathbf{g}_0\mathbf{g}_0\mathbf{g}_0\mathbf{g}_0}\overline{\mathbf{h}}^{(r)}}{\partial\boldsymbol{\beta}_5} = 12(\boldsymbol{\beta}_5^\top-\boldsymbol{\beta}_4^\top) \tag{195}$$

- The fifth-order Lie derivatives are as following:

$$\mathcal{L}^5_{\mathbf{g}_0\mathbf{g}_0\mathbf{g}_{2i}\mathbf{g}_0\mathbf{g}_{1j}}\overline{\mathbf{h}}^{(r)} = \nabla\mathcal{L}^4_{\mathbf{g}_0\mathbf{g}_0\mathbf{g}_{2i}\mathbf{g}_0}\overline{\mathbf{h}}^{(r)}\cdot\mathbf{g}_{1j} = 4\mathbf{e}_i^\top\lfloor\boldsymbol{\beta}_2\times\rfloor\lfloor\boldsymbol{\beta}_3\times\rfloor\mathbf{e}_j + 4\mathbf{e}_i^\top\lfloor\boldsymbol{\beta}_5\times\rfloor\mathbf{e}_j \tag{196}$$

while the corresponding gradients are:

$$\begin{aligned}\nabla\mathcal{L}^5_{\mathbf{g}_0\mathbf{g}_0\mathbf{g}_{2i}\mathbf{g}_0\mathbf{g}_{1j}}\overline{\mathbf{h}}^{(r)} &= \frac{\partial\mathcal{L}^5_{\mathbf{g}_0\mathbf{g}_0\mathbf{g}_{2i}\mathbf{g}_0\mathbf{g}_{1j}}\overline{\mathbf{h}}^{(r)}}{\partial\boldsymbol{\beta}} \\ &= \begin{bmatrix}\mathbf{0} & -4\mathbf{e}_j^\top\lfloor\boldsymbol{\beta}_3\times\rfloor\lfloor\mathbf{e}_i\times\rfloor & -4\mathbf{e}_i^\top\lfloor\boldsymbol{\beta}_2\times\rfloor\lfloor\mathbf{e}_j\times\rfloor & \mathbf{0} & -4\mathbf{e}_i^\top\lfloor\mathbf{e}_j\times\rfloor\end{bmatrix}\end{aligned} \tag{197}$$

Therefore, we can construct the $\Xi^{(r)}$ matrix (198) and we can find out that $\Xi^{(r)}$ is of full rank.

$$\Xi^{(r)} = \begin{bmatrix}\nabla\mathcal{L}^2_{\mathbf{g}_0\mathbf{g}_{21}}\overline{\mathbf{h}}^{(r)} \\ \nabla\mathcal{L}^2_{\mathbf{g}_0\mathbf{g}_{22}}\overline{\mathbf{h}}^{(r)} \\ \nabla\mathcal{L}^2_{\mathbf{g}_0\mathbf{g}_{23}}\overline{\mathbf{h}}^{(r)} \\ \nabla\mathcal{L}^5_{\mathbf{g}_0\mathbf{g}_0\mathbf{g}_{21}\mathbf{g}_0\mathbf{g}_{12}}\overline{\mathbf{h}}^{(r)} \\ \nabla\mathcal{L}^5_{\mathbf{g}_0\mathbf{g}_0\mathbf{g}_{22}\mathbf{g}_0\mathbf{g}_{13}}\overline{\mathbf{h}}^{(r)} \\ \nabla\mathcal{L}^5_{\mathbf{g}_0\mathbf{g}_0\mathbf{g}_{23}\mathbf{g}_0\mathbf{g}_{11}}\overline{\mathbf{h}}^{(r)} \\ \nabla\mathcal{L}^3_{\mathbf{g}_0\mathbf{g}_0\mathbf{g}_{21}}\overline{\mathbf{h}}^{(r)} \\ \nabla\mathcal{L}^3_{\mathbf{g}_0\mathbf{g}_0\mathbf{g}_{22}}\overline{\mathbf{h}}^{(r)} \\ \nabla\mathcal{L}^3_{\mathbf{g}_0\mathbf{g}_0\mathbf{g}_{23}}\overline{\mathbf{h}}^{(r)} \\ \nabla\mathcal{L}^4_{\mathbf{g}_0\mathbf{g}_0\mathbf{g}_{21}\mathbf{g}_0}\overline{\mathbf{h}}^{(r)} \\ \nabla\mathcal{L}^4_{\mathbf{g}_0\mathbf{g}_0\mathbf{g}_{22}\mathbf{g}_0}\overline{\mathbf{h}}^{(r)} \\ \nabla\mathcal{L}^4_{\mathbf{g}_0\mathbf{g}_0\mathbf{g}_{23}\mathbf{g}_0}\overline{\mathbf{h}}^{(r)} \\ \nabla\mathcal{L}^5_{\mathbf{g}_0\mathbf{g}_0\mathbf{g}_{21}\mathbf{g}_0\mathbf{g}_{13}}\overline{\mathbf{h}}^{(r)} \\ \nabla\mathcal{L}^5_{\mathbf{g}_0\mathbf{g}_0\mathbf{g}_{22}\mathbf{g}_0\mathbf{g}_{11}}\overline{\mathbf{h}}^{(r)} \\ \nabla\mathcal{L}^5_{\mathbf{g}_0\mathbf{g}_0\mathbf{g}_{23}\mathbf{g}_0\mathbf{g}_{12}}\overline{\mathbf{h}}^{(r)}\end{bmatrix} = \begin{bmatrix}-2\mathbf{e}_1^\top & \mathbf{0} & \mathbf{0} & \mathbf{0} & \mathbf{0} \\ -2\mathbf{e}_2^\top & \mathbf{0} & \mathbf{0} & \mathbf{0} & \mathbf{0} \\ -2\mathbf{e}_3^\top & \mathbf{0} & \mathbf{0} & \mathbf{0} & \mathbf{0} \\ \mathbf{0} & -4\mathbf{e}_2^\top\lfloor\boldsymbol{\beta}_3\times\rfloor\lfloor\mathbf{e}_1\times\rfloor & -4\mathbf{e}_1^\top\lfloor\boldsymbol{\beta}_2\times\rfloor\lfloor\mathbf{e}_2\times\rfloor & \mathbf{0} & -4\mathbf{e}_1^\top\lfloor\mathbf{e}_2\times\rfloor \\ \mathbf{0} & -4\mathbf{e}_3^\top\lfloor\boldsymbol{\beta}_3\times\rfloor\lfloor\mathbf{e}_2\times\rfloor & -4\mathbf{e}_2^\top\lfloor\boldsymbol{\beta}_2\times\rfloor\lfloor\mathbf{e}_3\times\rfloor & \mathbf{0} & -4\mathbf{e}_2^\top\lfloor\mathbf{e}_3\times\rfloor \\ \mathbf{0} & -4\mathbf{e}_1^\top\lfloor\boldsymbol{\beta}_3\times\rfloor\lfloor\mathbf{e}_3\times\rfloor & -4\mathbf{e}_3^\top\lfloor\boldsymbol{\beta}_2\times\rfloor\lfloor\mathbf{e}_1\times\rfloor & \mathbf{0} & -4\mathbf{e}_3^\top\lfloor\mathbf{e}_1\times\rfloor \\ \mathbf{0} & \mathbf{0} & 4\mathbf{e}_1^\top & \mathbf{0} & \mathbf{0} \\ \mathbf{0} & \mathbf{0} & 4\mathbf{e}_2^\top & \mathbf{0} & \mathbf{0} \\ \mathbf{0} & \mathbf{0} & 4\mathbf{e}_3^\top & \mathbf{0} & \mathbf{0} \\ \mathbf{0} & -4\mathbf{e}_1^\top\lfloor\boldsymbol{\beta}_3\times\rfloor & 4\mathbf{e}_1^\top\lfloor\boldsymbol{\beta}_2\times\rfloor & -4\mathbf{e}_1^\top & 4\mathbf{e}_1^\top \\ \mathbf{0} & -4\mathbf{e}_1^\top\lfloor\boldsymbol{\beta}_3\times\rfloor & 4\mathbf{e}_2^\top\lfloor\boldsymbol{\beta}_2\times\rfloor & -4\mathbf{e}_2^\top & 4\mathbf{e}_2^\top \\ \mathbf{0} & -4\mathbf{e}_1^\top\lfloor\boldsymbol{\beta}_3\times\rfloor & 4\mathbf{e}_3^\top\lfloor\boldsymbol{\beta}_2\times\rfloor & -4\mathbf{e}_3^\top & 4\mathbf{e}_3^\top \\ \mathbf{0} & -4\mathbf{e}_3^\top\lfloor\boldsymbol{\beta}_3\times\rfloor\lfloor\mathbf{e}_1\times\rfloor & -4\mathbf{e}_1^\top\lfloor\boldsymbol{\beta}_2\times\rfloor\lfloor\mathbf{e}_3\times\rfloor & \mathbf{0} & -4\mathbf{e}_1^\top\lfloor\mathbf{e}_3\times\rfloor \\ \mathbf{0} & -4\mathbf{e}_1^\top\lfloor\boldsymbol{\beta}_3\times\rfloor\lfloor\mathbf{e}_2\times\rfloor & -4\mathbf{e}_2^\top\lfloor\boldsymbol{\beta}_2\times\rfloor\lfloor\mathbf{e}_1\times\rfloor & \mathbf{0} & -4\mathbf{e}_2^\top\lfloor\mathbf{e}_1\times\rfloor \\ \mathbf{0} & -4\mathbf{e}_2^\top\lfloor\boldsymbol{\beta}_3\times\rfloor\lfloor\mathbf{e}_3\times\rfloor & -4\mathbf{e}_3^\top\lfloor\boldsymbol{\beta}_2\times\rfloor\lfloor\mathbf{e}_2\times\rfloor & \mathbf{0} & -4\mathbf{e}_3^\top\lfloor\mathbf{e}_2\times\rfloor\end{bmatrix} \tag{198}$$

Given random motion, the diagonal block of the $\Xi^{(r)}$ are all of full rank (3). Therefore, $\Xi^{(r)}$ is of full column rank.

H.3: Rank test for $\Xi^{(b)}$

For the analysis, with the generalized point measurement model(10)(11), we consider the noise free case, and define $\boldsymbol{\gamma} = \mathbf{b}_{\perp 1}$, $\boldsymbol{\gamma} = \mathbf{b}_{\perp 2}$. Then we will perform the nonlinear observability rank condition test according to [20].

- The zeroth-order Lie derivatives of the measurement function is:

$$\mathcal{L}^0\overline{\mathbf{h}}^{(b)} = \begin{bmatrix}\mathcal{L}^0\overline{\mathbf{h}}_1^{(b)} \\ \mathcal{L}^0\overline{\mathbf{h}}_2^{(b)}\end{bmatrix} = \begin{bmatrix}\boldsymbol{\gamma}_1^\top\boldsymbol{\beta}_1 \\ \boldsymbol{\gamma}_2^\top\boldsymbol{\beta}_1\end{bmatrix} = \begin{bmatrix}\boldsymbol{\gamma}_1^\top \\ \boldsymbol{\gamma}_2^\top\end{bmatrix}\boldsymbol{\beta}_1 \tag{199}$$

Then, the gradients of the zeroth-order Lie derivative is:

$$\nabla\mathcal{L}^0\overline{\mathbf{h}}^{(b)} = \begin{bmatrix}\nabla\mathcal{L}^0\overline{\mathbf{h}}_1^{(b)} \\ \nabla\mathcal{L}^0\overline{\mathbf{h}}_2^{(b)}\end{bmatrix} = \begin{bmatrix}\frac{\partial\overline{\mathbf{h}}_1^{(b)}}{\partial\boldsymbol{\beta}} \\ \frac{\partial\overline{\mathbf{h}}_2^{(b)}}{\partial\boldsymbol{\beta}}\end{bmatrix} = \begin{bmatrix}\boldsymbol{\gamma}_1^\top & \mathbf{0} & \mathbf{0} & \mathbf{0} & \mathbf{0} \\ \boldsymbol{\gamma}_2^\top & \mathbf{0} & \mathbf{0} & \mathbf{0} & \mathbf{0}\end{bmatrix} = \begin{bmatrix}\boldsymbol{\gamma}_1^\top \\ \boldsymbol{\gamma}_2^\top\end{bmatrix}\begin{bmatrix}\mathbf{I}_3 & \mathbf{0} & \mathbf{0} & \mathbf{0} & \mathbf{0}\end{bmatrix}$$

- The first-order Lie derivative of $\overline{\mathbf{h}}^{(b)}$ with respect to $\mathbf{g}_0$, $\mathbf{g}_{1i}$ and $\mathbf{g}_{2i}$ are computed respectively, as:

$$\mathcal{L}^1_{\mathbf{g}_0}\overline{\mathbf{h}}^{(b)} = \nabla\mathcal{L}^0\overline{\mathbf{h}}^{(b)}\cdot\mathbf{g}_0 = \begin{bmatrix} \nabla\mathcal{L}^0\overline{\mathbf{h}}^{(b)}_1\cdot\mathbf{g}_0 \\ \nabla\mathcal{L}^0\overline{\mathbf{h}}^{(b)}_2\cdot\mathbf{g}_0 \end{bmatrix} \tag{200}$$

$$= \begin{bmatrix} -\boldsymbol{\gamma}_1^\top\lfloor\boldsymbol{\beta}_1\times\rfloor\boldsymbol{\beta}_2 - \boldsymbol{\gamma}_1^\top\boldsymbol{\beta}_3 \\ -\boldsymbol{\gamma}_2^\top\lfloor\boldsymbol{\beta}_1\times\rfloor\boldsymbol{\beta}_2 - \boldsymbol{\gamma}_2^\top\boldsymbol{\beta}_3 \end{bmatrix} = \begin{bmatrix} \boldsymbol{\gamma}_1^\top \\ \boldsymbol{\gamma}_2^\top \end{bmatrix}[-\lfloor\boldsymbol{\beta}_1\times\rfloor\boldsymbol{\beta}_2 - \mathbf{I}_3\boldsymbol{\beta}_3] \tag{201}$$

$$\mathcal{L}^1_{\mathbf{g}_{1i}}\overline{\mathbf{h}}^{(b)} = \nabla\mathcal{L}^0\overline{\mathbf{h}}^{(b)}\cdot\mathbf{g}_{1i} = \begin{bmatrix} \nabla\mathcal{L}^0\overline{\mathbf{h}}^{(b)}_1\cdot\mathbf{g}_{1i} \\ \nabla\mathcal{L}^0\overline{\mathbf{h}}^{(b)}_2\cdot\mathbf{g}_{1i} \end{bmatrix} = \begin{bmatrix} \boldsymbol{\gamma}_1^\top\lfloor\boldsymbol{\beta}_1\times\rfloor\mathbf{e}_i \\ \boldsymbol{\gamma}_2^\top\lfloor\boldsymbol{\beta}_1\times\rfloor\mathbf{e}_i \end{bmatrix} = \begin{bmatrix} \boldsymbol{\gamma}_1^\top \\ \boldsymbol{\gamma}_2^\top \end{bmatrix}[\lfloor\boldsymbol{\beta}_1\times\rfloor\mathbf{e}_i] \tag{202}$$

$$\mathcal{L}^1_{\mathbf{g}_{2i}}\overline{\mathbf{h}}^{(b)} = \nabla\mathcal{L}^0\overline{\mathbf{h}}^{(b)}\cdot\mathbf{g}_{2i} = \begin{bmatrix} \nabla\mathcal{L}^0\overline{\mathbf{h}}^{(b)}_1\cdot\mathbf{g}_{2i} \\ \nabla\mathcal{L}^0\overline{\mathbf{h}}^{(b)}_2\cdot\mathbf{g}_{2i} \end{bmatrix} = \begin{bmatrix} \mathbf{0} \\ \mathbf{0} \end{bmatrix} \tag{203}$$

while the corresponding gradients are given by:

$$\nabla\mathcal{L}^1_{\mathbf{g}_0}\overline{\mathbf{h}}^{(b)} = \begin{bmatrix} \nabla\mathcal{L}^1_{\mathbf{g}_0}\overline{\mathbf{h}}^{(b)}_1 \\ \nabla\mathcal{L}^1_{\mathbf{g}_0}\overline{\mathbf{h}}^{(b)}_2 \end{bmatrix} = \begin{bmatrix} \frac{\partial\mathcal{L}^1_{\mathbf{g}_0}\overline{\mathbf{h}}^{(b)}_1}{\partial\boldsymbol{\beta}} \\ \frac{\partial\mathcal{L}^1_{\mathbf{g}_0}\overline{\mathbf{h}}^{(b)}_2}{\partial\boldsymbol{\beta}} \end{bmatrix} = \begin{bmatrix} \boldsymbol{\gamma}_1^\top\lfloor\boldsymbol{\beta}_2\times\rfloor & -\boldsymbol{\gamma}_1^\top\lfloor\boldsymbol{\beta}_1\times\rfloor & -\boldsymbol{\gamma}_1^\top & \mathbf{0} & \mathbf{0} \\ \boldsymbol{\gamma}_2^\top\lfloor\boldsymbol{\beta}_2\times\rfloor & -\boldsymbol{\gamma}_2^\top\lfloor\boldsymbol{\beta}_1\times\rfloor & -\boldsymbol{\gamma}_2^\top & \mathbf{0} & \mathbf{0} \end{bmatrix} \tag{204}$$

$$= \begin{bmatrix} \boldsymbol{\gamma}_1^\top \\ \boldsymbol{\gamma}_2^\top \end{bmatrix}\begin{bmatrix} \lfloor\boldsymbol{\beta}_2\times\rfloor & -\lfloor\boldsymbol{\beta}_1\times\rfloor & -\mathbf{I}_3 & \mathbf{0} & \mathbf{0} \end{bmatrix} \tag{205}$$

$$\nabla\mathcal{L}^1_{\mathbf{g}_{1i}}\overline{\mathbf{h}}^{(b)} = \begin{bmatrix} \nabla\mathcal{L}^1_{\mathbf{g}_{1i}}\overline{\mathbf{h}}^{(b)}_1 \\ \nabla\mathcal{L}^1_{\mathbf{g}_{1i}}\overline{\mathbf{h}}^{(b)}_2 \end{bmatrix} = \begin{bmatrix} \frac{\partial\mathcal{L}^1_{\mathbf{g}_{1i}}\overline{\mathbf{h}}^{(b)}_1}{\partial\boldsymbol{\beta}} \\ \frac{\partial\mathcal{L}^1_{\mathbf{g}_{1i}}\overline{\mathbf{h}}^{(b)}_2}{\partial\boldsymbol{\beta}} \end{bmatrix} = \begin{bmatrix} -\boldsymbol{\gamma}_1^\top\lfloor\mathbf{e}_i\times\rfloor & \mathbf{0} & \mathbf{0} & \mathbf{0} & \mathbf{0} \\ -\boldsymbol{\gamma}_2^\top\lfloor\mathbf{e}_i\times\rfloor & \mathbf{0} & \mathbf{0} & \mathbf{0} & \mathbf{0} \end{bmatrix} \tag{206}$$

$$= \begin{bmatrix} \boldsymbol{\gamma}_1^\top \\ \boldsymbol{\gamma}_2^\top \end{bmatrix}\begin{bmatrix} -\lfloor\mathbf{e}_i\times\rfloor & \mathbf{0} & \mathbf{0} & \mathbf{0} & \mathbf{0} \end{bmatrix} \tag{207}$$

$$\nabla\mathcal{L}^1_{\mathbf{g}_{1i}}\overline{\mathbf{h}}^{(b)} = \begin{bmatrix} \nabla\mathcal{L}^1_{\mathbf{g}_{1i}}\overline{\mathbf{h}}^{(b)}_1 \\ \nabla\mathcal{L}^1_{\mathbf{g}_{1i}}\overline{\mathbf{h}}^{(b)}_2 \end{bmatrix} = \begin{bmatrix} \frac{\partial\mathcal{L}^1_{\mathbf{g}_{1i}}\overline{\mathbf{h}}^{(b)}_1}{\partial\boldsymbol{\beta}} \\ \frac{\partial\mathcal{L}^1_{\mathbf{g}_{1i}}\overline{\mathbf{h}}^{(b)}_2}{\partial\boldsymbol{\beta}} \end{bmatrix} = \begin{bmatrix} \mathbf{0} \\ \mathbf{0} \end{bmatrix} \tag{208}$$

- The second-order Lie derivatives are as following:

$$\mathcal{L}^2_{\mathbf{g}_0\mathbf{g}_0}\overline{\mathbf{h}}^{(b)} = \nabla\mathcal{L}^1_{\mathbf{g}_0}\overline{\mathbf{h}}^{(b)}\cdot\mathbf{g}_0 = \begin{bmatrix} \nabla\mathcal{L}^1_{\mathbf{g}_0}\overline{\mathbf{h}}^{(b)}_1\cdot\mathbf{g}_0 \\ \nabla\mathcal{L}^1_{\mathbf{g}_0}\overline{\mathbf{h}}^{(b)}_2\cdot\mathbf{g}_0 \end{bmatrix} \tag{209}$$

$$= \begin{bmatrix} \boldsymbol{\gamma}_1^\top \\ \boldsymbol{\gamma}_2^\top \end{bmatrix}[-\lfloor\boldsymbol{\beta}_2\times\rfloor\lfloor\boldsymbol{\beta}_1\times\rfloor\boldsymbol{\beta}_2 - \lfloor\boldsymbol{\beta}_2\times\rfloor\boldsymbol{\beta}_3 + \lfloor\boldsymbol{\beta}_3\times\rfloor\boldsymbol{\beta}_2 - \boldsymbol{\beta}_5 + \boldsymbol{\beta}_4] \tag{210}$$

$$\mathcal{L}^2_{\mathbf{g}_0\mathbf{g}_{1i}}\overline{\mathbf{h}}^{(b)} = \nabla\mathcal{L}^1_{\mathbf{g}_0}\overline{\mathbf{h}}^{(b)}\cdot\mathbf{g}_{1i} = \begin{bmatrix} \nabla\mathcal{L}^1_{\mathbf{g}_0}\overline{\mathbf{h}}^{(b)}_1\cdot\mathbf{g}_{1i} \\ \nabla\mathcal{L}^1_{\mathbf{g}_0}\overline{\mathbf{h}}^{(b)}_2\cdot\mathbf{g}_{1i} \end{bmatrix} = \begin{bmatrix} \boldsymbol{\gamma}_1^\top \\ \boldsymbol{\gamma}_2^\top \end{bmatrix}[\lfloor\boldsymbol{\beta}_2\times\rfloor\lfloor\boldsymbol{\beta}_1\times\rfloor - \lfloor\boldsymbol{\beta}_3\times\rfloor]\,\mathbf{e}_i \tag{211}$$

$$\mathcal{L}^2_{\mathbf{g}_{1i}\mathbf{g}_0}\overline{\mathbf{h}}^{(b)} = \nabla\mathcal{L}^1_{\mathbf{g}_{1i}}\overline{\mathbf{h}}^{(b)}\cdot\mathbf{g}_0 = \begin{bmatrix} \nabla\mathcal{L}^1_{\mathbf{g}_{1i}}\overline{\mathbf{h}}^{(b)}_1\cdot\mathbf{g}_0 \\ \nabla\mathcal{L}^1_{\mathbf{g}_{1i}}\overline{\mathbf{h}}^{(b)}_2\cdot\mathbf{g}_0 \end{bmatrix} = \begin{bmatrix} \boldsymbol{\gamma}_1^\top \\ \boldsymbol{\gamma}_2^\top \end{bmatrix}[\lfloor\mathbf{e}_i\times\rfloor\lfloor\boldsymbol{\beta}_1\times\rfloor\boldsymbol{\beta}_2 + \lfloor\mathbf{e}_i\times\rfloor\boldsymbol{\beta}_3] \tag{212}$$

$$\mathcal{L}^2_{\mathbf{g}_{1i}\mathbf{g}_{1j}}\overline{\mathbf{h}}^{(b)} = \nabla\mathcal{L}^1_{\mathbf{g}_{1i}}\overline{\mathbf{h}}^{(b)}\cdot\mathbf{g}_{1j} = \begin{bmatrix} \nabla\mathcal{L}^1_{\mathbf{g}_{1i}}\overline{\mathbf{h}}^{(b)}_1\cdot\mathbf{g}_{1j} \\ \nabla\mathcal{L}^1_{\mathbf{g}_{1i}}\overline{\mathbf{h}}^{(b)}_2\cdot\mathbf{g}_{1j} \end{bmatrix} = \begin{bmatrix} \boldsymbol{\gamma}_1^\top \\ \boldsymbol{\gamma}_2^\top \end{bmatrix}[-\lfloor\mathbf{e}_i\times\rfloor\lfloor\boldsymbol{\beta}_1\times\rfloor\mathbf{e}_j] \tag{213}$$

with the corresponding gradients as:

$$\nabla\mathcal{L}^2_{\mathbf{g}_0\mathbf{g}_0}\overline{\mathbf{h}}^{(b)} = \begin{bmatrix} \nabla\mathcal{L}^2_{\mathbf{g}_0\mathbf{g}_0}\overline{\mathbf{h}}^{(b)}_1 \\ \nabla\mathcal{L}^2_{\mathbf{g}_0\mathbf{g}_0}\overline{\mathbf{h}}^{(b)}_2 \end{bmatrix} = \begin{bmatrix} \frac{\partial\mathcal{L}^2_{\mathbf{g}_0\mathbf{g}_0}\overline{\mathbf{h}}^{(b)}_1}{\partial\boldsymbol{\beta}} \\ \frac{\partial\mathcal{L}^2_{\mathbf{g}_0\mathbf{g}_0}\overline{\mathbf{h}}^{(b)}_2}{\partial\boldsymbol{\beta}} \end{bmatrix} \tag{214}$$

$$= \begin{bmatrix} \boldsymbol{\gamma}^\top_1 \\ \boldsymbol{\gamma}^\top_2 \end{bmatrix} \begin{bmatrix} \lfloor\boldsymbol{\beta}_2\times\rfloor^2 & -\lfloor\boldsymbol{\beta}_2\times\rfloor\lfloor\boldsymbol{\beta}_1\times\rfloor + \lfloor\lfloor\boldsymbol{\beta}_1\times\rfloor\boldsymbol{\beta}_2\times\rfloor + 2\lfloor\boldsymbol{\beta}_3\times\rfloor & -2\lfloor\boldsymbol{\beta}_2\times\rfloor & \mathbf{I}_3 & -\mathbf{I}_3 \end{bmatrix}$$

$$\nabla\mathcal{L}^2_{\mathbf{g}_0\mathbf{g}_{1i}}\overline{\mathbf{h}}^{(b)} = \begin{bmatrix} \nabla\mathcal{L}^2_{\mathbf{g}_0\mathbf{g}_{1i}}\overline{\mathbf{h}}^{(b)}_1 \\ \nabla\mathcal{L}^2_{\mathbf{g}_0\mathbf{g}_{1i}}\overline{\mathbf{h}}^{(b)}_2 \end{bmatrix} = \begin{bmatrix} \frac{\partial\mathcal{L}^2_{\mathbf{g}_0\mathbf{g}_{1i}}\overline{\mathbf{h}}^{(b)}_1}{\partial\boldsymbol{\beta}} \\ \frac{\partial\mathcal{L}^2_{\mathbf{g}_0\mathbf{g}_{1i}}\overline{\mathbf{h}}^{(b)}_2}{\partial\boldsymbol{\beta}} \end{bmatrix} \tag{215}$$

$$= \begin{bmatrix} \boldsymbol{\gamma}^\top_1 \\ \boldsymbol{\gamma}^\top_2 \end{bmatrix} \begin{bmatrix} -\lfloor\boldsymbol{\beta}_2\times\rfloor\lfloor\mathbf{e}_i\times\rfloor & -\lfloor\lfloor\boldsymbol{\beta}_1\times\rfloor\mathbf{e}_i\times\rfloor & \lfloor\mathbf{e}_i\times\rfloor & \mathbf{0} & \mathbf{0} \end{bmatrix} \tag{216}$$

$$\nabla\mathcal{L}^2_{\mathbf{g}_{1i}\mathbf{g}_0}\overline{\mathbf{h}}^{(b)} = \begin{bmatrix} \nabla\mathcal{L}^2_{\mathbf{g}_{1i}\mathbf{g}_0}\overline{\mathbf{h}}^{(b)}_1 \\ \nabla\mathcal{L}^2_{\mathbf{g}_{1i}\mathbf{g}_0}\overline{\mathbf{h}}^{(b)}_2 \end{bmatrix} = \begin{bmatrix} \frac{\partial\mathcal{L}^2_{\mathbf{g}_{1i}\mathbf{g}_0}\overline{\mathbf{h}}^{(b)}_1}{\partial\boldsymbol{\beta}} \\ \frac{\partial\mathcal{L}^2_{\mathbf{g}_{1i}\mathbf{g}_0}\overline{\mathbf{h}}^{(b)}_2}{\partial\boldsymbol{\beta}} \end{bmatrix} \tag{217}$$

$$= \begin{bmatrix} \boldsymbol{\gamma}^\top_1 \\ \boldsymbol{\gamma}^\top_2 \end{bmatrix} \begin{bmatrix} -\lfloor\mathbf{e}_i\times\rfloor\lfloor\boldsymbol{\beta}_2\times\rfloor & \lfloor\mathbf{e}_i\times\rfloor\lfloor\boldsymbol{\beta}_1\times\rfloor & \lfloor\mathbf{e}_i\times\rfloor & \mathbf{0} & \mathbf{0} \end{bmatrix} \tag{218}$$

$$\nabla\mathcal{L}^2_{\mathbf{g}_{1i}\mathbf{g}_{1j}}\overline{\mathbf{h}}^{(b)} = \begin{bmatrix} \nabla\mathcal{L}^2_{\mathbf{g}_{1i}\mathbf{g}_{1j}}\overline{\mathbf{h}}^{(b)}_1 \\ \nabla\mathcal{L}^2_{\mathbf{g}_{1i}\mathbf{g}_{1j}}\overline{\mathbf{h}}^{(b)}_2 \end{bmatrix} = \begin{bmatrix} \frac{\partial\mathcal{L}^2_{\mathbf{g}_{1i}\mathbf{g}_{1j}}\overline{\mathbf{h}}^{(b)}_1}{\partial\boldsymbol{\beta}} \\ \frac{\partial\mathcal{L}^2_{\mathbf{g}_{1i}\mathbf{g}_{1j}}\overline{\mathbf{h}}^{(b)}_2}{\partial\boldsymbol{\beta}} \end{bmatrix} = \begin{bmatrix} \boldsymbol{\gamma}^\top_1 \\ \boldsymbol{\gamma}^\top_2 \end{bmatrix} \begin{bmatrix} \lfloor\mathbf{e}_i\times\rfloor\lfloor\mathbf{e}_j\times\rfloor & \mathbf{0} & \mathbf{0} & \mathbf{0} & \mathbf{0} \end{bmatrix} \tag{219}$$

- The third-order Lie derivatives are as following:

$$\mathcal{L}^3_{\mathbf{g}_0\mathbf{g}_0\mathbf{g}_{1i}}\overline{\mathbf{h}}^{(b)} = \nabla\mathcal{L}^2_{\mathbf{g}_0\mathbf{g}_0}\overline{\mathbf{h}}^{(b)}\cdot\mathbf{g}_{1i} = \begin{bmatrix} \nabla\mathcal{L}^2_{\mathbf{g}_0\mathbf{g}_0}\overline{\mathbf{h}}^{(b)}_1\cdot\mathbf{g}_{1i} \\ \nabla\mathcal{L}^2_{\mathbf{g}_0\mathbf{g}_0}\overline{\mathbf{h}}^{(b)}_2\cdot\mathbf{g}_{1i} \end{bmatrix} \tag{220}$$

$$= \begin{bmatrix} \boldsymbol{\gamma}^\top_1 \\ \boldsymbol{\gamma}^\top_2 \end{bmatrix} \left[\lfloor\boldsymbol{\beta}_2\times\rfloor^2\lfloor\boldsymbol{\beta}_1\times\rfloor - 2\lfloor\boldsymbol{\beta}_2\times\rfloor\lfloor\boldsymbol{\beta}_3\times\rfloor - \lfloor\boldsymbol{\beta}_5\times\rfloor\right]\mathbf{e}_i \tag{221}$$

$$\mathcal{L}^3_{\mathbf{g}_0\mathbf{g}_0\mathbf{g}_{2i}}\overline{\mathbf{h}}^{(b)} = \nabla\mathcal{L}^2_{\mathbf{g}_0\mathbf{g}_0}\overline{\mathbf{h}}^{(b)}\cdot\mathbf{g}_{2i} = \begin{bmatrix} \nabla\mathcal{L}^2_{\mathbf{g}_0\mathbf{g}_0}\overline{\mathbf{h}}^{(b)}_1\cdot\mathbf{g}_{2i} \\ \nabla\mathcal{L}^2_{\mathbf{g}_0\mathbf{g}_0}\overline{\mathbf{h}}^{(b)}_2\cdot\mathbf{g}_{2i} \end{bmatrix} = \begin{bmatrix} \boldsymbol{\gamma}^\top_1 \\ \boldsymbol{\gamma}^\top_2 \end{bmatrix} \left[-2\lfloor\boldsymbol{\beta}_2\times\rfloor\right]\mathbf{e}_i \tag{222}$$

$$\tag{223}$$

$$\mathcal{L}^3_{\mathbf{g}_0\mathbf{g}_{1i}\mathbf{g}_0}\overline{\mathbf{h}}^{(b)} = \nabla\mathcal{L}^2_{\mathbf{g}_0\mathbf{g}_{1i}}\overline{\mathbf{h}}^{(b)}\cdot\mathbf{g}_0 = \begin{bmatrix} \nabla\mathcal{L}^2_{\mathbf{g}_0\mathbf{g}_{1i}}\overline{\mathbf{h}}^{(b)}_1\cdot\mathbf{g}_0 \\ \nabla\mathcal{L}^2_{\mathbf{g}_0\mathbf{g}_{1i}}\overline{\mathbf{h}}^{(b)}_2\cdot\mathbf{g}_0 \end{bmatrix} \tag{224}$$

$$= \begin{bmatrix} \boldsymbol{\gamma}^\top_1 \\ \boldsymbol{\gamma}^\top_2 \end{bmatrix} \left[\lfloor\boldsymbol{\beta}_2\times\rfloor\lfloor\mathbf{e}_i\times\rfloor\lfloor\boldsymbol{\beta}_1\times\rfloor\boldsymbol{\beta}_2 + \lfloor\boldsymbol{\beta}_2\times\rfloor\lfloor\mathbf{e}_i\times\rfloor\boldsymbol{\beta}_3 - \lfloor\mathbf{e}_i\times\rfloor\lfloor\boldsymbol{\beta}_3\times\rfloor\boldsymbol{\beta}_2 + \lfloor\mathbf{e}_i\times\rfloor\boldsymbol{\beta}_5 - \lfloor\mathbf{e}_i\times\rfloor\boldsymbol{\beta}_4\right]$$

with the corresponding gradients as:

$$\nabla\mathcal{L}^3_{\mathbf{g}_0\mathbf{g}_0\mathbf{g}_{1i}}\overline{\mathbf{h}}^{(b)} = \begin{bmatrix} \nabla\mathcal{L}^3_{\mathbf{g}_0\mathbf{g}_0\mathbf{g}_{1i}}\overline{\mathbf{h}}^{(b)}_1 \\ \nabla\mathcal{L}^3_{\mathbf{g}_0\mathbf{g}_0\mathbf{g}_{1i}}\overline{\mathbf{h}}^{(b)}_2 \end{bmatrix} = \begin{bmatrix} \frac{\partial\mathcal{L}^3_{\mathbf{g}_0\mathbf{g}_0\mathbf{g}_{1i}}\overline{\mathbf{h}}^{(b)}_1}{\partial\boldsymbol{\beta}} \\ \frac{\partial\mathcal{L}^3_{\mathbf{g}_0\mathbf{g}_0\mathbf{g}_{1i}}\overline{\mathbf{h}}^{(b)}_2}{\partial\boldsymbol{\beta}} \end{bmatrix} \tag{225}$$

$$= \begin{bmatrix} \boldsymbol{\gamma}^\top_1 \\ \boldsymbol{\gamma}^\top_2 \end{bmatrix} \begin{bmatrix} \frac{\partial\mathcal{L}^3_{\mathbf{g}_0\mathbf{g}_0\mathbf{g}_{1i}}\overline{\mathbf{h}}^{(b)}}{\partial\boldsymbol{\beta}_1} & \frac{\partial\mathcal{L}^3_{\mathbf{g}_0\mathbf{g}_0\mathbf{g}_{1i}}\overline{\mathbf{h}}^{(b)}}{\partial\boldsymbol{\beta}_2} & \frac{\partial\mathcal{L}^3_{\mathbf{g}_0\mathbf{g}_0\mathbf{g}_{1i}}\overline{\mathbf{h}}^{(b)}}{\partial\boldsymbol{\beta}_3} & \frac{\partial\mathcal{L}^3_{\mathbf{g}_0\mathbf{g}_0\mathbf{g}_{1i}}\overline{\mathbf{h}}^{(b)}}{\partial\boldsymbol{\beta}_4} & \frac{\partial\mathcal{L}^3_{\mathbf{g}_0\mathbf{g}_0\mathbf{g}_{1i}}\overline{\mathbf{h}}^{(b)}}{\partial\boldsymbol{\beta}_5} \end{bmatrix} \tag{226}$$

$$\nabla\mathcal{L}^3_{\mathbf{g}_0\mathbf{g}_{1i}\mathbf{g}_0}\overline{\mathbf{h}}^{(b)} = \begin{bmatrix} \nabla\mathcal{L}^3_{\mathbf{g}_0\mathbf{g}_{1i}\mathbf{g}_0}\overline{\mathbf{h}}^{(b)}_1 \\ \nabla\mathcal{L}^3_{\mathbf{g}_0\mathbf{g}_{1i}\mathbf{g}_0}\overline{\mathbf{h}}^{(b)}_2 \end{bmatrix} = \begin{bmatrix} \frac{\partial\mathcal{L}^3_{\mathbf{g}_0\mathbf{g}_{1i}\mathbf{g}_0}\overline{\mathbf{h}}^{(b)}_1}{\partial\boldsymbol{\beta}} \\ \frac{\partial\mathcal{L}^3_{\mathbf{g}_0\mathbf{g}_{1i}\mathbf{g}_0}\overline{\mathbf{h}}^{(b)}_2}{\partial\boldsymbol{\beta}} \end{bmatrix} \tag{227}$$

$$= \begin{bmatrix} \boldsymbol{\gamma}^\top_1 \\ \boldsymbol{\gamma}^\top_2 \end{bmatrix} \begin{bmatrix} \frac{\partial\mathcal{L}^3_{\mathbf{g}_0\mathbf{g}_{1i}\mathbf{g}_0}\overline{\mathbf{h}}^{(b)}}{\partial\boldsymbol{\beta}_1} & \frac{\partial\mathcal{L}^3_{\mathbf{g}_0\mathbf{g}_{1i}\mathbf{g}_0}\overline{\mathbf{h}}^{(b)}}{\partial\boldsymbol{\beta}_2} & \frac{\partial\mathcal{L}^3_{\mathbf{g}_0\mathbf{g}_{1i}\mathbf{g}_0}\overline{\mathbf{h}}^{(b)}}{\partial\boldsymbol{\beta}_3} & -\lfloor\mathbf{e}_i\rfloor & \lfloor\mathbf{e}_i\rfloor \end{bmatrix} \tag{228}$$

$$\nabla\mathcal{L}^3_{\mathbf{g}_0\mathbf{g}_0\mathbf{g}_{2i}}\overline{\mathbf{h}}^{(b)} = \begin{bmatrix} \nabla\mathcal{L}^3_{\mathbf{g}_0\mathbf{g}_0\mathbf{g}_{2i}}\overline{\mathbf{h}}^{(b)}_1 \\ \nabla\mathcal{L}^3_{\mathbf{g}_0\mathbf{g}_0\mathbf{g}_{2i}}\overline{\mathbf{h}}^{(b)}_2 \end{bmatrix} = \begin{bmatrix} \frac{\partial\mathcal{L}^3_{\mathbf{g}_0\mathbf{g}_0\mathbf{g}_{2i}}\overline{\mathbf{h}}^{(b)}_1}{\partial\boldsymbol{\beta}} \\ \frac{\partial\mathcal{L}^3_{\mathbf{g}_0\mathbf{g}_0\mathbf{g}_{2i}}\overline{\mathbf{h}}^{(b)}_2}{\partial\boldsymbol{\beta}} \end{bmatrix} = \begin{bmatrix} \boldsymbol{\gamma}^\top_1 \\ \boldsymbol{\gamma}^\top_2 \end{bmatrix} \begin{bmatrix} \mathbf{0} & \mathbf{0} & 2\lfloor\mathbf{e}_i\times\rfloor & \mathbf{0} & \mathbf{0} \end{bmatrix} \tag{229}$$

where in the equations:

$$\frac{\partial \mathcal{L}^3_{\mathbf{g}_0\mathbf{g}_0\mathbf{g}_{1i}} \overline{\mathbf{h}}^{(b)}}{\partial \boldsymbol{\beta}_1} = \begin{bmatrix} \frac{\partial \mathcal{L}^3_{\mathbf{g}_0\mathbf{g}_0\mathbf{g}_{1i}} \overline{\mathbf{h}}^{(b)}_1}{\partial \boldsymbol{\beta}_1} \\ \frac{\partial \mathcal{L}^3_{\mathbf{g}_0\mathbf{g}_0\mathbf{g}_{1i}} \overline{\mathbf{h}}^{(b)}_2}{\partial \boldsymbol{\beta}_1} \end{bmatrix} = \begin{bmatrix} \boldsymbol{\gamma}_1^\top \\ \boldsymbol{\gamma}_2^\top \end{bmatrix} \left[-\lfloor \boldsymbol{\beta}_2 \times \rfloor^2 \lfloor \mathbf{e}_i \times \rfloor \right] \tag{230}$$

$$\frac{\partial \mathcal{L}^3_{\mathbf{g}_0\mathbf{g}_0\mathbf{g}_{1i}} \overline{\mathbf{h}}^{(b)}}{\partial \boldsymbol{\beta}_2} = \begin{bmatrix} \frac{\partial \mathcal{L}^3_{\mathbf{g}_0\mathbf{g}_0\mathbf{g}_{1i}} \overline{\mathbf{h}}^{(b)}_1}{\partial \boldsymbol{\beta}_2} \\ \frac{\partial \mathcal{L}^3_{\mathbf{g}_0\mathbf{g}_0\mathbf{g}_{1i}} \overline{\mathbf{h}}^{(b)}_2}{\partial \boldsymbol{\beta}_2} \end{bmatrix} \tag{231}$$

$$= \begin{bmatrix} \boldsymbol{\gamma}_1^\top \\ \boldsymbol{\gamma}_2^\top \end{bmatrix} \left[-\lfloor \lfloor \boldsymbol{\beta}_2 \times \rfloor \lfloor \boldsymbol{\beta}_1 \times \rfloor \mathbf{e}_i \times \rfloor - \lfloor \boldsymbol{\beta}_2 \times \rfloor \lfloor \lfloor \boldsymbol{\beta}_1 \times \rfloor \mathbf{e}_i \times \rfloor + 2 \lfloor \lfloor \boldsymbol{\beta}_3 \times \rfloor \mathbf{e}_i \times \rfloor \right] \tag{232}$$

$$\frac{\partial \mathcal{L}^3_{\mathbf{g}_0\mathbf{g}_0\mathbf{g}_{1i}} \overline{\mathbf{h}}^{(b)}}{\partial \boldsymbol{\beta}_3} = \begin{bmatrix} \frac{\partial \mathcal{L}^3_{\mathbf{g}_0\mathbf{g}_0\mathbf{g}_{1i}} \overline{\mathbf{h}}^{(b)}_1}{\partial \boldsymbol{\beta}_3} \\ \frac{\partial \mathcal{L}^3_{\mathbf{g}_0\mathbf{g}_0\mathbf{g}_{1i}} \overline{\mathbf{h}}^{(b)}_2}{\partial \boldsymbol{\beta}_3} \end{bmatrix} = \begin{bmatrix} \boldsymbol{\gamma}_1^\top \\ \boldsymbol{\gamma}_2^\top \end{bmatrix} \left[2 \lfloor \boldsymbol{\beta}_2 \times \rfloor \lfloor \mathbf{e}_i \times \rfloor \right] \tag{233}$$

$$\frac{\partial \mathcal{L}^3_{\mathbf{g}_0\mathbf{g}_0\mathbf{g}_{1i}} \overline{\mathbf{h}}^{(b)}}{\partial \boldsymbol{\beta}_4} = \begin{bmatrix} \frac{\partial \mathcal{L}^3_{\mathbf{g}_0\mathbf{g}_0\mathbf{g}_{1i}} \overline{\mathbf{h}}^{(b)}_1}{\partial \boldsymbol{\beta}_4} \\ \frac{\partial \mathcal{L}^3_{\mathbf{g}_0\mathbf{g}_0\mathbf{g}_{1i}} \overline{\mathbf{h}}^{(b)}_2}{\partial \boldsymbol{\beta}_4} \end{bmatrix} = \begin{bmatrix} \mathbf{0} \\ \mathbf{0} \end{bmatrix} \tag{234}$$

$$\frac{\partial \mathcal{L}^3_{\mathbf{g}_0\mathbf{g}_0\mathbf{g}_{1i}} \overline{\mathbf{h}}^{(b)}}{\partial \boldsymbol{\beta}_5} = \begin{bmatrix} \frac{\partial \mathcal{L}^3_{\mathbf{g}_0\mathbf{g}_0\mathbf{g}_{1i}} \overline{\mathbf{h}}^{(b)}_1}{\partial \boldsymbol{\beta}_5} \\ \frac{\partial \mathcal{L}^3_{\mathbf{g}_0\mathbf{g}_0\mathbf{g}_{1i}} \overline{\mathbf{h}}^{(b)}_2}{\partial \boldsymbol{\beta}_5} \end{bmatrix} = \begin{bmatrix} \boldsymbol{\gamma}_1^\top \\ \boldsymbol{\gamma}_2^\top \end{bmatrix} \left[\lfloor \mathbf{e}_i \times \rfloor \right] \tag{235}$$

$$\frac{\partial \mathcal{L}^3_{\mathbf{g}_0\mathbf{g}_{1i}\mathbf{g}_0} \overline{\mathbf{h}}^{(b)}}{\partial \boldsymbol{\beta}_1} = \begin{bmatrix} \frac{\partial \mathcal{L}^3_{\mathbf{g}_0\mathbf{g}_{1i}\mathbf{g}_0} \overline{\mathbf{h}}^{(b)}_1}{\partial \boldsymbol{\beta}_1} \\ \frac{\partial \mathcal{L}^3_{\mathbf{g}_0\mathbf{g}_{1i}\mathbf{g}_0} \overline{\mathbf{h}}^{(b)}_2}{\partial \boldsymbol{\beta}_1} \end{bmatrix} = \begin{bmatrix} \boldsymbol{\gamma}_1^\top \\ \boldsymbol{\gamma}_2^\top \end{bmatrix} \left[-\lfloor \boldsymbol{\beta}_2 \times \rfloor \lfloor \mathbf{e}_i \times \rfloor \lfloor \boldsymbol{\beta}_2 \times \rfloor \right] \tag{236}$$

$$\frac{\partial \mathcal{L}^3_{\mathbf{g}_0\mathbf{g}_{1i}\mathbf{g}_0} \overline{\mathbf{h}}^{(b)}}{\partial \boldsymbol{\beta}_2} = \begin{bmatrix} \frac{\partial \mathcal{L}^3_{\mathbf{g}_0\mathbf{g}_{1i}\mathbf{g}_0} \overline{\mathbf{h}}^{(b)}_1}{\partial \boldsymbol{\beta}_1} \\ \frac{\partial \mathcal{L}^3_{\mathbf{g}_0\mathbf{g}_{1i}\mathbf{g}_0} \overline{\mathbf{h}}^{(b)}_2}{\partial \boldsymbol{\beta}_1} \end{bmatrix} = \begin{bmatrix} \boldsymbol{\gamma}_1^\top \\ \boldsymbol{\gamma}_2^\top \end{bmatrix} \left[\lfloor \boldsymbol{\beta}_2 \times \rfloor \lfloor \mathbf{e}_i \times \rfloor \lfloor \boldsymbol{\beta}_1 \times \rfloor - \lfloor \lfloor \mathbf{e}_i \times \rfloor \lfloor \boldsymbol{\beta}_1 \times \rfloor \boldsymbol{\beta}_2 \times \rfloor - \lfloor \mathbf{e}_i \times \rfloor \lfloor \boldsymbol{\beta}_3 \times \rfloor - \lfloor \lfloor \mathbf{e}_i \times \rfloor \boldsymbol{\beta}_3 \times \rfloor \right]$$

$$\frac{\partial \mathcal{L}^3_{\mathbf{g}_0\mathbf{g}_{1i}\mathbf{g}_0} \overline{\mathbf{h}}^{(b)}}{\partial \boldsymbol{\beta}_3} = \begin{bmatrix} \frac{\partial \mathcal{L}^3_{\mathbf{g}_0\mathbf{g}_{1i}\mathbf{g}_0} \overline{\mathbf{h}}^{(b)}_1}{\partial \boldsymbol{\beta}_1} \\ \frac{\partial \mathcal{L}^3_{\mathbf{g}_0\mathbf{g}_{1i}\mathbf{g}_0} \overline{\mathbf{h}}^{(b)}_2}{\partial \boldsymbol{\beta}_1} \end{bmatrix} = \begin{bmatrix} \boldsymbol{\gamma}_1^\top \\ \boldsymbol{\gamma}_2^\top \end{bmatrix} \left[\lfloor \boldsymbol{\beta}_2 \times \rfloor \lfloor \mathbf{e}_i \times \rfloor + \lfloor \mathbf{e}_i \times \rfloor \lfloor \boldsymbol{\beta}_2 \times \rfloor \right] \tag{237}$$

Therefore, we can construct the $\Xi^{(b)}$ matrix as (238). Note that the diagonal block are all of full column

rank and, hence the matrix $\Xi^{(b)}$ is of full column rank.

$$\Xi^{(b)} = \begin{bmatrix} \nabla\mathcal{L}^1_{\mathbf{g}_{11}}\overline{\mathbf{h}}^{(b)} \\ \nabla\mathcal{L}^1_{\mathbf{g}_{12}}\overline{\mathbf{h}}^{(b)} \\ \nabla\mathcal{L}^1_{\mathbf{g}_{13}}\overline{\mathbf{h}}^{(b)} \\ \nabla\mathcal{L}^3_{\mathbf{g}_0\mathbf{g}_0\mathbf{g}_{21}}\overline{\mathbf{h}}^{(b)} \\ \nabla\mathcal{L}^3_{\mathbf{g}_0\mathbf{g}_0\mathbf{g}_{22}}\overline{\mathbf{h}}^{(b)} \\ \nabla\mathcal{L}^3_{\mathbf{g}_0\mathbf{g}_0\mathbf{g}_{23}}\overline{\mathbf{h}}^{(b)} \\ \nabla\mathcal{L}^2_{\mathbf{g}_{11}\mathbf{g}_0}\overline{\mathbf{h}}^{(b)} \\ \nabla\mathcal{L}^2_{\mathbf{g}_{12}\mathbf{g}_0}\overline{\mathbf{h}}^{(b)} \\ \nabla\mathcal{L}^2_{\mathbf{g}_{13}\mathbf{g}_0}\overline{\mathbf{h}}^{(b)} \\ \nabla\mathcal{L}^3_{\mathbf{g}_0\mathbf{g}_{11}\mathbf{g}_0}\overline{\mathbf{h}}^{(b)} \\ \nabla\mathcal{L}^3_{\mathbf{g}_0\mathbf{g}_{11}\mathbf{g}_0}\overline{\mathbf{h}}^{(b)} \\ \nabla\mathcal{L}^3_{\mathbf{g}_0\mathbf{g}_{11}\mathbf{g}_0}\overline{\mathbf{h}}^{(b)} \\ \nabla\mathcal{L}^3_{\mathbf{g}_0\mathbf{g}_0\mathbf{g}_{11}}\overline{\mathbf{h}}^{(b)} \\ \nabla\mathcal{L}^3_{\mathbf{g}_0\mathbf{g}_0\mathbf{g}_{12}}\overline{\mathbf{h}}^{(b)} \\ \nabla\mathcal{L}^3_{\mathbf{g}_0\mathbf{g}_0\mathbf{g}_{13}}\overline{\mathbf{h}}^{(b)} \end{bmatrix} = \begin{bmatrix} -\boldsymbol{\gamma}_1^\top\lfloor\mathbf{e}_1\times\rfloor & \mathbf{0} & \mathbf{0} & \mathbf{0} & \mathbf{0} \\ -\boldsymbol{\gamma}_2^\top\lfloor\mathbf{e}_1\times\rfloor & \mathbf{0} & \mathbf{0} & \mathbf{0} & \mathbf{0} \\ -\boldsymbol{\gamma}_1^\top\lfloor\mathbf{e}_2\times\rfloor & \mathbf{0} & \mathbf{0} & \mathbf{0} & \mathbf{0} \\ -\boldsymbol{\gamma}_2^\top\lfloor\mathbf{e}_2\times\rfloor & \mathbf{0} & \mathbf{0} & \mathbf{0} & \mathbf{0} \\ -\boldsymbol{\gamma}_1^\top\lfloor\mathbf{e}_3\times\rfloor & \mathbf{0} & \mathbf{0} & \mathbf{0} & \mathbf{0} \\ -\boldsymbol{\gamma}_2^\top\lfloor\mathbf{e}_3\times\rfloor & \mathbf{0} & \mathbf{0} & \mathbf{0} & \mathbf{0} \\ \mathbf{0} & 2\boldsymbol{\gamma}_1^\top\lfloor\mathbf{e}_1\times\rfloor & \mathbf{0} & \mathbf{0} & \mathbf{0} \\ \mathbf{0} & 2\boldsymbol{\gamma}_2^\top\lfloor\mathbf{e}_1\times\rfloor & \mathbf{0} & \mathbf{0} & \mathbf{0} \\ \mathbf{0} & 2\boldsymbol{\gamma}_1^\top\lfloor\mathbf{e}_2\times\rfloor & \mathbf{0} & \mathbf{0} & \mathbf{0} \\ \mathbf{0} & 2\boldsymbol{\gamma}_2^\top\lfloor\mathbf{e}_2\times\rfloor & \mathbf{0} & \mathbf{0} & \mathbf{0} \\ \mathbf{0} & 2\boldsymbol{\gamma}_1^\top\lfloor\mathbf{e}_3\times\rfloor & \mathbf{0} & \mathbf{0} & \mathbf{0} \\ \mathbf{0} & 2\boldsymbol{\gamma}_2^\top\lfloor\mathbf{e}_3\times\rfloor & \mathbf{0} & \mathbf{0} & \mathbf{0} \\ -\boldsymbol{\gamma}_1^\top\lfloor\mathbf{e}_1\times\rfloor\lfloor\boldsymbol{\beta}_2\times\rfloor & \boldsymbol{\gamma}_1^\top\lfloor\mathbf{e}_1\times\rfloor\lfloor\boldsymbol{\beta}_1\times\rfloor & \boldsymbol{\gamma}_1^\top\lfloor\mathbf{e}_1\times\rfloor & \mathbf{0} & \mathbf{0} \\ -\boldsymbol{\gamma}_2^\top\lfloor\mathbf{e}_1\times\rfloor\lfloor\boldsymbol{\beta}_2\times\rfloor & \boldsymbol{\gamma}_2^\top\lfloor\mathbf{e}_1\times\rfloor\lfloor\boldsymbol{\beta}_1\times\rfloor & \boldsymbol{\gamma}_2^\top\lfloor\mathbf{e}_1\times\rfloor & \mathbf{0} & \mathbf{0} \\ -\boldsymbol{\gamma}_1^\top\lfloor\mathbf{e}_2\times\rfloor\lfloor\boldsymbol{\beta}_2\times\rfloor & \boldsymbol{\gamma}_1^\top\lfloor\mathbf{e}_2\times\rfloor\lfloor\boldsymbol{\beta}_1\times\rfloor & \boldsymbol{\gamma}_1^\top\lfloor\mathbf{e}_2\times\rfloor & \mathbf{0} & \mathbf{0} \\ -\boldsymbol{\gamma}_2^\top\lfloor\mathbf{e}_2\times\rfloor\lfloor\boldsymbol{\beta}_2\times\rfloor & \boldsymbol{\gamma}_2^\top\lfloor\mathbf{e}_2\times\rfloor\lfloor\boldsymbol{\beta}_1\times\rfloor & \boldsymbol{\gamma}_2^\top\lfloor\mathbf{e}_2\times\rfloor & \mathbf{0} & \mathbf{0} \\ -\boldsymbol{\gamma}_1^\top\lfloor\mathbf{e}_3\times\rfloor\lfloor\boldsymbol{\beta}_2\times\rfloor & \boldsymbol{\gamma}_1^\top\lfloor\mathbf{e}_3\times\rfloor\lfloor\boldsymbol{\beta}_1\times\rfloor & \boldsymbol{\gamma}_1^\top\lfloor\mathbf{e}_3\times\rfloor & \mathbf{0} & \mathbf{0} \\ -\boldsymbol{\gamma}_2^\top\lfloor\mathbf{e}_3\times\rfloor\lfloor\boldsymbol{\beta}_2\times\rfloor & \boldsymbol{\gamma}_2^\top\lfloor\mathbf{e}_3\times\rfloor\lfloor\boldsymbol{\beta}_1\times\rfloor & \boldsymbol{\gamma}_2^\top\lfloor\mathbf{e}_3\times\rfloor & \mathbf{0} & \mathbf{0} \\ \frac{\partial\mathcal{L}^3_{\mathbf{g}_0\mathbf{g}_{11}\mathbf{g}_0}\overline{\mathbf{h}}_1^{(b)}}{\partial\boldsymbol{\beta}_1} & \frac{\partial\mathcal{L}^3_{\mathbf{g}_0\mathbf{g}_{11}\mathbf{g}_0}\overline{\mathbf{h}}_1^{(b)}}{\partial\boldsymbol{\beta}_2} & \frac{\partial\mathcal{L}^3_{\mathbf{g}_0\mathbf{g}_{11}\mathbf{g}_0}\overline{\mathbf{h}}_1^{(b)}}{\partial\boldsymbol{\beta}_3} & -\boldsymbol{\gamma}_1^\top\lfloor\mathbf{e}_1\times\rfloor & \boldsymbol{\gamma}_1^\top\lfloor\mathbf{e}_1\times\rfloor \\ \frac{\partial\mathcal{L}^3_{\mathbf{g}_0\mathbf{g}_{11}\mathbf{g}_0}\overline{\mathbf{h}}_2^{(b)}}{\partial\boldsymbol{\beta}_1} & \frac{\partial\mathcal{L}^3_{\mathbf{g}_0\mathbf{g}_{11}\mathbf{g}_0}\overline{\mathbf{h}}_2^{(b)}}{\partial\boldsymbol{\beta}_2} & \frac{\partial\mathcal{L}^3_{\mathbf{g}_0\mathbf{g}_{11}\mathbf{g}_0}\overline{\mathbf{h}}_2^{(b)}}{\partial\boldsymbol{\beta}_3} & -\boldsymbol{\gamma}_2^\top\lfloor\mathbf{e}_1\times\rfloor & \boldsymbol{\gamma}_2^\top\lfloor\mathbf{e}_1\times\rfloor \\ \frac{\partial\mathcal{L}^3_{\mathbf{g}_0\mathbf{g}_{12}\mathbf{g}_0}\overline{\mathbf{h}}_1^{(b)}}{\partial\boldsymbol{\beta}_1} & \frac{\partial\mathcal{L}^3_{\mathbf{g}_0\mathbf{g}_{12}\mathbf{g}_0}\overline{\mathbf{h}}_1^{(b)}}{\partial\boldsymbol{\beta}_2} & \frac{\partial\mathcal{L}^3_{\mathbf{g}_0\mathbf{g}_{12}\mathbf{g}_0}\overline{\mathbf{h}}_1^{(b)}}{\partial\boldsymbol{\beta}_3} & -\boldsymbol{\gamma}_1^\top\lfloor\mathbf{e}_2\times\rfloor & \boldsymbol{\gamma}_1^\top\lfloor\mathbf{e}_2\times\rfloor \\ \frac{\partial\mathcal{L}^3_{\mathbf{g}_0\mathbf{g}_{12}\mathbf{g}_0}\overline{\mathbf{h}}_2^{(b)}}{\partial\boldsymbol{\beta}_1} & \frac{\partial\mathcal{L}^3_{\mathbf{g}_0\mathbf{g}_{12}\mathbf{g}_0}\overline{\mathbf{h}}_2^{(b)}}{\partial\boldsymbol{\beta}_2} & \frac{\partial\mathcal{L}^3_{\mathbf{g}_0\mathbf{g}_{12}\mathbf{g}_0}\overline{\mathbf{h}}_2^{(b)}}{\partial\boldsymbol{\beta}_3} & -\boldsymbol{\gamma}_2^\top\lfloor\mathbf{e}_2\times\rfloor & \boldsymbol{\gamma}_2^\top\lfloor\mathbf{e}_2\times\rfloor \\ \frac{\partial\mathcal{L}^3_{\mathbf{g}_0\mathbf{g}_{13}\mathbf{g}_0}\overline{\mathbf{h}}_1^{(b)}}{\partial\boldsymbol{\beta}_1} & \frac{\partial\mathcal{L}^3_{\mathbf{g}_0\mathbf{g}_{13}\mathbf{g}_0}\overline{\mathbf{h}}_1^{(b)}}{\partial\boldsymbol{\beta}_2} & \frac{\partial\mathcal{L}^3_{\mathbf{g}_0\mathbf{g}_{13}\mathbf{g}_0}\overline{\mathbf{h}}_1^{(b)}}{\partial\boldsymbol{\beta}_3} & -\boldsymbol{\gamma}_1^\top\lfloor\mathbf{e}_3\times\rfloor & \boldsymbol{\gamma}_1^\top\lfloor\mathbf{e}_3\times\rfloor \\ \frac{\partial\mathcal{L}^3_{\mathbf{g}_0\mathbf{g}_{13}\mathbf{g}_0}\overline{\mathbf{h}}_2^{(b)}}{\partial\boldsymbol{\beta}_1} & \frac{\partial\mathcal{L}^3_{\mathbf{g}_0\mathbf{g}_{13}\mathbf{g}_0}\overline{\mathbf{h}}_2^{(b)}}{\partial\boldsymbol{\beta}_2} & \frac{\partial\mathcal{L}^3_{\mathbf{g}_0\mathbf{g}_{13}\mathbf{g}_0}\overline{\mathbf{h}}_2^{(b)}}{\partial\boldsymbol{\beta}_3} & -\boldsymbol{\gamma}_2^\top\lfloor\mathbf{e}_3\times\rfloor & \boldsymbol{\gamma}_2^\top\lfloor\mathbf{e}_3\times\rfloor \\ \frac{\partial\mathcal{L}^3_{\mathbf{g}_0\mathbf{g}_0\mathbf{g}_{11}}\overline{\mathbf{h}}_1^{(b)}}{\partial\boldsymbol{\beta}_1} & \frac{\partial\mathcal{L}^3_{\mathbf{g}_0\mathbf{g}_0\mathbf{g}_{11}}\overline{\mathbf{h}}_1^{(b)}}{\partial\boldsymbol{\beta}_2} & \frac{\partial\mathcal{L}^3_{\mathbf{g}_0\mathbf{g}_0\mathbf{g}_{11}}\overline{\mathbf{h}}_1^{(b)}}{\partial\boldsymbol{\beta}_3} & \mathbf{0} & \boldsymbol{\gamma}_1^\top\lfloor\mathbf{e}_1\times\rfloor \\ \frac{\partial\mathcal{L}^3_{\mathbf{g}_0\mathbf{g}_0\mathbf{g}_{11}}\overline{\mathbf{h}}_2^{(b)}}{\partial\boldsymbol{\beta}_1} & \frac{\partial\mathcal{L}^3_{\mathbf{g}_0\mathbf{g}_0\mathbf{g}_{11}}\overline{\mathbf{h}}_2^{(b)}}{\partial\boldsymbol{\beta}_2} & \frac{\partial\mathcal{L}^3_{\mathbf{g}_0\mathbf{g}_0\mathbf{g}_{11}}\overline{\mathbf{h}}_2^{(b)}}{\partial\boldsymbol{\beta}_3} & \mathbf{0} & \boldsymbol{\gamma}_2^\top\lfloor\mathbf{e}_1\times\rfloor \\ \frac{\partial\mathcal{L}^3_{\mathbf{g}_0\mathbf{g}_0\mathbf{g}_{12}}\overline{\mathbf{h}}_1^{(b)}}{\partial\boldsymbol{\beta}_1} & \frac{\partial\mathcal{L}^3_{\mathbf{g}_0\mathbf{g}_0\mathbf{g}_{12}}\overline{\mathbf{h}}_1^{(b)}}{\partial\boldsymbol{\beta}_2} & \frac{\partial\mathcal{L}^3_{\mathbf{g}_0\mathbf{g}_0\mathbf{g}_{12}}\overline{\mathbf{h}}_1^{(b)}}{\partial\boldsymbol{\beta}_3} & \mathbf{0} & \boldsymbol{\gamma}_1^\top\lfloor\mathbf{e}_2\times\rfloor \\ \frac{\partial\mathcal{L}^3_{\mathbf{g}_0\mathbf{g}_0\mathbf{g}_{12}}\overline{\mathbf{h}}_2^{(b)}}{\partial\boldsymbol{\beta}_1} & \frac{\partial\mathcal{L}^3_{\mathbf{g}_0\mathbf{g}_0\mathbf{g}_{12}}\overline{\mathbf{h}}_2^{(b)}}{\partial\boldsymbol{\beta}_2} & \frac{\partial\mathcal{L}^3_{\mathbf{g}_0\mathbf{g}_0\mathbf{g}_{12}}\overline{\mathbf{h}}_2^{(b)}}{\partial\boldsymbol{\beta}_3} & \mathbf{0} & \boldsymbol{\gamma}_2^\top\lfloor\mathbf{e}_2\times\rfloor \\ \frac{\partial\mathcal{L}^3_{\mathbf{g}_0\mathbf{g}_0\mathbf{g}_{13}}\overline{\mathbf{h}}_1^{(b)}}{\partial\boldsymbol{\beta}_1} & \frac{\partial\mathcal{L}^3_{\mathbf{g}_0\mathbf{g}_0\mathbf{g}_{13}}\overline{\mathbf{h}}_1^{(b)}}{\partial\boldsymbol{\beta}_2} & \frac{\partial\mathcal{L}^3_{\mathbf{g}_0\mathbf{g}_0\mathbf{g}_{13}}\overline{\mathbf{h}}_1^{(b)}}{\partial\boldsymbol{\beta}_3} & \mathbf{0} & \boldsymbol{\gamma}_1^\top\lfloor\mathbf{e}_3\times\rfloor \\ \frac{\partial\mathcal{L}^3_{\mathbf{g}_0\mathbf{g}_0\mathbf{g}_{13}}\overline{\mathbf{h}}_2^{(b)}}{\partial\boldsymbol{\beta}_1} & \frac{\partial\mathcal{L}^3_{\mathbf{g}_0\mathbf{g}_0\mathbf{g}_{13}}\overline{\mathbf{h}}_2^{(b)}}{\partial\boldsymbol{\beta}_2} & \frac{\partial\mathcal{L}^3_{\mathbf{g}_0\mathbf{g}_0\mathbf{g}_{13}}\overline{\mathbf{h}}_2^{(b)}}{\partial\boldsymbol{\beta}_3} & \mathbf{0} & \boldsymbol{\gamma}_2^\top\lfloor\mathbf{e}_3\times\rfloor \end{bmatrix} \tag{238}$$

References

[1] J.A. Hesch et al. "Consistency Analysis and Improvement of Vision-aided Inertial Navigation". In: *IEEE Transactions on Robotics* PP.99 (2013), pp. 1–19. DOI: 10.1109/TRO.2013.2277549.

[2] J.A. Hesch et al. "Camera-IMU-based localization: Observability analysis and consistency improvement". In: *International Journal of Robotics Research* 33 (2014), pp. 182–201.

[3] M. Li and A. I. Mourikis. "High-Precision, Consistent EKF-based Visual-Inertial Odometry". In: *International Journal of Robotics Research* 32.6 (2013), pp. 690–711.

[4] Stefan Leutenegger et al. "Keyframe-based visual-inertial odometry using nonlinear optimization". In: *International Journal of Robotics Research* (Dec. 2014).

[5] Guoquan Huang, Michael Kaess, and John Leonard. "Towards Consistent Visual-Inertial Navigation". In: *IEEE International Conference on Robotics and Automation*. Hong Kong, China, 2014, pp. 4926–4933. DOI: 10.1109/ICRA.2014.6907581.

[6] Tong Qin, Peiliang Li, and Shaojie Shen. "VINS-Mono: A Robust and Versatile Monocular Visual-Inertial State Estimator". In: *arXiv preprint arXiv:1708.03852* (2017).

[7] Raúl Mur-Artal and Juan D Tardós. "Visual-inertial monocular SLAM with map reuse". In: *IEEE Robotics and Automation Letters* 2.2 (2017), pp. 796–803.

[8] Kevin Eckenhoff, Patrick Geneva, and Guoquan Huang. "Direct visual-inertial navigation with analytical preintegration". In: *Robotics and Automation (ICRA), 2017 IEEE International Conference on*. IEEE. 2017, pp. 1429–1435.

[9] Ji Zhang and Sanjiv Singh. "Enabling aggressive motion estimation at low-drift and accurate mapping in real-time". In: *International Conference on Robotics and Automation*. IEEE. Singapore, 2017, pp. 5051–5058.

[10] Chao X Guo and Stergios I Roumeliotis. "IMU-RGBD camera navigation using point and plane features". In: *International Conference on Intelligent Robots and Systems*. Tokyo, Japan, 2013, pp. 3164–3171.

[11] Yulin Yang and Guoquan Huang. "Acoustic-Inertial Underwater Navigation". In: *Proc. of the IEEE International Conference on Robotics and Automation*. Singapore, 2017.

[12] Guoquan Huang, Anastasios I. Mourikis, and Stergios I. Roumeliotis. "Observability-based Rules for Designing Consistent EKF SLAM Estimators". In: *International Journal of Robotics Research* 29.5 (Apr. 2010), pp. 502–528. DOI: 10.1177/0278364909353640.

[13] A. I. Mourikis and S. I. Roumeliotis. "A multi-state constraint Kalman filter for vision-aided inertial navigation". In: *International Conference on Robotics and Automation*. Rome, Italy, 2007, pp. 3565–3572.

[14] Guoquan Huang. "Improving the Consistency of Nonlinear Estimators: Analysis, Algorithms, and Applications". PhD thesis. Department of Computer Science and Engineering, University of Minnesota, 2012. URL: http://people.csail.mit.edu/ghuang/paper/thesis.pdf.

[15] Eagle S. Jones and Stefano Soatto. "Visual-inertial Navigation, Mapping and Localization: A Scalable Real-time Causal Approach". In: *International Journal of Robotics Research* 30.4 (Apr. 2011), pp. 407–430. DOI: 10.1177/0278364910388963.

[16] Joshua Hernandez, Konstantine Tsotsos, and Stefano Soatto. "Observability, identifiability and sensitivity of vision-aided inertial navigation". In: *2015 IEEE International Conference on Robotics and Automation (ICRA)*. IEEE. Seattle, Washington, 2015, pp. 2319–2325.

[17] A. Martinelli. "Vision and IMU Data Fusion: Closed-Form Solutions for Attitude, Speed, Absolute Scale, and Bias Determination". In: *IEEE Transactions on Robotics* 28.1 (2012), pp. 44–60.

[18] A. Martinelli. "Visual-inertial structure from motion: Observability and resolvability". In: *Proc. of the IEEE/RSJ International Conference on Intelligent Robots and Systems*. Tokyo, Japan, Nov. 2013, pp. 4235–4242.

[19] Dimitrios G. Kottas et al. "On the Consistency of Vision-aided Inertial Navigation". In: *International Symposium on Experimental Robotics*. Quebec City, Canada, 2012.

[20] R. Hermann and A. Krener. "Nonlinear controllability and observability". In: *IEEE Transactions on Automatic Control* 22.5 (Oct. 1977), pp. 728 –740.

[21] Chao Guo and Stergios Roumeliotis. "IMU-RGBD Camera 3D Pose Estimation and Extrinsic Calibration: Observability Analysis and Consistency Improvement". In: *International Conference on Robotics and Automation*. Karlsruhe, Germany, 2013.

[22] Kejian J Wu et al. "VINS on wheels". In: *International Conference on Robotics and Automation*. IEEE. Singapore, 2017, pp. 5155–5162.

[23] H. Yu and A. I. Mourikis. "Vision-aided inertial navigation with line features and a rolling-shutter camera". In: *International Conference on Robotics and Intelligent Systems*. Hamburg, Germany, 2015, pp. 892–899.

[24] Ghazaleh Panahandeh et al. "Observability analysis of a vision-aided inertial navigation system using planar features on the ground". In: *International Conference on Intelligent Robots and Systems*. IEEE. Tokyo, Japan, 2013, pp. 4187–4194.

[25] Dimitrios G Kottas and Stergios I Roumeliotis. "Efficient and consistent vision-aided inertial navigation using line observations". In: *International Conference on Robotics and Automation*. Karlsruhe, Germany, 2013, pp. 1540–1547.

[26] Adrien Bartoli and Peter Sturm. "Structure From Motion Using Lines: Representation, Triangulation and Bundle Adjustment". In: *Computer Vision and Image Understanding* 100.3 (2005), pp. 416–441.

[27] Nikolas Trawny and Stergios I. Roumeliotis. *Indirect Kalman Filter for 3D Attitude Estimation*. Tech. rep. University of Minnesota, Dept. of Comp. Sci. & Eng., Mar. 2005.

[28] X. Zuo et al. "Robust Visual SLAM with Point and Line Features". In: *Proc. of the IEEE/RSJ International Conference on Intelligent Robots and Systems*. Vancouver, Canada, 2017.

[29] Y. Bar-Shalom and T. E. Fortmann. *Tracking and Data Association*. New York: Academic Press, 1988.

[30] Yulin Yang and Guoquan Huang. "Map-Based Localization Under Adversarial Attacks". In: *Proc. of the International Symposium on Robotics Research*. Puerto Varas, Chile, 2017.

[31] A. Martinelli. "Nonlinear Unknown Input Observability: Extension of the Observability Rank Condition". In: *IEEE Transactions on Automatic Control* (2018), pp. 1–1. ISSN: 0018-9286. DOI: 10.1109/TAC.2018.2798806.

[32] Z. Yang and S. Shen. "Monocular visual-inertial fusion with online initialization and camera-IMU calibration". In: *IEEE International Symposium on Safety, Security, and Rescue Robotics (SSRR)*. West Lafayette, Indiana, 2015, pp. 1–8. DOI: 10.1109/SSRR.2015.7442952.

[33] G. Panahandeh et al. "Observability analysis of a vision-aided inertial navigation system using planar features on the ground". In: *International Conference on Intelligent Robots and Systems*. 2013, pp. 4187–4194. DOI: 10.1109/IROS.2013.6696956.

[34] M. D. Shuster. "A survey of attitude representations". In: *Journal of the Astronautical Sciences* 41.4 (1993), pp. 439–517.